PEOPLE'S DEMOCRATIC REPUBLIC OF ALGERIA
MINISTRY OF HIGHER EDUCATION AND SCIENTIFIC RESEARCH

UNIVERSITY KASDI MERBAH OUARGLA

FACULTY OF APPLIED SCIENCES

DEPARTMENT OF MECHANICAL ENGINEERING

ACADEMIC MASTER'S THESIS

Field: Science and Technology

Sector: Mechanical Engineering

Specialty: Energetic

Presented by :

ZEHARI Houssam Eddine

ARIBI Taha

Theme

Energy Efficiency in Algerian Residential Buildings

Impact of Insulation and Renewable Energy in Various Climates

Publicly supported : 14-06-2025

The Jury :

Mr. Imad KEMERCHOU	**Associate Professor (A)**	**UKM Ouargla**	**President**
Mr. Mohamed Mebrouk DRID	**Associate Professor (B)**	**UKM Ouargla**	**Examiner**
Ms. Nadia SAIFI	**Professor**	**UKM Ouargla**	**Promoter**

Academic year: 2024–2025

Acknowledgments

We thank Allah Almighty, with all gratitude, for guiding us to the path of light and knowledge, and for granting us the health and strength to complete this work.

We extend our sincere thanks and deep appreciation to our supervisor, ***Dr. Nadia SAIFI****, Professor at the University of Kasdi Merbah Ouargla, for the trust she placed in us by assigning this topic, and for her continuous support, follow-up, and valuable guidance throughout the completion of this work.*

We also express our heartfelt gratitude to ***Dr. Imad KEMERCHOU****, Associate Professor at the University of Kasdi Merbah Ouargla, for kindly agreeing to chair the defense committee, and to* ***Dr. Mohamed Mebrouk DRID****, also Associate Professor at the same university, for accepting to examine and evaluate this work.*

In conclusion, we warmly thank our fellow Master's students and everyone who supported us directly or indirectly in completing this research work.

We extend our heartfelt thanks and sincere appreciation to our dear families for their constant encouragement and unwavering support throughout our academic journey.

We also thank everyone who contributed in any way to assisting us during this scientific endeavor.

Finally, we would like to thank each other for the spirit of collaboration and dedication that marked our teamwork throughout the course of this project.

Dedication

To those who, after Allah, have had the greatest impact on every step of my journey…

*To my **mother** and **father**, the heartbeat of my life and my true source of strength, thank you for your patience, unwavering support, and the prayers that accompanied me at every moment. Without your sacrifices, I would not have reached this achievement. You are the wellspring of endless love and giving, and every success rightfully belongs to you before it belongs to me.*

*To my dear uncle **Z.Omar**, who was always there with encouraging words, sincere advice, and constant support, your presence in my life is a blessing I am proud of, and it is an honor for me to dedicate a part of this success to you.*

*And to my colleague and brother in this journey, **Taha** thank you for your spirit of collaboration, shared effort, and the mutual understanding that brought us together throughout this project. You were a true partner, and your presence was essential to the success of this dissertation.*

To all of you, I dedicate this work with sincerity, love, and endless gratitude.

ZEHARI Houssam Eddine

Dedication

In the name of Allah, the Most Gracious, the Most Merciful.

All praise is due to Allah, who granted me strength, patience, and guidance throughout this journey.

To my beloved parents,

Your endless love, sincere prayers, and constant support have been my greatest blessings. This accomplishment is the result of your sacrifices and faith in me. May Allah reward you with the highest ranks in Jannah.

*To my dear **brothers** and **sisters**,*

Thank you for your love, encouragement, and for always being there when I needed you. Your presence brought me peace and strength.

To my wonderful friends,

Your motivation, kindness, and companionship made this path lighter and more joyful. I'm grateful Allah placed you in my life.

*To my esteemed colleague **Houssam**,*

Your dedication, persistence, and valuable contributions were instrumental throughout the work on this thesis. I deeply appreciate your commitment, teamwork, and the positive spirit you brought to every stage of this journey. It was truly an honor to collaborate with you.

ARIBI Taha

Contents

List of Figures

List of Tables

Nomenclature

$C_{cooling}$	Annual cooling cost	$/m²
C_{el}	Cost of electricity	$/kWh
C_{eng}	Energy consumption cost	$/m²
C_g	Cost of natural gas	$/kWh
$C_{heating}$	Annual heating cost	$/m²
C_i	cost of insulation material	$/m²
C_{i1}	Cost of extruded polystyrene	$/m³
C_{i2}	Cost of glass wool	$/m³
C_p	Specific heat capacity	J/kg·K
e	Thickness of the material	m
$E_{cooling}$	Annual cooling energy requirement	kWh/m²
$E_{heating}$	Annual heating energy requirement	kWh/m²
h_{in}	Enthalpy of entering air	kJ/kg
h_{out}	Enthalpy of leaving air	kJ/kg
LHV_{gaz}	Lower heating value of natural gas	MJ/m³
m	Amount of substance mol number	kmol/m²·year
M	Molar mass of fuel	kg/kmol
$\dot{m}_{air}$	Mass flow rate of air	Kg/s
m_{CO_2}	Annual CO_2 emissions per unit area	$kgCO_2/m^2 \cdot year$
N	Building lifetime	years
P_{comp}	Compressor power consumption	kW
P_{fan}	Fan power consumption	kW
Q_{abs}	Heat absorbed from the environment heating mode	kW
Qcooling	Annual Cooling transmission load	kWh
Qheatin	Annual heating transmission load	kWh
Q_{latent}	Latent cooling capacity	kW
Q_{rej}	Heat rejected to the environment cooling mode	kW
Q_{sens}	Sensible cooling capacity	kW
Q_{total}	Total capacity heating or cooling	kW
RH	Relative humidity	%
T_b	Base temperature for heating/cooling	°C
T_m	Mean daily outdoor temperature	°C
TC	Total cost	$/m²

U	Overall heat transfer coefficient of wall	$W/m^2 \cdot K$
Greek Letters		
λ	Thermal conductivity	kJ/h·m·K
ηs	Efficiency of the heating system	-
ρ	Material density	kg/m^3
Abbreviations		
HVAC	Heating, Ventilation, and Air Conditioning	
CDD	Cooling Degree Days	
COP	Coefficient of Performance	
DHW	Domestic Hot Water	
DTR	Thermal Regulation Document Algeria	
HDD	Heating Degree Days	
HP	Heat Pump Pompe à chaleur	
ONM	National Office of Meteorology Algeria	
PWF	Present Worth Factor	
TRNSYS	Transient System Simulation Tool	

General Introduction

General Introduction

Energy performance in buildings has become a critical issue in hot and semi-arid regions, where extreme climatic conditions such as high summer temperatures and minimal rainfall exert considerable pressure on cooling and heating systems (Alyami, M. M., 2022). In this context, the search for sustainable solutions to ensure indoor thermal comfort while reducing energy consumption has become a central objective in modern building design.

In Algeria, particularly in the southern regions, residential buildings represent a significant share of the national energy demand due to their reliance on mechanical air conditioning systems. The building sector is one of the most energy-consuming sectors in Algeria, accounting for 42% of the total energy consumption among all sectors (Meftah, N., & Mahri, Z. L., 2022) .To address this challenge, passive strategies such as thermal insulation, combined with active systems like air-to-air heat pumps powered by renewable energy sources, offer promising and effective alternatives. These solutions not only reduce heat loss in winter and heat gain in summer but also promote clean and efficient energy production and usage.

Several studies in the literature have emphasized the importance of adapting materials and construction methods to local climatic conditions. The use of insulating materials with low thermal conductivity, such as glass wool and extruded polystyrene, combined with efficient heat pump systems, has been shown to significantly enhance thermal comfort while reducing both energy consumption and greenhouse gas emissions. However, such strategies require a comprehensive assessment that considers climatic variability, building orientation, seasonal energy needs, and financial and environmental factors.

The main objective of this work is to evaluate the impact of integrating thermal insulation with an air-to-air heat pump system on energy consumption, indoor thermal conditions, and CO_2 emissions in residential buildings located in hot and semi-arid regions of Algeria. To achieve this, a dual approach was adopted: numerical simulations using TRNSYS software and a detailed economic and environmental analysis of various proposed scenarios.

This thesis is structured into three interrelated chapters.

The first chapter presents the national energy context in Algeria and highlights the challenges and opportunities in improving energy performance in the building sector. It reviews

the key factors influencing energy consumption and emphasizes the importance of adapting construction strategies to regional climatic conditions.

The second chapter describes the adopted methodology, including the selection of insulation materials, the modeling of a typical residential building, and the simulation procedures used to analyze energy loads. It also outlines the indicators used to assess energy, economic, and environmental performance across several southern Algerian provinces.

The third chapter presents a comparative analysis of the simulation results, focusing on energy savings, indoor thermal comfort, and emissions reduction. Special attention is given to the economic feasibility of each configuration and the identification of optimal insulation thicknesses for different climates.

The main conclusions drawn from this research are presented in the general conclusion, along with practical recommendations to promote the implementation of these strategies in sustainable construction projects throughout Algeria’s arid and semi-arid zones.

CHAPTER I

Energy Efficiency with Insulation and Renewable Energy

1. Introduction

The increasing global demand for energy and the intensifying effects of climate change have made energy efficiency in buildings a top priority for sustainable development. In Algeria, the building sector alone accounts for nearly 42% of total energy consumption, a figure driven by population growth, urban sprawl, and reliance on fossil fuels. Addressing this issue is critical for reducing greenhouse gas emissions, conserving resources, and improving occupant comfort. The residential sector, in particular, presents a significant opportunity for intervention through improved insulation, passive design strategies, and the integration of renewable energy systems. This chapter explores the multifaceted aspects of energy consumption in Algerian residential buildings. It begins by underlining the national importance of energy efficiency, followed by an examination of key factors influencing energy demand such as thermal insulation, HVAC systems, building orientation, and user behavior. Special attention is given to the challenges of accurately forecasting energy use in diverse climatic conditions. Furthermore, the chapter analyzes the Algerian climate and its influence on building energy performance across various regions, highlighting the necessity of region-specific design solutions. Finally, it delves into the principles of thermal comfort, emphasizing both environmental and individual parameters that must be considered in designing energy-efficient and comfortable living spaces.

2. Energy efficiency in residential buildings

2.1. Importance of energy efficiency in Algeria's building sector

The building sector in Algeria represents one of the main contributors to national energy consumption, accounting for nearly 42% of total energy demand (APRUE, 2020). The growing population, rapid urbanization, and dependency on fossil fuels have increased pressure on the sector. Energy efficiency is therefore vital for reducing consumption, minimizing greenhouse gas emissions, and achieving sustainable development goals (Benouar & Messaoud, 2019). National strategies have emphasized the need for integrating renewable energies and thermal insulation techniques, particularly in the residential sector.

2.2. Main factors affecting building energy consumption

Several parameters influence the energy consumption of buildings in Algeria. These include low thermal insulation, inefficient HVAC systems, building envelope characteristics, orientation, and user behavior (Bensaid et al., 2021). Moreover, construction practices often fail

to adhere to bioclimatic design principles, especially in older housing stocks. Climate variability between regions significantly affects energy loads, further complicating energy planning (Ghrib et al., 2018).

2.3. Challenges in predicting energy use

Forecasting energy use in buildings is complex due to the interplay of dynamic variables such as climate, occupancy schedules, and envelope performance. Limited access to local consumption data, lack of calibration in simulation models, and differences in user behavior introduce uncertainties in energy predictions (Mebarki et al., 2020). While simulation tools like TRNSYS and Energy Plus are widely used, they require adaptation to the Algerian context for reliable results.

2.4. Energy performance diagnosis and evaluation methods

Energy performance assessments in Algeria increasingly rely on dynamic thermal simulation tools, such as TRNSYS, EnergyPlus, and DesignBuilder (Chel et al., 2019). These tools enable the evaluation of different architectural and technical interventions, including passive cooling, improved glazing, solar chimneys, and insulation strategies. Studies have demonstrated that integrating such methods can lead to a 30–50% reduction in energy demand for heating and cooling (Messaoudi et al., 2021).

3. Climate analysis and its impact on energy use

3.1. Algerian climate and its influence on energy patterns

Algeria spans a diverse climatic spectrum ranging from the Mediterranean in the north to the arid Sahara in the south (ONM, 2021). These variations lead to different energy demands: heating in the north and cooling in the south. Rising temperatures and increased frequency of heatwaves due to climate change amplify energy needs and strain existing infrastructure (Bouabdallah et al., 2020). Additionally, desertification and water scarcity further complicate energy management and resource planning (UNDP, 2022).

3.2. Geographical and climatic zones of Algeria

Algeria covers an area of 2,381,741 km². It is located between 18° and 38° north latitude and between 9° and 12° east longitude. The Algerian territory is characterized by a diversity of climatic zones, classified into four categories, namely (Figure I.1):

Zone A: Coastal marine area;

Zone B: Mountainous hinterland;

Zone C: High plateaus;

Zone D: Pre-Saharan and Saharan region.

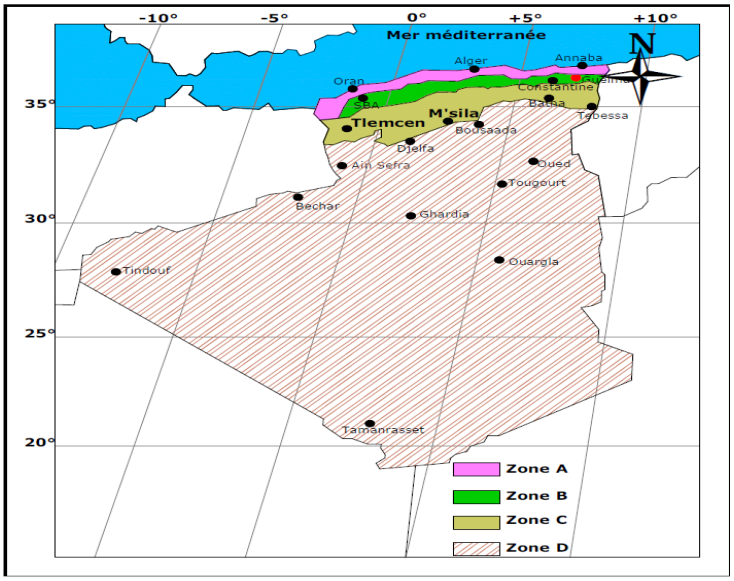

Figure I.1: Climat classification in Algeria (Medjelekh, 2006)

3.2.1. Coastal areas (climate and urban concentration):

Coastal cities such as Algiers and Oran face relatively milder climates but experience dense urban development. This leads to heat island effects and rising energy demand for cooling (Benamrane et al., 2018). The stable climate offers potential for solar energy integration in buildings and urban infrastructure.

3.2.2. Mountainous areas (tell atlas and saharan atlas):

These areas experience notable diurnal and seasonal temperature variations. Energy needs fluctuate between heating and cooling, depending on the time of year. The complex topography influences wind flow and solar exposure, which can be leveraged in passive design approaches (Cherif et al., 2017).

3.2.3. High plateaus (hauts plateaux):

The High Plateaus region of Algeria is characterized by a semi-arid climate, with low and irregular precipitation ranging from 200 to 400 mm per year. This zone experiences significant

temperature variations and is covered mainly by steppe vegetation. It acts as a transitional climatic zone between the Mediterranean coastal areas and the arid Sahara Desert. The climatic conditions significantly influence the energy needs for heating and cooling in buildings located in this region (Office National de la Météorologie - ONM, 2021).

3.2.4. Desert areas (extreme conditions and their implications):

The Saharan region, comprising over 80% of Algeria's territory, is subject to extreme solar radiation, low humidity, and significant temperature fluctuations (CNES, 2021). Buildings in these areas require high-performance insulation and passive cooling systems to maintain indoor comfort. Moreover, the high solar potential makes it ideal for photovoltaic and solar thermal applications (Saheb et al., 2019).

3.3. Bottom-up approach for estimating residential energy demand in Algeria

Understanding future energy demand in the residential sector is crucial for developing effective national energy policies and sustainability strategies. In this context, researchers have conducted studies using advanced modeling techniques to predict energy consumption trends across different climatic regions of Algeria. One such significant study is that of Ghedamsi et al., which utilizes a bottom-up approach to assess and project energy needs through the year 2040. Ghedamsi et al. (2016) employed a bottom-up modeling approach to simulate and forecast the energy consumption of Algerian buildings through the year 2040. To estimate annual energy consumption, the Algerian territory was divided into climatic zones based on the annual cost of energy used for heating and cooling in the residential sector. The annual heating and cooling demands of buildings in various regions of Algeria (48 meteorological stations) were evaluated using the degree-day method. Subsequently, Geographic Information System (GIS) techniques were applied to develop a climatic zoning map. Within each zone, energy consumption was calculated for heating, cooling, and household appliances. The results indicated that final energy consumption increased from 73.23 TWh in 2008 to 179.78 TWh in 2040. Additionally, Algeria's climate was classified into seven distinct zones, with Zone 7 accounting for approximately 73% of the country's total final energy consumption.

Lazher Messoudi et al (2024) developed a bottom-up modeling approach to analyze and forecast residential energy consumption in Algeria until the year 2040. The study aimed to identify regional differences in energy demand for heating and cooling across the country.

To achieve this, the Algerian territory was divided into distinct climatic zones based on annual heating and cooling needs. These needs were evaluated using the degree-days method at 48 meteorological stations nationwide. A Geographic Information System (GIS) was employed to map and visualize the climatic zones. Within each zone, energy demands were calculated for space heating, cooling, and household appliances. This comprehensive modeling allowed the researchers to assess regional consumption variations. The final energy consumption in the residential sector was estimated to increase significantly over time. It rose from 73.23 TWh in 2008 to a projected 179.78 TWh in 2040. The analysis revealed that the climatic zone labeled "Zone 7" accounted for approximately 73% of the total final energy consumption. This high share is attributed to extreme climatic conditions requiring both substantial heating and cooling. The methodology demonstrated the relevance of tailored strategies for each zone instead of a national one-size-fits-all approach. This includes improving building insulation, promoting energy-efficient systems, and adjusting thermal standards by region. The study provides a foundation for the development of climate-responsive building regulations. It emphasizes the role of spatial planning and climate analysis in shaping energy policies. Incorporating GIS helped visualize spatial disparities in energy demand, enabling targeted interventions. The approach supports the design of localized energy-saving measures and sustainable urban development. By considering regional climate data and building needs, policymakers can optimize future energy planning. The study concludes that understanding energy use by climate zone is essential for reducing national energy consumption. These findings serve as a strategic reference for decision-makers in Algeria's energy and housing sectors.

4. Thermal comfort:

In built environments, thermal comfort is a crucial requirement that designers must address. The thermal environment is defined by four physical variables: air temperature, solar radiation intensity, humidity, and air velocity. These factors interact with human activity and clothing to determine the body's thermal state, forming six fundamental parameters governing heat exchange between humans and their surroundings (Figure I.2).

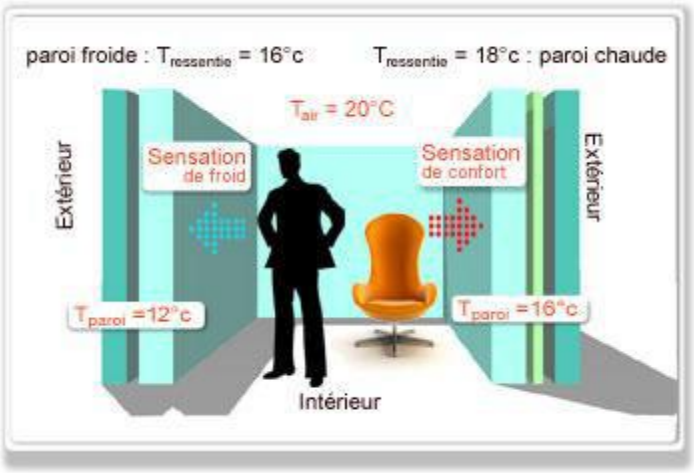

Figure I.2: Thermal comfort (Ecodom, 2013).

4.1. Environmental climatic factors

Thermal comfort depends on four environmental factors: air temperature, humidity, mean radiant temperature, and air velocity, which vary over time and space. These factors influence how humans perceive their thermal environment and are essential in designing comfortable indoor spaces (Benlatreche T, 2006).

4.1.1. Air Temperature

Air temperature is the main external factor affecting thermal comfort. It includes the ambient air temperature, which should be kept between 19 and 26 °C indoors. Wall temperature also matters; a cold wall causes discomfort even if the air is warm. The operative temperature, combining air and wall temperatures, better reflects the actual sensation. A temperature difference of 3 °C between the feet and head can cause discomfort for some occupants, (Figure I.3).

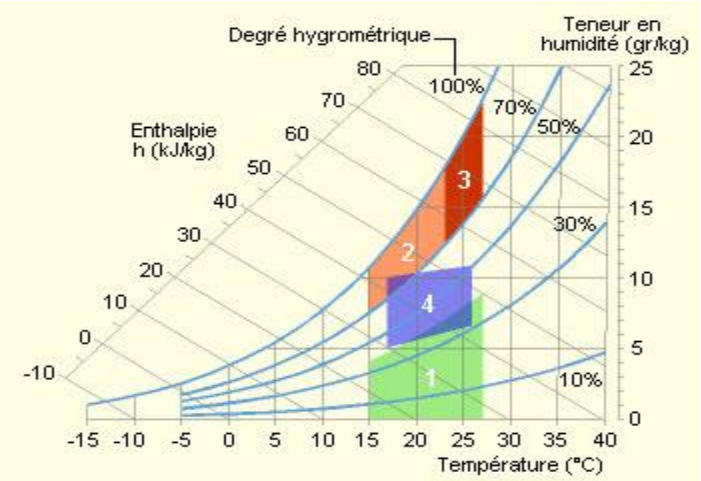

Figure I.3: Example of a comfort zone on the psychrometric chart (Thiers S, 2008).

4.1.2. Humidity

Humidity affects comfort and health, with an optimal range between 35% and 70% relative humidity. Outside this range, dry air can cause discomfort, and high humidity can promote microbial growth such as bacteria, molds, or dust mites. Maintaining floor temperatures between 19 and 29 °C also helps keep the discomfort rate low (Thiers S, 2008).

4.1.3. Air movement and velocity

Air movement affects the perceived temperature by increasing heat exchange from the body. It cools more when the air is cold but can cause discomfort if the velocity exceeds 0.15 m/s in winter or 0.25 m/s in summer, leading to drafts. Proper air-tightness is crucial to prevent unwanted airflow inside buildings (Mazouz S, 2010).

4.2. Individual factors

4.2.1. Clothing

Clothing creates a thermal barrier, maintaining a microclimate around the body. Its thermal resistance is quantified by the Clo index (Figure I.4). Different fabrics, garment cuts, and wearer activities influence heat exchange, helping maintain comfort throughout seasonal changes and various environments (Figure I.4).

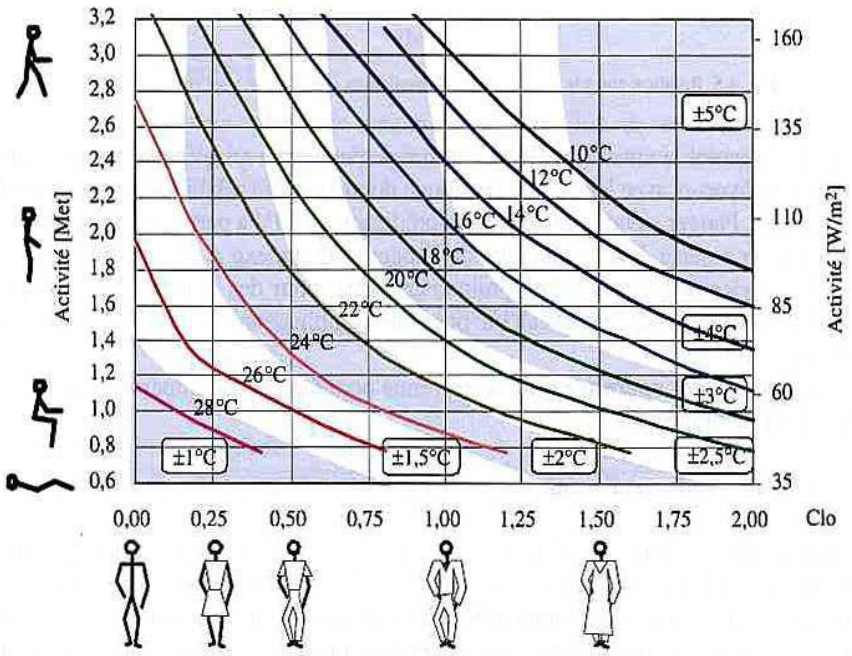

Figure I.4: Optimal operative temperature as a function of metabolism (ISO EN 7730, 1994).

4.2.2. Metabolism

The metabolic rate measures heat produced by the human body, depending on activity level, physiology, and individual characteristics (Figure I.5). Basal metabolism covers minimal life functions, resting metabolism applies to quiet sitting, and working metabolism varies with physical activity intensity. These metabolic differences affect thermal comfort needs (Merzeg A, 2010; Fernandez P, 2009).

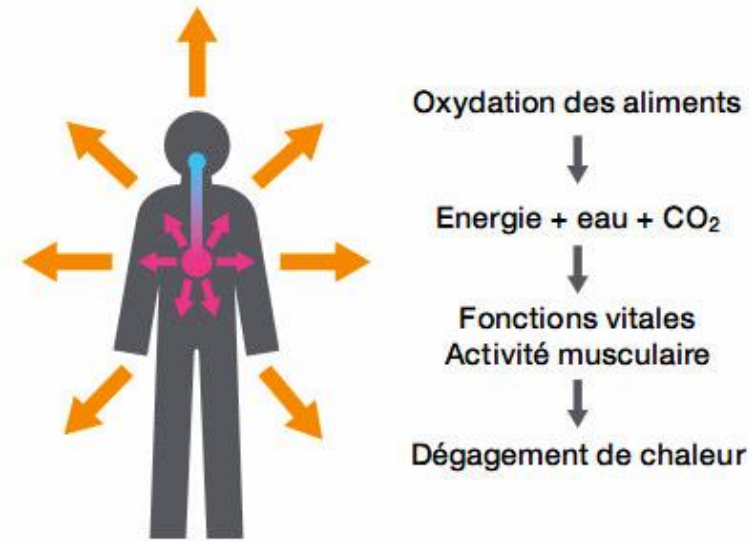

Figure I.5: Human metabolism.(Ref)

5. Design and construction materials

Thermal mass and insulation: Choosing the right building materials is essential for energy efficiency. High thermal mass materials can help control indoor temperatures in areas with extreme temperatures, lowering the demand for active heating and cooling systems. In arid regions, for instance, classic adobe buildings are made to have chilly interiors during the day and warm ones at night (Mebarki A. et al, 2020).
Energy Efficiency Requirements: In order to lower overall energy usage, the Algerian government has been supporting improved insulation and energy-efficient designs as part of its efforts to raise building energy efficiency standards (Messaoudi L. et al, 2021).

5.1. Material selection and climate adaptation

Despite Algeria's diverse climate, the current building materials widely used do not adequately consider climatic conditions, relying heavily on reinforced concrete and industrial

materials that lack thermal efficiency, which increases energy consumption for heating and cooling systems. Consequently, the Algerian government has been promoting thermal insulation and improved building designs to enhance energy efficiency and reduce consumption (Figure I.7) (MHU,2010).

Traditionally, buildings in arid regions utilized local materials such as sun-dried clay bricks and natural plaster,(Figure I.6) which possess high thermal mass, helping regulate indoor temperatures by keeping interiors cool during the day and warm at night. Combining these traditional techniques with modern insulation technologies and material selection can significantly improve thermal comfort and reduce mechanical system dependency, thereby supporting sustainability and energy efficiency efforts in the construction sector.

Figure I.6: Use of concrete and current building materials in Ouargla.

Figure I.7: Use of local materials (stone) in Ouargla.

5.2. Insulation Techniques and Innovations

Insulation always plays a beneficial role: in winter, it slows down the loss of heat from the home to the outside. In summer, on the contrary, it cools the living space by limiting heat gain. Insulation also prevents unpleasant condensation and the feeling of a 'cold wall,' which would otherwise force overheating the air to maintain a sufficient level of comfort.

5.2.1. Types of Insulation Materials Used in Residential Buildings

a. Fiberglass:

Fiberglass insulation is made from fine strands of glass and is one of the most common materials used today. It is available in batts, rolls, and loose-fill forms, allowing flexible installation in walls, attics, and floors(Figure I.8).

Figure I.8: Fiberglass

Its cost-effectiveness combined with R-values between R-2.9 and R-4.3 per inch makes it a popular choice (Benamrane 2018). (Saheb, Y 2019)

b. Mineral Wool

Mineral wool, including rock wool and slag wool, is produced from natural minerals and industrial waste. It is naturally fire-resistant without the need for additional chemicals and is available as batts, rolls, or loose-fill. This insulation is known for high recycled content and excellent thermal and acoustic properties (Figure I.9), (UNDP. 2022).

Figure I.9: Mineral wool

c. Cellulose

Cellulose insulation is largely made from recycled paper products and contains 82% to 85% recycled content. Treated with fire retardants, it can be installed densely packed or as loose-fill in new or existing buildings. Cellulose offers strong thermal performance and contributes to sustainable construction (Figure I.10), (Saheb, Y.et al, 2019).

Figure I.10 : Cellulose, (Saheb, Y.et al, 2019).

d. Organic Textiles

Natural fiber insulations include cotton, sheep's wool, straw, and hemp. These materials are treated to resist fire, mold, and pests, making them durable and environmentally friendly options. Although less common, hemp shares thermal properties comparable to other fibrous insulations (Figure I.11), (Derradji, L. et al 2019).

Figure I.11: Organic Textiles (Derradji, L. et al 2019).

e. Polystyrene

Polystyrene insulation comes in rigid foam boards and loose-fill forms, offering lightweight but effective thermal resistance. Its R-value varies with density, and it is widely used for insulation due to its versatility in different applications. It provides good moisture resistance and durability (Figure I.12), (Derradji, L. et al 2017).

Figure I.12: Polystyrene (Derradji, L. et al 2017).

f. Polyurethane with Polyisocyanurate

These rigid thermosetting foam insulations have high R-values and are commonly used as foam boards or spray foam. They expand to fill gaps, improving airtightness and insulation continuity. Their high thermal resistance makes them suitable for various residential insulation needs (Figure I.13), (Neya, I. et al, 2021).

Figure I.13: Polyurethane with polyisocyanurate (Neya, I. et al, 2021).

g. Glass wool

Glass wool is considered to be the most effective, and environmentally friendly insulation product to use as it is non-combustible, and meets the requirements for optimal thermal and acoustic insulation performance in accordance with the highest international standards (EN, FM, ASTM). Centrifugal glass wool product is a kind of thin fiber, low thermal conductivity insulation material, the special structure determines that it can be very good Imprison the air, so that it cannot flow, put an end to the air convection heat transfer, but also can quickly reduce the transmission of sound, so as to heat and sound-absorbing effect. glass wool includes 7 series of glass wool blanket, glass wool board, glass wool tube, glass wool batt, Foil-clad glass wool, colorful glass wool, high-temperature glass wool.(Figure I,14), (Kimco Insulation, 2024).

Figure I.14: Glass wool (Kimco Insulation, 2024).

5.2.2 Effect of Insulation Materials on Energy Loss and Occupant Comfort

Insulation materials greatly influence both energy efficiency and the comfort of occupants in a building. Proper insulation reduces energy consumption by limiting heat transfer between indoor and outdoor environments, thus lowering heating and cooling costs Khoukhi, M. (2018)

By minimizing unwanted heat gain in summer and heat loss in winter, good insulation materials help maintain a steady indoor climate. Additionally, well-installed insulation reduces air leaks, which are major contributors to energy waste and discomfort caused by drafts (Ozel, M.2019) (Elsayed, 2019)

Beyond thermal benefits, many insulation materials also provide acoustic dampening and help control indoor humidity. This combination enhances occupant comfort by creating quieter indoor spaces and reducing the risk of mold, contributing to healthier indoor air quality (Kaushik, A. et al, 2022)

5.2.3. Thermal Properties and Performance of Insulation Materials

a. Thermal Conductivity

Thermal conductivity refers to the amount of heat that passes through a material one meter thick per square meter of surface, given a temperature difference of one degree Celsius between both sides. It is expressed in watts per meter per degree Celsius (W/m·°C). This property is specific to each material and indicates its inherent insulating capability (Saheb, Y 2019)

b. Thermal Resistance

Thermal resistance (R-value) measures how well a material resists heat flow. The higher the R-value, the better the insulation. It depends on both the thickness of the material and its thermal conductivity, combining to indicate the overall insulating performance (UNDP. 2022)

c. Thermal Diffusivity

Thermal diffusivity describes a material’s ability to transmit temperature changes over time. It increases with higher thermal conductivity and decreases with greater volumetric heat capacity. Essentially, it reflects the speed at which heat spreads within a material (UNDP, 2022).

d. Thermal effusivity

Thermal effusivity reflects how quickly a material responds to heat input whether from an internal source or solar radiation. Materials with high effusivity absorb heat rapidly, which can moderate temperature increases inside the room by quickly transferring heat into the building structure (UNDP, 2022).

e. Heat Capacity

Heat capacity (per unit volume) indicates a material's ability to store thermal energy. It is influenced by three key factors: the material's thermal conductivity (λ), specific heat capacity, and density. These properties together define how much heat a material can retain and for how long (Derradji, L, 2017).

5.2.4. Literature Review on Thermal Insulation

Numerous studies have been conducted to evaluate the thermal properties and performance of insulation materials, highlighting their critical role in enhancing energy efficiency and indoor comfort. This section reviews key research contributions related to different types of insulation, their thermal behavior, and their impact on building energy consumption.

L. Derradji et al. (2017) studied the impact of expanded polystyrene insulation thickness on the thermal performance of a prototype building in Algeria compared to a traditional one. Results showed that good insulation stabilizes indoor temperatures and can save up to 70% of heating and cooling energy. Optimal insulation thickness ranges from 1 to 2.5 cm for cooling and 1 to 7 cm for heating, depending on materials and energy sources. Highest energy savings were observed with electricity, and the lowest with natural gas. The study highlights the importance of proper insulation thickness for energy efficiency in Algerian buildings.

Ibrahim Neya et al. (2021) evaluated the thermal performance of compressed stabilized earth block walls in a hot, dry climate using insulation materials like glass wool and straw-lime mixtures. Their simulations showed similar thermal performance for 0.10 m glass wool and 0.15 m straw with 0.02 m lime insulation. Optimal wall thickness varied depending on insulation, with 0.22 m and 0.35 m thick uninsulated walls performing well, while 0.14 m thickness sufficed with insulation. The study highlights the importance of choosing appropriate wall thickness and insulation for thermal comfort and energy efficiency in tropical regions, supporting sustainable building practices.

Khoukhi, M. (2018) investigated how heat and humidity affect the thermal conductivity of polystyrene insulation in buildings. The study showed that moisture content and temperature significantly increase the insulation's thermal conductivity, leading to higher cooling loads up to 8% more at 28 °C with 30% moisture. The impact is greater on roofs than walls and is influenced by building color, weight, and volume. Dark-colored roofs and light-weight buildings increase cooling demand. The findings stress the importance of considering moisture and temperature effects on insulation properties for accurate energy performance assessments in hot, humid climates.

Ozel, M. (2019) numerically studied how glazing area percentage (GAP) and wall orientation affect the optimum insulation thickness in Elazığ, Turkey. Results show that as GAP

increases, optimum insulation thickness and energy savings decrease, while payback periods increase for all wall orientations and glazing types (single and double). South-facing walls require thicker insulation with lower GAP values. Double glazing reduces optimum thickness more than single glazing. Heating and cooling loads are significantly influenced by glazing area, glazing type, and wall orientation. The study highlights the importance of balancing glazing and insulation for energy efficiency.

Elsayed, Mohamed F. et al. (2019) studied optimal insulation thickness for building walls in Palestine using Life Cycle Cost (LCC) analysis. The study highlighted that buildings consume about 43% of Palestine's energy, yet insulation remains optional despite its low cost and clear benefits. They analyzed different insulation materials, weather conditions, energy prices, and equipment efficiencies across eight regions. Results showed insulation type and climate had the greatest impact on optimal thickness, which ranged from 0.4 to 9 cm. Payback periods were short, between 0.9 and 1.6 years, confirming financial viability. The study recommended developing building codes to mandate insulation use.

Despite numerous studies on insulation materials and their thermal performance under various climatic conditions, there remains a need for integrated research that considers the combined effects of moisture, climate variability, and the incorporation of modern renewable energy systems. Such studies are essential to optimize insulation strategies and enhance overall energy efficiency for achieving true sustainability in diverse built environments.

6. Renewable Energy Systems and Their Integration with Residential Buildings

Potential for Solar Energy: Algeria has a lot of potential for solar energy, particularly in its arid areas. Building designs that use solar panels can assist meet energy needs in a sustainable way, minimizing energy costs and dependency on fossil fuels (Messoudi, L, 2024) Government Initiatives: By offering cleaner energy sources, the Algerian government hopes to raise the proportion of renewable energy in its energy mix, which can help buildings' energy requirements (ONM, 2021).

Residential buildings are progressively incorporating renewable energy systems to improve sustainability, lower carbon footprints, and increase energy efficiency. This is a summary of the several kinds of renewable energy systems that are frequently installed in homes, along with information on how they are integrated.

6.2. Solar Energy Technologies:

6.1. 1.Photovoltaic panels

Photovoltaic panels use semiconductor materials, usually silicon, to directly convert sunlight into electricity. Key information regarding PV panels is as follows:

a. Functionality:

Direct current (DC) power produced by sunlight striking photovoltaic cells can be transformed into alternating current (AC) for usage in residences and commercial buildings. Efficiency: Under ideal circumstances, modern photovoltaic panels may attain efficiencies of up to 22.5%, which means they transform a sizable amount of sunshine into electrical power that can be used (ADEME, 2023).

b. Installation:

PV systems are adaptable to a variety of property types since they can be set up as ground-mounted arrays or on rooftops. Additionally, they can be combined with battery storage devices to supply electricity when the sun isn't shining (IRENA, 2020).

c. Grid Connection:

By enabling homes to sell excess electricity back to the utility, PV systems can be linked to the electrical grid and help reduce energy expenses (CSTB, 2022).

Figure I.15: Photovoltaic panels mounted on a building

6.1. 2. Water heaters powered by the sun

Solar water heaters heat water for use in homes and businesses using solar energy. They work especially well to lower the energy expenses related to water heating. Important elements consist of:

a. System types

Solar water heating systems come in two primary varieties:

Active Systems: These move water or a heat-transfer fluid through the solar collectors using pumps and controllers. Residential applications are where they are more prevalent. Installing passive systems is easier and frequently less expensive because they rely on natural convection rather than pumps (Bhatia, S. C. 2014).

Solar collectors, a storage tank, and occasionally a backup heating system for overcast days or times of high demand are the components of a conventional solar water heating system. Depending on the use and climate, the collectors might be either evacuated-tube or flat-plate kinds, each with unique benefits.

Energy Savings: Depending on the system and regional temperature, solar water heaters can cut traditional energy use for water heating by 60% to 75%.

Figure I.16: Water heaters powered by the sun.

6.3. Heat pump

6.3.1. Definition of a Heat Pump (HP):

In general, from a thermodynamic perspective, refrigeration machines and heat pumps are thermal machines that operate in reverse: they consume mechanical energy to extract heat from a cold source and transfer it to a hot source. The heat pump is the core component of a geothermal or aerothermal installation. It enables the recovery of heat from the ground or air, amplifies it, and then releases it inside buildings to provide heating. The goal is to produce heat from a free low-temperature source in order to warm a space or maintain it at a sufficiently high temperature. In such cases, the thermal machine is referred to as a heat pump (HP). Heat pumps are categorized as systems that utilize renewable energy, as they extract heat from the environment for the heating of premises or dwellings (Kinab, E., 2009).

Figure I.17: Heat pump **(**Jason Brown Plumbing & Gas., 2005).

6.3.2. Working Principle

Naturally, heat is transferred from a hot source to a cold sink. The heat pump is a thermodynamic system that enables reverse heat transfer, i.e. from a lower temperature level to a higher temperature level. requires the input of mechanical work. The ideal thermodynamic cycle of a vapor-compression heat pump (Figure 1.4) consists of

- diabatic and reversible (isentropic) compression
- Isobaric heat rejection (condensation and subcooling)
- Isenthalpic expansion
- Isobaric heat addition (evaporation and superheating)

This theoretical refrigeration cycle is a far cry from a Carnot cycle, but has the advantage of technological simplicity.

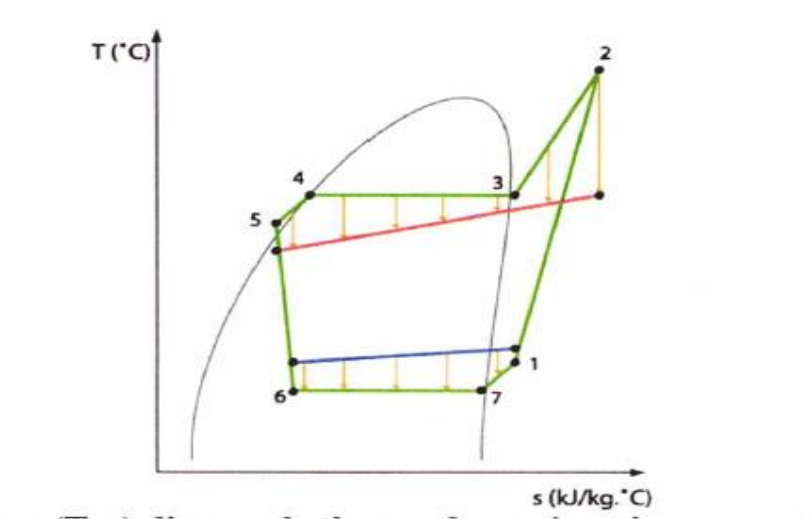

Figure I.18: Diagram (T,S) of a thermodynamic cycle with mechanical vapor compression cycle.

The heat pump has four main components (Figure I.18**):**

- A compressor for quasi-adiabatic compression,
- A condenser, which condenses the refrigerant and transfers heat to the hot with the hot well,
- An expansion valve for isenthalpic expansion,
- An evaporator, which evaporates the refrigerant and transfers heat with the cold source,

Another important “component” of a heat pump is the refrigerant. Variety of refrigerants; among the most widely used today in heat pumps and air conditioning R-407C, R-410A and R-134a; R-407C is a zeotropic fluid that has a very low a zeotropic fluid that exhibits temperature creep.

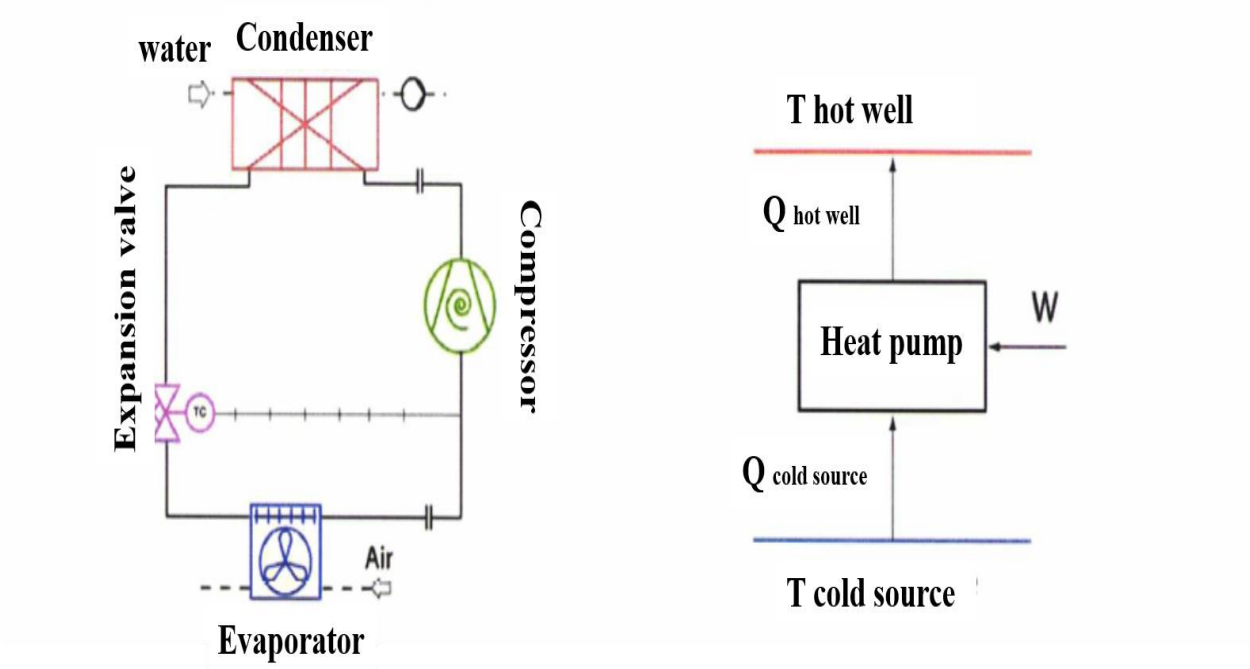

Figure I.19: Simplified heat pump diagram.

6.3.3. Types of Heat Pump

This comparison table provides an overview of the most common types of heat pumps, highlighting their energy source, primary function, installation complexity, domestic hot water capability, and suitability for cold climates. Each type offers advantages suited to specific housing needs and environmental conditions.

Table.I.1: Comparison table of different types of heat pumps.

Heat Pump Type	Heat Source	Main Use	Installation Complexity
Air to air (Xiao, B. et al 2020)	Outdoor air	Air heating/cooling	Very simple (no water circui)
Water to water (Rahhal, C. 2006)	Outdoor air	Water heating + DHW	Simple (no drilling required)
Brine to water (Luis S-M.et al, 2023)	Groundwater/aquifers	Water heating	Complex (drilling + permits)
Ground to water (Zhang, S et al., 2017)	Underground soil	Water heating	Complex (buried collectors)
Ground to ground (S.J. Self et al, 2013)	Underground soil	Underfloor heating directly	Technical (soil/building study)
Inverter (variable capacity) (Umer Khalid, A. 2012)	Depends on system type	Adaptive heating/cooling	Medium (advanced technology)

Choosing the right heat pump depends on several factors such as your local climate, available space, budget, and whether domestic hot water is needed. While air-source pumps are easier to install, ground or water-based systems offer superior performance in colder regions and higher energy savings in the long term.

6.3.4. Advantages of the Heat Pump (Itho Daalderop, 2024)

- Combined heating and cooling: year-round comfort temperature

- Domestic hot water for the whole family
- Low energy consumption: around 75% less than a traditional boiler
- Carbon neutral thanks to green energy
- Subsidies and renovation incentives available
- Positive impact on the Energy Performance Level (E-level) in new buildings

6.3.5. Disadvantages

- High initial investment costs.
- Performance depends on outdoor temperatures, especially for air-source systems (CSTB, 2022).
- Requires good building insulation to operate efficiently.

6.3.6. Literature Review on Heat Pumps

Sârbu, I. et al (2010) discussed the efficiency of heat pumps as a viable heating and cooling solution in buildings, particularly emphasizing their economic and environmental advantages compared to conventional gas or oil systems. They presented a case study analyzing the heating of a 240 m² residential building using a water-to-water heat pump system sourced from underground water. The study evaluated both the existing building envelope and a thermally rehabilitated version, showing a significant reduction in heating demand after insulation. The authors concluded that, although the initial investment in a heat pump system is higher, the operational cost savings make it economically favorable in the long term.

Rosti et al (2020) investigated optimal insulation thickness in Iran, finding that it ranged from 0 to 4 cm across different climate zones and materials such as classic gray brick, hollow clay block, LECA block, and AAC block. Their study highlighted variations in energy-saving metrics and payback periods among countries.

Zhuang et al. (2023) conducted a comprehensive study on the application of a sewage-source heat pump system for heating and cooling a 28,000 m² office building in Qingdao, China. The system employed a specially designed sewage heat exchanger to address fouling and corrosion challenges. Based on one year of operational data, the average sewage temperature was 13.5 °C in

winter and 22 °C in summer, with corresponding system COPs of 2.96 and 3.25. The system's energy consumption was significantly lower than that of conventional systems, consuming only 50.81% of the energy used by a coal-fired boiler in winter and 61.56% of the energy consumed by an air-source heat pump in summer. Despite its promising energy-saving and environmental benefits, the study noted issues such as scaling and reduced heat transfer performance over time, suggesting the need for improved sewage heat exchange and online descaling technologies.

Zhang et al (2017) carried out a field investigation of a direct sewage-source heat pump system implemented in a hotel in Changchun City. Their study analyzed the relationships between cooling capacity, COP, and sewage temperature, while also highlighting the system's economic and energy-saving advantages.

In summary, while previous studies have demonstrated the effectiveness of heat pumps and thermal insulation separately in improving building energy efficiency, there remains a noticeable research gap concerning their combined application. The existing literature lacks comprehensive evaluations of how these two technologies interact to enhance overall performance. Therefore, this study addresses that gap by investigating the synergistic impact of integrating a heat pump system with thermal insulation, aiming to offer a more complete and effective solution for optimizing energy use in buildings, especially in regions with high heating and cooling requirements.

7. Conclusion

In conclusion, the residential building sector in Algeria represents both a challenge and an opportunity in the pursuit of energy efficiency and sustainable development. The country's diverse climate zones, from Mediterranean coastal cities to arid Saharan regions, significantly impact energy consumption patterns, necessitating tailored strategies rather than uniform national policies. As this chapter has illustrated, improving energy efficiency involves more than just technical upgrades it requires a deep understanding of regional climatic conditions, building characteristics, and occupant behavior.

Dynamic simulation tools and geographic modeling techniques have emerged as effective means to evaluate energy performance and predict future consumption trends. Studies employing bottom-up approaches underscore the urgency of targeted interventions, especially in high-consumption zones. In parallel, ensuring thermal comfort remains essential to occupant well-being and energy-conscious design. By harmonizing environmental factors, user habits, and building technologies, Algeria can reduce its energy footprint while enhancing indoor living conditions.

The insights presented in this chapter provide a foundational framework for policymakers, architects, and engineers to promote a resilient, energy-efficient built environment in Algeria.

CHAPTER II

Methodology, Modeling and Simulation

1. Introduction

The southern regions of Algeria are among the most affected by harsh climatic conditions, characterized by high temperatures in summer and significant cold in winter. This climatic variability increases the need for effective solutions to ensure thermal comfort inside buildings while reducing energy consumption. In this context, the topic of thermal insulation and the use of renewable energy systems, such as heat pumps, is of great importance, as it forms a fundamental pillar for achieving sustainable development in the building sector. Several studies have shown that integrating high-performance insulation materials can reduce energy consumption by more than 30% in buildings located in hot climates (Benouaz & Belhamel, 2002). Additionally, other research has demonstrated the effectiveness of heat pump systems, especially air-to-air types, in reducing energy demand and maintaining stable thermal comfort throughout the year (Chaturvedi, Henderson, & Douglas, 1998). This chapter aims to study the impact of integrating thermal insulation materials in residential buildings in selected southern Algerian regions, analyzing the effectiveness of this integration in reducing cooling and heating energy demands based on climatic indicators such as Cooling Degree Days (CDD) and Heating Degree Days (HDD). Furthermore, it examines the feasibility of integrating a heat pump system as a renewable energy solution, along with performing financial and environmental analyses to compare various proposed scenarios. Through this study, the focus will be on selecting suitable insulation materials, developing a simulation model using TRNSYS software, and analyzing the energy, economic, and environmental performance results of the proposed solutions. This will contribute to formulating practical recommendations to improve energy efficiency in residential buildings in southern Algeria.

2. Research methodology

An analytical methodology based on numerical simulation was adopted to enhance the thermal performance of the building by integrating passive design strategies, such as thermal insulation, with high-efficiency active systems, such as heat pumps. In the initial phase, essential data related to the building's geometry, construction materials, usage patterns, and climatic conditions for each region were collected. A detailed 3D model of the building was developed using SketchUp, where all structural components walls, roofs, and floors were assigned to separate layers to allow for precise material manipulation. Two insulation materials, extruded polystyrene and glass wool, were introduced into the building envelope, and their thicknesses were varied to determine the optimal value for each climatic zone, with the goal of minimizing heat loss and

enhancing energy efficiency. An economic study was conducted to assess the cost-effectiveness of each insulation type, complemented by an environmental assessment to evaluate the carbon footprint associated with each option. After reducing the thermal load, a heat pump system was integrated as an active HVAC solution due to its high efficiency and energy-saving potential. The TRNSYS software, through the TRNBuild interface, was used to define thermal zones and simulate building performance. Key performance indicators such as energy consumption, heating and cooling loads, and indoor thermal comfort levels were analyzed, enabling a comprehensive evaluation of the effectiveness of each intervention and a comparison between the proposed configurations.

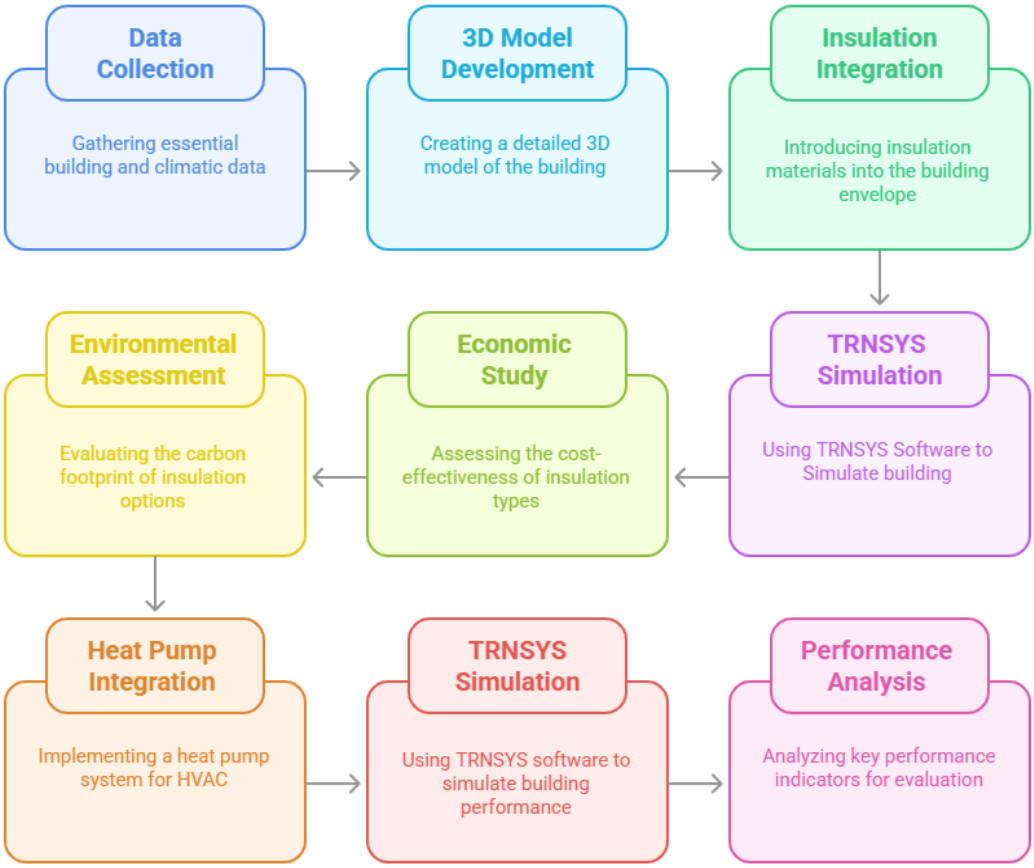

Figure II.1: Applied methodology diagram.

3. Selection of southern Algerian regions

Based on the Document of Thermal Regulation in Buildings (DTR, 2010), which divides Algeria into five climatic zones according to heating and cooling needs, and the classification proposed by Ghedamssi et al. (2015), which identifies seven climatic zones using GIS techniques

based on annual energy cost for thermal comfort, the southern Algerian wilayas were selected as representative of the most extreme climatic conditions. These areas, particularly those falling within Zone 7, account for the highest share of energy consumption due to elevated temperatures and significant cooling demands. Therefore, they offer a relevant context for assessing the effectiveness of thermal insulation and the integration of renewable energy technologies such as heat pumps to enhance energy efficiency and ensure sustainable indoor thermal comfort.

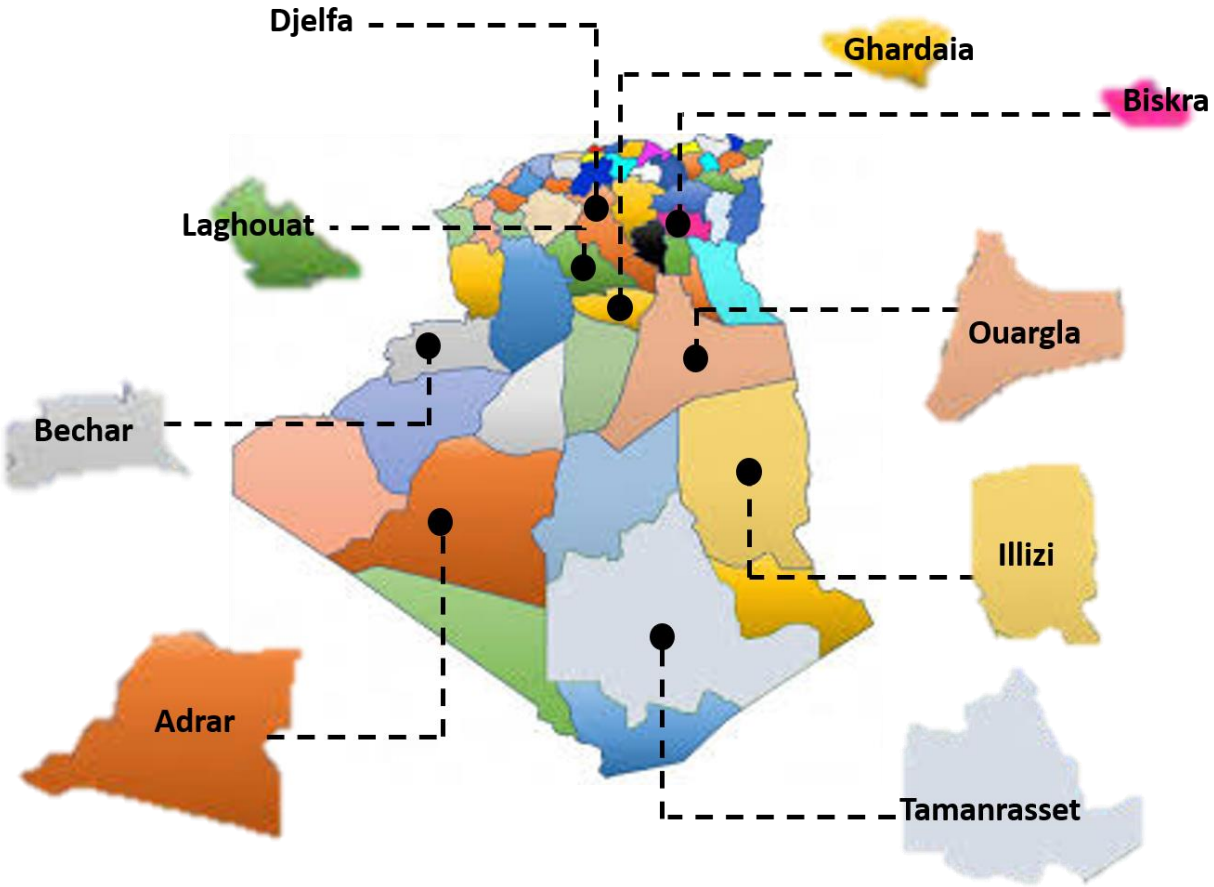

Figure II.2: Geographic distribution of the selected southern Algerian wilayas with arid and semi-arid climates.

3.1. Adrar

The wilaya of Adrar is located 1,300 km southwest of Algiers, on the western edge of the Tademaït plateau. It has a continental desert climate, characterized by high solar radiation (7–8 hours/day in winter and 10–11 hours/day in summer), extremely high temperatures in summer and low temperatures in winter, with very low annual rainfall not exceeding 550 mm. Rainfall is rare, sudden, and largely ineffective due to rapid evaporation, which negatively affects traditional brick

constructions. The region's climate was analyzed based on 21 years of meteorological data from the Adrar Airport weather station.

The wilaya of Adrar experiences significant temperature variations throughout the year. During the summer months (June to August), temperatures can exceed 45 °C, while in winter (December and January), they may drop to 0 °C. The region is known for its high average temperatures, which directly affect energy availability and the biological growth cycle of vegetation, often measured using degree-days. According to the table, July is the hottest month, with temperatures rising above 46 °C, while January is the coldest, with minimum temperatures around 5 °C. This intense heat, coupled with very low annual rainfall (about 23 mm), extremely high evapotranspiration (2751 mm/year), and prolonged sunshine (averaging over 10 hours/day in summer), reinforces the region's hyper-arid climate and imposes substantial challenges for energy efficiency and sustainable building design.

3.2. Béchar

The wilaya of Béchar is characterized by an arid desert climate with significant temperature fluctuations. The hottest month is July, with average temperatures exceeding 35 °C, while January is the coldest, with averages around 9.75 °C. Wind speeds peak in April (5 m/s), enhancing evaporation, and drop to their lowest in December (2.48 m/s). Relative humidity is lowest in July (16.86%) and highest in December (55.16%). Atmospheric pressure varies slightly, with the lowest recorded in April (92.14 kPa) and the highest in January (92.89 kPa). The region receives intense solar radiation, especially in summer, with values exceeding 7.5 kWh/m²/day in June.

3.3. Biskra

The wilaya of Biskra is marked by a hot arid climate with sharp seasonal contrasts. The hottest month is August, with average temperatures reaching 40.86 °C, while January is the coldest, with a minimum of 8.25 °C and a maximum of 17.45 °C. Rainfall is very low and irregular, with a peak of only 21.27 mm in April and a minimum of 0.95 mm in July, reflecting a highly variable and drought-prone environment. Relative humidity ranges from 24.92% in July to 52.22% in December, influenced by high temperatures and large thermal amplitudes. Wind speeds peak in June (14.75 km/h) and are lowest in November (10.8 km/h). These climatic extremes pose serious challenges for water management, agriculture, and sustainable building design in the region.

3.4. Djelfa

Djelfa Wilaya has a predominantly semi-arid to arid climate with a continental influence. The northern and central parts experience semi-arid conditions, while the southern area is more arid. Due to higher elevations in the central region, annual rainfall there averages between 250 and 300 mm, decreasing to about 250 mm in the north and around 150 mm or less in the south. Rainfall is irregular and often occurs as storms, which intensify soil erosion. The wet season lasts from September to May, peaking in January with about 31 mm of rain, while the summer months (June to August) are dry.

Temperatures range from winter lows around 1–2°C in December and January to summer highs reaching up to 35.6°C in July. The hot season spans approximately four months in the north and center and extends to five months in the south.

3.5. Ghardaïa

Ghardaïa has a desert climate characterized by dry air and strong temperature variations. The average monthly temperatures range from 11.3°C in January to 34.9°C in August, with minimum temperatures between 4.9°C (January) and 27.6°C (July). Annual rainfall is very low, about 22.86 mm, with the highest monthly precipitation of 9.4 mm in April. Winter winds come from the northwest and are cold and humid, while summer winds from the northeast are strong and hot. Sandstorms from the southeast occur approximately 20 days per year, mainly in March, April, and May. Relative humidity ranges from about 18.8% in July to 57.8% in December.

3.6. Illizi

Illizi, located in the extreme southeast of Algeria, is characterized by a hot and arid Saharan climate. Annual temperature variations are significant, with minimum temperatures dropping to around 6°C in January and maximum values reaching approximately 43°C in July (The Weather Channel, 2025). The region receives extremely low rainfall, with an annual average of only 1.89 mm, making it one of the driest areas in the country (Weather and climate). Relative humidity remains low throughout the year, averaging about 35%. Predominant winds blow from the northeast and southeast, with speeds typically ranging from 15 to 30 km/h, further increasing evaporation and aridity (The Weather Channel, 2025). According to Emberger's bioclimatic classification, Illizi falls within the Saharan bioclimatic stage, characterized by extremely hot

summers and mild winters. These severe climate conditions influence local biodiversity and limit human settlement and agriculture.

3.7. Laghouat

Laghouat lies between two climatic zones: the Mediterranean in the north and the desert in the south (Gaussen, H. ,1957). The average annual temperature is 17.4°C, with January being the coldest month (8.73°C) and July the hottest (32.20°C). The annual precipitation averages 155.27 mm, with the wettest month being September (27.53 mm) and the driest month June (7.45 mm). Temperature and rainfall data cover the period from 2008 to 2017 (ONM,2018). The Gaussen ombrothermic diagram shows a clear dry period during most of the year. Climate significantly impacts local biodiversity and water availability. Rainfall is influenced by altitude, exposure, and orientation (Gaussen, H. ,1957). Overall, Laghouat experiences hot dry summers and cold dry winters.

3.8. Ouargla

The climate of Ouargla is classified as hot desert (Saharan type), marked by extremely hot and long summers and short, mild winters. The annual average temperature is 23.9°C, with peaks reaching 38.9°C in July and the lowest around 12.7°C in December. The relative humidity averages 36.2%, peaking at 52.5% in December and dropping to 15.5% in July. Annual evaporation is extremely high, totaling 2890.4 mm, with a maximum of 566.6 mm in July. Rainfall is scarce and irregular, averaging only 24.8 mm/year, with September being the wettest month (11 mm). The ombrothermic diagram confirms that the dry season lasts the entire year, indicating a persistent aridity. The sunshine duration is high, with an annual average of 264.8 hours/month, peaking at 321.2 hours in August. Winds are most frequent and intense between March and September, with a maximum speed of 13.1 km/h in March. This extreme climate poses significant challenges to biological and agricultural activities in the region (Bechahe, K., 2021).

3.9. Tamanrasset

Tamanrasset is characterized by a typical Saharan desert climate—hot, dry, and extremely arid. Summers are very long and intense, with daytime temperatures reaching up to 45 °C, while winters are short and mild, with nighttime lows occasionally below 5 °C. The region receives very little rainfall, averaging less than 60 mm per year, confirming its hyper-arid classification. Relative

humidity is generally low, which accelerates evaporation, while intense solar radiation exceeds 300 hours per month, particularly in summer. Hot, dry winds laden with dust are frequent, further impacting thermal comfort. Traditional dwellings, built using local materials like mud, stone, and palm fibers, demonstrate effective passive cooling, creating favorable indoor microclimates. These characteristics make thermal insulation and sustainable design crucial for improving energy performance in buildings (Hamdi K., 2016).

4. Typical construction

The choice of the housing model for thermal simulations (Figure 5) was based on prior research conducted by Semahi et al. (2020), Mokhtara et al. (2019a), Mokhtara et al. (2020), and Kadraoui et al. (2019). These studies focused on the energy demand and thermal performance of residential buildings under Algerian climatic conditions. In particular, the study by Mokhtara et al. (2020) guided the selection of a representative building configuration. The adopted model corresponds to the standard "F2" residential unit as defined by Algerian construction norms. This typical housing unit comprises a bedroom, living room, hallway, bathroom, and kitchen, with a total floor area of 80 m^2 and a ceiling height of 3 meters. Figure (II.3) illustrates a 3D representation of the selected model.

Figure II.3: 3D model of the reference building before insulation

Residential buildings in Algeria typically rely on multi-layered construction systems to enhance thermal insulation and improve the building's energy efficiency. As shown in Figure (II.4), the standard composition of the exterior wall includes four layers arranged from the outside to the inside: a cement render, a brick layer, an air gap for insulation, and finally an interior plaster finish. This combination offers a balance between thermal performance and structural durability.

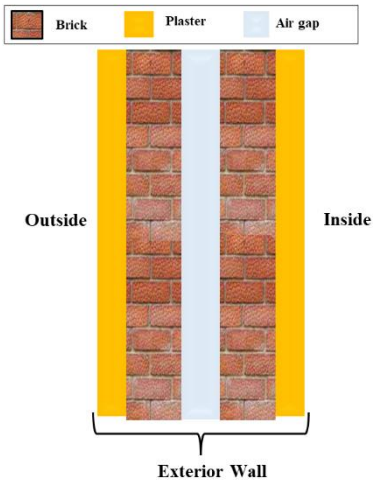

Figure II.4: Layered composition of an exterior wall.

The interior walls (Figure II.5) follow a similar multi-layered approach but are adapted to suit interior space requirements. Each interior wall typically consists of an initial plaster layer, a brick core, and a second plaster finish on the opposite side. This configuration ensures both acoustic insulation and interior comfort.

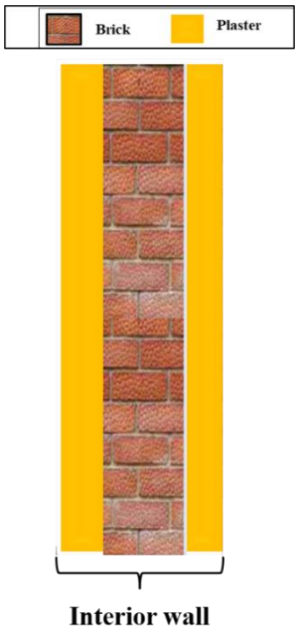

Figure II.5: Layered composition of an interior wall.

To assess the thermal performance of the different components of the building envelope, the physical properties of the materials used in the walls, roof, and floor were compiled. The roof

structure comprises several layers: a mortar layer, a layer of heavy-weight concrete, Hourdis hollow blocks, and an internal plaster ceiling finish. The floor (ground slab) is constructed using a concrete base layer (béton), covered with a mortar screed, and finished with ceramic tiling. These elements work together to ensure thermal stability and structural strength. The relevant physical properties such as specific heat capacity, thermal conductivity, and density are summarized in Table (II.1).

Table II.1: Thermo-physical properties of building materials (Khenfer, A., Chacha, A. 2018.).

	Materials	**Conductivity (kJ/h.m. K)**	**Specific heat (Kj/kg.K)**	**Density (kg/m^3)**	**Thickness e (m)**
Exterior wall	Cement_Mor	5.04	1	2000	0.01
	Brick	1.697	0.794	720	0.1
	Air_space	0.216	1.227	100	0.01
	Brick	1.697	0.794	720	0.1
	Cement_Mor	5.04	1	2000	0.01
Interior wall	Plaster	1.264	1	1500	0.01
	Brick	1.697	0.794	720	0.1
	Plaster	1.264	1	1500	0.01
Roof	Bitumenroo	0.61	1	1200	0.01
	Cement mor	5.04	1	2000	0.01
	Bton lourd	6.318	0.92	2300	0.2
	Cement_mor	5.04	1	2000	0.01
Ground floor	Enduit ext	4.152	1	1700	0.1
	Poly ext	0.105	1.18	35	0.04
	Enduit ext	4.152	1	1700	0.1
	Ceramics	4.32	1	2000	0.02

5. Thermal insulation

5.1. Selected Insulation Materials

The thermal insulation materials are selected to evaluate their impact on energy consumption in buildings. These materials are Glass Wool, and Extruded Polystyrene (XPS). The insulation materials are chosen based on several important criteria.

Firstly, these materials offer a good balance between availability and cost, making them suitable for most projects. Secondly, they have effective thermal performance due to their low thermal conductivity, which helps reduce energy consumption by maintaining indoor temperatures.

Thirdly, these materials provide physical properties such as lightweight and flexibility in installation, facilitating their use in various types of buildings. Fourthly, some of these materials, such as Glass Wool, are more environmentally friendly due to their recyclability. Lastly, they possess high durability and strength, making them suitable for diverse conditions and strict insulation requirements (Saif, N. et al, 2024). The main physical characteristics of the selected insulation materials are summarized in Table (II.2).

Table II.2: Characteristics of selected insulation materials (Daouas N., 2011).

	Conductivity λ (kJ/h.m.K)	**Specific heat Cp (J/kg.K)**	**Density ρ (kg/m^3)**
Extruded polystyrene	0.11	1.18	35
Glass wool	0.15	0.84	12

5.2. Integration of insulation in the model

This study focuses on the external wall structure in the calculations for selected insulation materials across all regions in Algeria. The wall structure involves multiple layers, including an insulation layer situated between the bricklayer and an air space (Figure II.6) (Saif, N. et al, 2024).

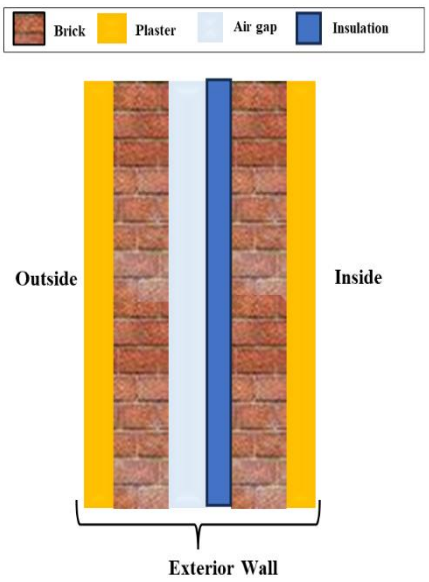

Figure II.6: Exterior wall with insulation.

5.3. Cooling and heating degree-days (CDD and HDD)

The construction of the zones was carried out according to the criteria of the number of winter degree days and the number of summer degree days. The degree-days method is one way to calculate how much energy a building will use for heating and cooling. The approach assumes that the energy needs for a building are proportional to the difference between the average outdoor air temperature and the base temperature measured, a reference temperature that expresses the domestic heating or air conditioning needs. The total number of annual heating and cooling degree-days (HDD and CDD) is calculated by (Ozel 2019; Mourshed 2012)

$$\mathrm{HDD} = \sum_{i=1}^{365} |T_m - T_b| \qquad (II.1)$$

$$\mathrm{CCD} = \sum_{i=1}^{365} |T_b - T_m| \qquad (II.2)$$

HDD: Heating degree day.

CDD: air conditioning degree-days.

T_m: Mean temperature for the day (typically in °C).

T_b: Base temperature for heating (typically 18 °C) and base temperature for cooling (typically 26 °C) (Omer 2012; Monjur Mourshed 2012).

The result of HDD and CDD is typically in degree days (°C-day or °F-day), which quantifies the number of degrees by which the average daily temperature falls below the base temperature over a period. The notion of degree days makes it possible to assess the severity of the heating and air conditioning season. It is therefore possible to compare the heat needs of different buildings or the same building at various times, avoiding variations related to place and time, and consequently variations in weather. This method makes it possible to measure the air conditioning needs during the hot summer months against a reference temperature of Tb. The degree-days method, heating and cooling transmission loads per unit area are expressed as follows:

$$Q_{heating} = 86400 \times \mathrm{HDD} \times U \qquad (II.3)$$

$$Q_{cooling} = 86400 \times \mathrm{CDD} \times U \qquad (II.4)$$

where U is the overall heat transfer coefficient for a typical wall.

Annual fuel consumption can be calculated by dividing the annual heat loss by the efficiency η_s and$LHV_{gaz}$of the heating system, and by dividing the annual heat loss COP by the cooling system (M. Ozel 2011).

$$E_{heeting} = \frac{Q_{heating}}{\eta_s LHV_{gaz}} \quad (II.5)$$

where:

$E_{heeting}$: annual heating requirement (kWh/m^2),

$Q_{heating}$: Heating transmission load (kWh).

Similarly, for cooling, it is given by:

$$E_{cooling} = \frac{Q_{cooling}}{COP} \quad (II.6)$$

where:

$E_{Cooling}$: Annual cooling requirement (kWh/m^2).

Table II.3: The parameters used in calculations.

Variable	Description	Value	Source
η_s	Efficiency of the heating system	0.93	(N. Daouas 2011)
LHV_{gaz}	Lower heating value of natural gas	42 MJ/m^3	(Alsayeda M. F., et al. 2019)
COP	Cooling system's coefficient of performance	3	(Alsayeda M. F., et al. 2019)

5.4. Cost and financial analysis methods

The annual gas cost per unit area is expressed as follow:

$$C_{heating} = E_{heaiting}\, C_g \quad (II.7)$$

The annual electricity cost per unit area is expressed as follow:

$$C_{cooling} = E_{cooling} C_{el} \quad \text{(II. 8)}$$

where $\boldsymbol{C_g}$ is the cost of natural gas in \$/kWh and $\boldsymbol{C_{el}}$ the cost of electricity in \$/kWh.

The total cost mainly depends on the cost of insulation material, energy cost, annual heating and cooling costs, efficiency of the heating system, cooling equipment's coefficient of performance, building lifespan, inflation rate, and interest rates.

The total cost is the sum of the insulation material cost and the present value of the energy consumption cost over the building's lifetime. The total cost per unit wall area is given by:

$$TC = PWF \times C_{enr} + C_i e_i = RC + IC \quad \text{(II. 9)}$$

where C_{enr} is the cost of energy consumption (\$/m^2), PWF is Present Worth Factor, C_i is the insulation cost the per unit of area (\$/m^2) and is$e_i$the thickness of insulation (m). The Present Worth Factor (PWF) defined as:

Where:

$$PWF = \frac{(1+r)r^N - 1}{r(1+r)^N}, \begin{cases} i > g, r = \dfrac{i-g}{i+g} \\ i < g, r = \dfrac{g-1}{g+1} \end{cases} \quad \text{(II. 10)}$$

$$PWF = \frac{N}{1+i}, i = g \quad \text{(II. 11)}$$

Where $\boldsymbol{N}$ is building lifetime, $\boldsymbol{i}$ is the interest rate, $\boldsymbol{g}$ is the inflation rate and $\boldsymbol{r}$ is the discount rate.

Table II.4: Average isolation and energy prices in Algeria.

Variable	Description	Value
C_{i1} (Assly, 2025).	Cost of extruded polystyrene	80.6 \$/m^3
C_{i2}(Alger Froid,2023)	Cost of glass wool	51.85 \$/m^3
Cg (Mesaoudi L et al, 2023)	Cost of natural gas	0.028 \$/kWh
Cel (Eurostat. 2024)	Cost of electricity	0.3 \$/kWh
N	Lifetime of the building	10 years

The cost of energy and building lifetime are given in Table (II.4).

5.5. Environmental indicators

The annual C_{O2} emissions per unit area of building exterior walls can be derived using the following equations (Dobayci 2007; Yuan et al 2017)

$$m = \frac{(E_{heating+}E_{cooling})}{M} \quad \text{(II. 12)}$$

For natural gas:

$$m_{CO2} = 1{,}05 \times m \times M_{CO2} \quad \text{(II. 13)}$$

For electricity:

$$m_{CO2} = \frac{a \times Q_{cooling}}{cop} \quad \text{(II. 14)}$$

The variables in these equations are defined as follows:

m: The mol number, measured in (kmol/m^2. Year).

M: The molar mass of fuel, which is 17.5 (kg/kmol) for natural gas.

5.6. Initial comparison of scenarios

The effects of thermal insulation and the installation of a renewable energy system on the thermal loads associated with heating and cooling in a desert-climate residential building were compared in this study. Due to substantial heat gain in the summer and substantial heat loss in the winter, the first case a design devoid of thermal insulation reported high energy consumption, placing a major thermal burden on traditional heating and cooling systems.

In the second instance, thermal insulation materials with exceptional thermal resistance, such polystyrene and glass wool, were installed on the walls. This update greatly increased indoor thermal comfort while reducing energy use by up to 60% for heating and 40% for cooling, depending on usage patterns and seasonal conditions.

In the third instance, no additional wall insulation was added; instead, a heat pump system was utilized to provide both heating and cooling. When compared to conventional systems, the system's high efficiency helped to reduce electricity use, particularly for heating requirements. However, the system had to run for longer periods of time due to continuous thermal losses caused by the lack of insulation, especially during severe weather. This example shows how effective heat

pumps are as an energy-efficient option, but they are still not as good as combining them with appropriate thermal insulation.

Table II.5: Description of the different comparison scenarios

Scenario	Description	Remarks
Without Insulation	Building without any thermal insulation	Significant energy losses due to poor thermal resistance; high heating/cooling demand.
With Insulation (Glass Wool or Polystyrene)	Building insulated with glass wool or polystyrene	Energy consumption drops considerably due to improved thermal performance of walls and roofs.
With Insulation + Heat Pump	Insulated building using a high-efficiency heat pump system	Combined effect of insulation and efficient heat pump results in optimal energy performance.

6. Integration of a heat pump system as a renewable energy source

6.1. Heat pump description

The heat pump, commonly called PAC, recovers the heat contained in the air, earth or water to transfer it inside a building to be heated or, sometimes, to pro produce domestic hot water (DHW). The reversible heat pump, in addition to the heat in winter, also produces cold in the summer (Bhatia, A., 2024).

There are different types of PAC classified according to the cap and the heat diffusion system. Some may be reversible, i.e. operate in reverse for

making cold in the summer (air conditioning). We distinguish:

6.1.1. Air-to-air heat pump model – Type 119

6.1.1.1. Description of heat pump Type 119

Type 119 is a model used to simulate the performance of air-to-air heat pumps based on manufacturer catalog data. It allows for the inclusion of air mixing effects on the indoor side of the evaporator, enhancing the accuracy of simulations in systems that combine outdoor fresh air with return air. This type supports three auxiliary heating options: no auxiliary heating, electric resistance heating (one or two stages), or gas heating.

6.1.1.2. Data specifications

The number of data points in the input files must exactly match the number defined in the model's parameters. Any mismatch may lead to simulation errors or inaccurate results.

It is assumed that the electric consumption data includes the power used by both the compressor and the fans. However, the model separates compressor and fan power consumption in the output results. If a separate fan component (another TRNSYS Type) is used in the system model, the input data should only reflect the compressor power consumption, excluding the fan power.

6.1.1.3. Operating mechanism

The heat pump operates based on a vapor compression refrigeration cycle and can be reversed to provide either heating or cooling. Being an "air-source" heat pump, air flows over both the evaporator and condenser heat exchangers. The system may be a compact unit or a split configuration with the condenser located remotely.

The model uses manufacturer catalog data to simulate heating and cooling performance, making it suitable for representing various commercial and residential heat pump systems. On the indoor side, two air streams (return air and outdoor air) are mixed using a damper controlled by a signal input.

6.1.1.4. Air mixing algorithm

Type 119 first determines the properties of the mixed air using psychrometric functions from the TRNSYS utility library. The enthalpy and humidity ratio of the mixed air are computed using the following equations:

$$h_{air,Fanln} = \gamma_{damper}\, h_{air,primary} + (1-\gamma_{damper}) h_{air,secondary} \quad \text{(II.15)}$$

$$\omega_{air,Fanln} = \gamma_{damper}\, \omega_{air,primary} + (1-\gamma_{damper}) \omega_{air,secondary} \quad \text{(II. 16)}$$

It is assumed that the mixing occurs at the pressure of the primary air stream (typically the return air), and pressure equilibrium is maintained across the damper between the two streams.

6.1.1.5. Saturation adjustment and enthalpy correction

If the calculated relative humidity of the mixed air exceeds the saturation level at the given temperature, the model adjusts the humidity ratio to the saturation value and issues a warning in the TRNSYS output file.

If condensation is expected due to this adjustment, the enthalpy is recalculated considering the latent heat of condensation:

$$h_{air,Fanln} = \gamma_{damper}\, h_{air,priary} + (1-\gamma_{damper}) h_{air,secondary} - h_{cond} \frac{\dot{m}_{cond}}{\dot{m}_{air}} \qquad \text{(II. 17)}$$

The mixed air state is considered *converged* when the difference between the calculated enthalpy and the enthalpy obtained from the psychrometric function falls within a defined tolerance.

6.1.1.6. Mode Determination

Once the mixed air state is determined, the model evaluates the operating mode of the heat pump. It may function in :

- Cooling mode
- Heating mode
- Fan-only operation (no active heating or cooling)

The performance data from the catalog is then used to determine the heat pump's operation under the detected mode.

6.1.1.7. Schematic Diagram of Type 119

Figure (II.7) illustrates the configuration of the heat pump system, highlighting key components such as the outdoor and indoor coils (evaporator and condenser), the air stream inputs with mixing occurring at the damper, auxiliary heating elements which can be electric or gas-based, and the damper control mechanism responsible for regulating air mixing.

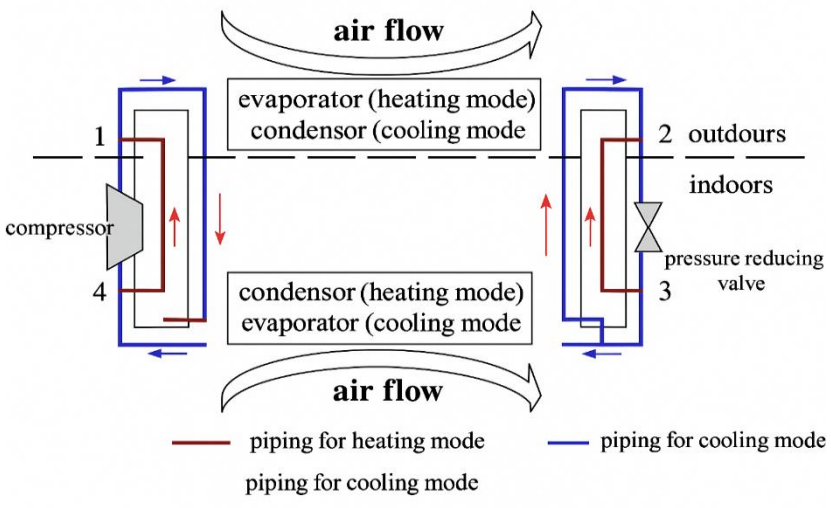

Figure II.7: Air Source Heat Pump Schematic (TRNSYS 18., 2015).

6.1.2. Operation of a Heat Pump in Cooling Mode:

The heat pump in cooling mode operates as a conventional air-conditioner with the indoor coil as an evaporator and the outdoor coil as a condenser. The refrigerant (upon leaving the compressor via the red line in the figure below) first flows through the reversing valve where it is directed to the outdoor coil. Since the refrigerant always flows to the condenser first after leaving the compressor, the outdoor coil is acting as the condenser. In this mode of operation, the heat from the refrigerant is rejected to the outside air. From the outdoor coil, the refrigerant flows through the expansion device and then to the indoor coil, where the refrigerant picks up or absorbs heat from the air in the area being cooled. The refrigerant then flows back to the compressor via the reversing valve and the cycle repeats itself (Bhatia, A., 2024).

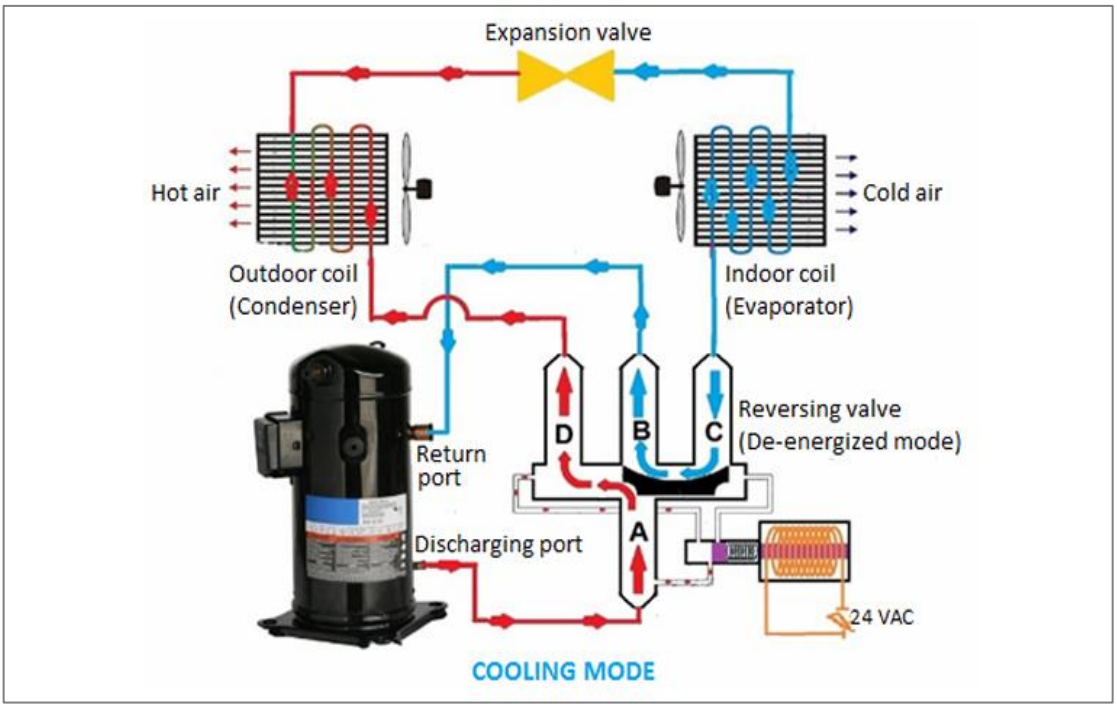

Figure II.8: Operating principle of the heat pump for cooling (Bhatia, A., 2024).

The model queries TRNSYS's Interpolate Data subroutine to obtain cooling performance data for the current conditions. The software verifies the consistency of catalog data; for example, if the sensible cooling load exceeds the total cooling load, the total value is increased accordingly, a standard practice in industry (TRNSYS 18., 2015).

The enthalpy of the air exiting the evaporator is calculated as:

$$h_{air,Evapout} = h_{air,EvapIn} - \frac{\dot{Q}_{tot,cool}}{\dot{m}_{air}} \qquad \text{(II. 18)}$$

Next, psychrometric functions calculate other air properties, including the effect of indoor fan pressure rise. The total cooling capacity is recalculated from the enthalpy difference of the air entering and leaving the evaporator.

The sensible cooling capacity is given by:

$$\dot{Q}_{sens,cool} = \dot{m}_{air} Cp_{air} \left(T_{Evap,in} - T_{Evap,out}\right) \quad \text{(II. 19)}$$

Latent cooling capacity is then derived as the difference between the total and sensible cooling values. To calculate the compressor power P_{comp} , the rated power of the indoor and outdoor fans (provided as parameters) is subtracted from the total power reported in the data file. This compressor power is used to determine the heat rejection energy as follows:

$$\dot{Q}_{rejection} = \dot{Q}_{tot,cool} + \dot{P}_{comp} \quad \text{(II. 20)}$$

Finally, the coefficient of performance (COP) in cooling mode is defined by:

$$COP = \frac{\dot{Q}_{tot,cool}}{\dot{P}_{comp} + \dot{P}_{fan,Outdoor} + \dot{P}_{fan,Indoor}} \quad \text{(II. 21)}$$

This formulation accounts for the total cooling capacity relative to the combined electrical power consumption of the compressor and fans.

6.1.3. Operation of a Heat Pump in Heating Mode:

In heating mode, the refrigerant leaves the compressor (shown by the red line in the figure) and passes through the reversing valve, directing it first to the indoor coil. Since the refrigerant always flows to the condenser immediately after the compressor, the indoor coil acts as the condenser in this mode. Heat is then rejected to the indoor air space. From the indoor coil, the refrigerant flows through the expansion device to the outdoor coil, where it absorbs heat from the outside air. The refrigerant returns to the compressor via the reversing valve, completing the cycle (Bhatia, A., 2024).

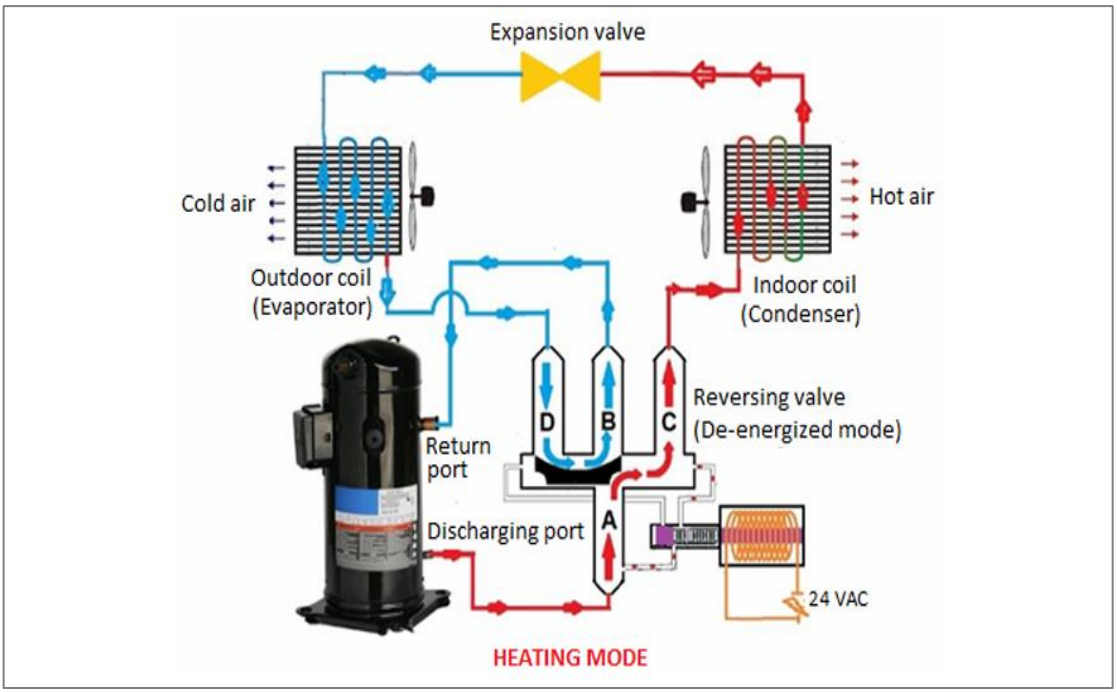

Figure II.9: Operating principle of the heat pump for heating (Bhatia, A., 2024).

Heating performance data specifications closely resemble those for cooling. The heating data file must include two values: total heating capacity and power consumption. Power consumption should cover both compressor and indoor/outdoor fan power. Type 119 performs linear interpolation between heating performance data points based on the current indoor air flow rate (l/s), indoor dry bulb temperature (°C), and outdoor dry bulb temperature (°C). The model does not extrapolate beyond the data range; if inputs fall outside this range, the closest maximum or minimum values are used, and warnings are recorded in the TRNSYS log files (TRNSYS 18., 2015).

The relevant air flow rate is the indoor coil air flow, as the heating performance is assumed independent of outdoor coil air flow rate.

The air state leaving the condenser is calculated based on enthalpy, accounting for the fan-induced pressure rise:

$$h_{air,condenserOut} = h_{air,condenserIn} + \frac{\dot{Q}_{tot,cool}}{\dot{m}_{air}} \qquad \text{(II. 22)}$$

Psychrometric routines finalize the air state, possibly adjusting the enthalpy. Heating power is recalculated as the product of air mass flow and the enthalpy difference between inlet and outlet air.

The energy absorbed by the indoor air stream and the heat pump's coefficient of performance (COP) are given by:

$$\dot{Q}_{absorption} = \dot{Q}_{tot,heat} - \dot{P}_{comp} \quad \text{(II. 23)}$$

$$COP = \frac{\dot{Q}_{tot,heat}}{\dot{P}_{comp} + \dot{P}_{fan,Outdoor} + \dot{P}_{fan,Indoor}} \quad \text{(II. 24)}$$

7. System Modeling in TRNSYS:

This Table presents the key TRNSYS components used to model the system. Each component performs a specific function that contributes to building an integrated simulation model reflecting the thermal and operational behavior of the system. The following table lists these components, their types, and a brief description of their roles in the simulation.

Table II.6: TRNSYS components used for system representation.

Types	Component name	Logo	Description
56	Multi-Zone Building		This component models the thermal behavior of a building having multiple thermal zones.
119	Heat Pump		Type119 models an air source heat pump with air mixing and damper control, supporting no, electric, or gas auxiliary heating.
15	weather data file		This component reads and interpolates weather data, providing radiation, mains water temperature, sky temperature, and seasonal forcing functions.
166	Simple Room Thermostat		A simple room thermostat is modeled to output on/off control functions that can be used to control a system having a heating source and a cooling source.
65	Online graphical plotter		The online graphics component displays variables live during simulation without creating output files.

14	Time Dependent Forcing Function		Type14 generates time-dependent forcing functions with repeating patterns based on discrete data points and linear interpolation. The cycle repeats every N hours, with values given in dimensionless units for general use.
41	Load Profile Sequencer - Unique Days of the Week		This component organizes daily profiles from Type14 into a full-year schedule, supporting up to 20 schedules per day and allowing one forcing function per weekday.

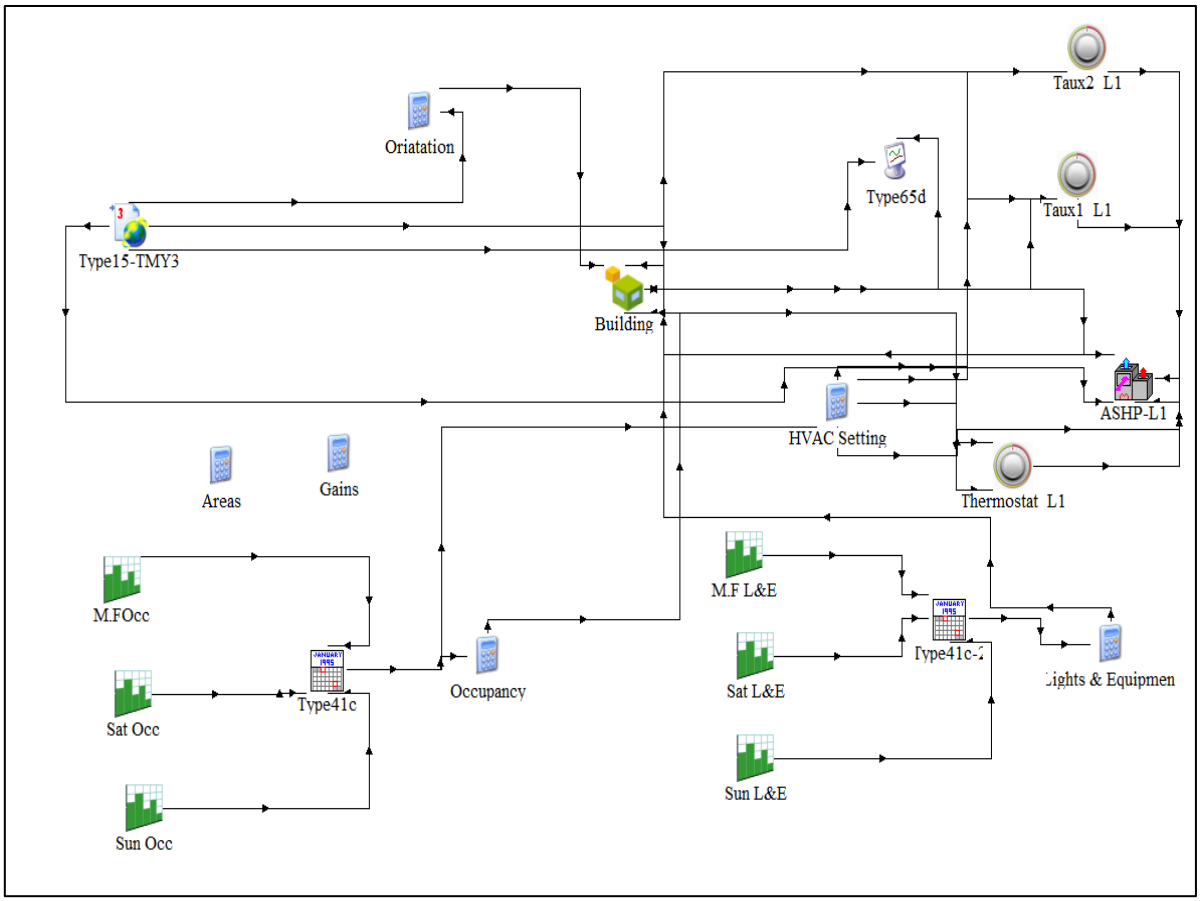

Figure II.10 : shows a schematic representation of the heat pump system within the TRNSYS simulation environment. The diagram illustrates the main components such as the indoor and outdoor coils, airflow streams, air mixing damper, and auxiliary heating units, providing a clear overview of the system's operation and its integration in the model.

8. Time dependent load profiles for heating and cooling in a southern Algerian residential building

8.1. Cooling load weekdays (Sunday to Thursday)

This schedule represents the cooling demand during typical weekdays in a southern Algerian home using a heat pump. The cooling load rises significantly during mid-day due to high solar radiation and outdoor temperatures, then decreases during the evening and night hours.

Table II.7: Weekday cooling load profile for a southern Algerian house (Sunday to Thursday

Time (h:m)	Cooling Load (Relative) (W/m^2)	Notes
00:00-10:00	0.0	No cooling needed
10:00-13:00	0.4	Morning heat build-up
13:00-18:00	1.0	Peak cooling period
18:00-22:00	0.7	Gradual decline
22:00-00:00	0.1	Night cooling minimized

8.2. Cooling Load Weekend (Friday and Saturday)

On weekends, occupants remain at home more often, leading to a more sustained cooling load throughout the day, though the pattern still peaks during mid-afternoon and tapers in the evening.

Table II.8: Weekend cooling load profile for a southern Algerian house (Friday and Saturday)

Time (h:m)	Cooling Load (Relative) (W/m^2)	Notes
00:00-10:00	0.0	No significant cooling
10:00-13:00	0.5	Gradual warming indoors
13:00-18:00	1.0	Maximum cooling period
18:00-22:00	0.8	Warm early evening
22:00-00:00	0.2	Cooling reduced at night

8.3. Heating load weekdays (Sunday to Thursday)

This schedule reflects the typical heating requirements during winter weekdays. Heating demand is highest in the early morning and evening, with a reduction during the warmer midday hours.

Table II.9: Weekday heating load profile for a southern Algerian house (Sunday to Thursday)

Time (h:m)	Cooling Load (Relative)(W/m^2)	Notes
00:00-10:00	0.6	Cold nighttime conditions
10:00-13:00	0.5	Morning occupancy
13:00-18:00	0.2	Reduced heating need
18:00-22:00	0.6	Evening heat up
22:00-00:00	0.3	Mild heating during bedtime

8.4. Heating Load – Weekend (Friday and Saturday)

Weekend heating demand is moderate throughout the day, as people stay home longer and benefit from internal heat gains. Heating is lower overnight and early morning compared to weekdays.

Table II.10: Weekend heating load profile for a southern Algerian house (Friday and Saturday)

Time (h:m)	Cooling Load (Relative)(W/m^2)	Notes
00:00-10:00	0.4	Moderate night heating
10:00-13:00	0.5	Slight morning warm up
13:00-18:00	0.3	Indoor gains reduce demand
18:00-22:00	0.6	Evening warmth needed
22:00-00:00	0.2	Reduced heating overnight

9. Conclusion:

This chapter presented a comprehensive overview of the theoretical framework and numerical modeling approach adopted to optimize building energy performance and ensure thermal comfort. The methodology was structured in two key phases: the application of passive insulation materials (glass wool and polystyrene) to reduce thermal loads, followed by the integration of an active HVAC system using a high-efficiency heat pump. TRNSYS was utilized as the primary simulation tool to evaluate the impact of each intervention on energy consumption, thermal loads, and indoor comfort conditions.

The modeling results provide a foundation for the analysis presented in the next chapter. Chapter Three will focus on the detailed results and discussion, highlighting the performance of the proposed strategy across different climatic conditions, and assessing the effectiveness of combining passive and active energy solutions in sustainable building design.

CHAPTER III

Results and discussion

1. Introduction

This chapter presents the results of the energy performance assessment of a typical residential building in nine Algerian provinces representing climatic gradients within the dry and semi-arid desert zones. An analytical approach was adopted based on precise numerical simulations of a series of thermal scenarios covering a gradual range of insulation thicknesses, from the uninsulated case (0.00 m) up to 0.30 m. The study also included the role of the heat pump as an active heating and cooling system, testing its impact in four main modes: the reference case without insulation and without a heat pump, the case with insulation only (passive control), the case with the heat pump only (active control), and finally the combined case with both insulation and heat pump (mixed control). These scenarios enabled a comprehensive evaluation of a set of indicators including annual energy consumption, economic costs related to investment and operation, carbon emissions resulting from electricity consumption, as well as fluctuations in indoor temperatures directly affecting occupant comfort. By aligning these analyses with the climatic characteristics of each province, regional differences within the desert framework were identified, allowing the derivation of optimal scenarios that simultaneously consider thermal, economic, and environmental factors.

2. Resultants and discussions

2.1.Validation of simulation results

To assess the accuracy of the simulation results, a comparative analysis was carried out between the outcomes of our current study and those obtained by Ghedamsi et al. (2016) for the same case study locations. The aim is to validate the thermal energy consumption estimations by evaluating the consistency of cooling, heating, and total energy demands.

Table III.1: Comparison between the results of this study and those of Ghedamsi et al. (2016).

	(R. Ghedamsi et al,2016)			This study			Relative difference (%)
	Cooling (kWh/m^2)	Heating (kWh/m^2)	Total (kWh/m^2)	Cooling (kWh/m^2)	Heating (kWh/m^2)	Total	
Adrar	45,8	16,43	62,23	50,99	16,17	67,17	7,35
Ain safra	15,45	41,38	56,83	18,00	38,29	56,29	0,94
Annaba	2,61	29,71	32,32	5,92	30,57	36,49	11,43

This comparison aims to validate the results of our current study by comparing them with a previous study conducted by Ghedamsi et al. (2016) for the same case studies. The findings show a noticeable consistency, confirming the reliability of our simulation model. In Adrar, the total energy consumption reached 67.17 kWh/m² in our study, compared to 62.23 kWh/m² in Ghedamsi's study, resulting in a relative difference of 7.35%. In Ain Safra, the difference was minimal, only 0.94%, indicating a high level of accuracy in the estimated results. In Annaba, the relative difference was 11.43%, mainly due to higher cooling demand in our model, which may be attributed to variations in climatic input data or occupancy assumptions. Overall, these differences remain within acceptable margins for validation purposes and confirm the robustness of the thermal modeling approach adopted in our study.

a. Insulation

Figure III.1 presents the relationship between insulation thickness and annual energy consumption for extruded polystyrene and glass wool across nine Algerian wilayas, highlighting the impact of climatic variation on insulation performance. The subsequent analysis details the trends observed in each region.

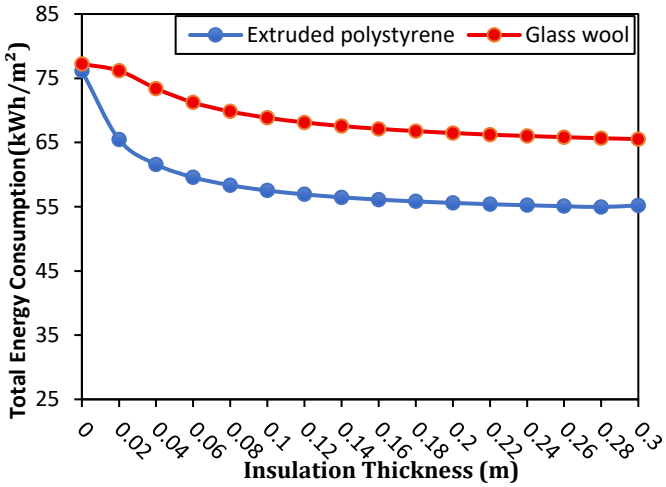
Extruded polystyrene
Glass wool
Total Energy Consumption(kWh/m²)
85
75
65
55
45
35
25
0 0.02 0.04 0.06 0.08 0.1 0.12 0.14 0.16 0.18 0.2 0.22 0.24 0.26 0.28 0.3
Insulation Thickness (m)

(a)

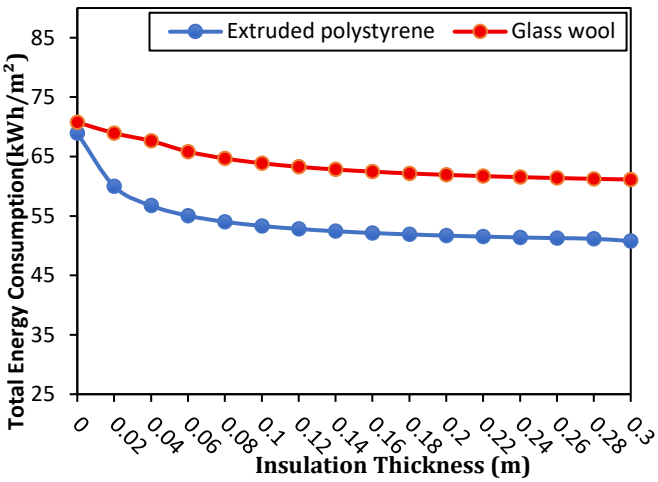
Extruded polystyrene
Glass wool
Total Energy Consumption(kWh/m²)
85
75
65
55
45
35
25
0 0.02 0.04 0.06 0.08 0.1 0.12 0.14 0.16 0.18 0.2 0.22 0.24 0.26 0.28 0.3
Insulation Thickness (m)

(b)

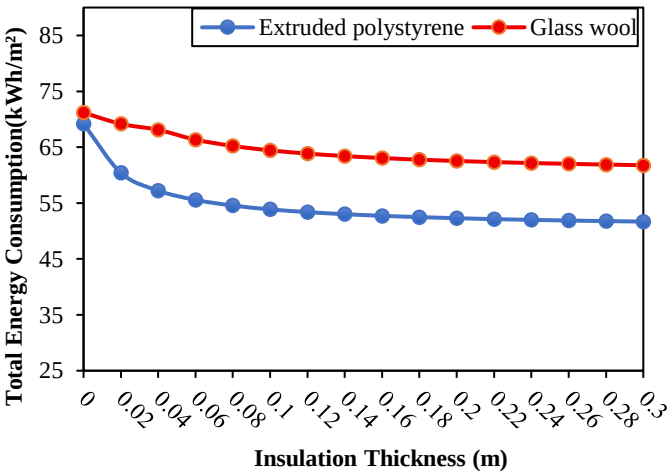
Extruded polystyrene
Glass wool
Total Energy Consumption(kWh/m²)
85
75
65
55
45
35
25
0 0.02 0.04 0.06 0.08 0.1 0.12 0.14 0.16 0.18 0.2 0.22 0.24 0.26 0.28 0.3
Insulation Thickness (m)

(c)

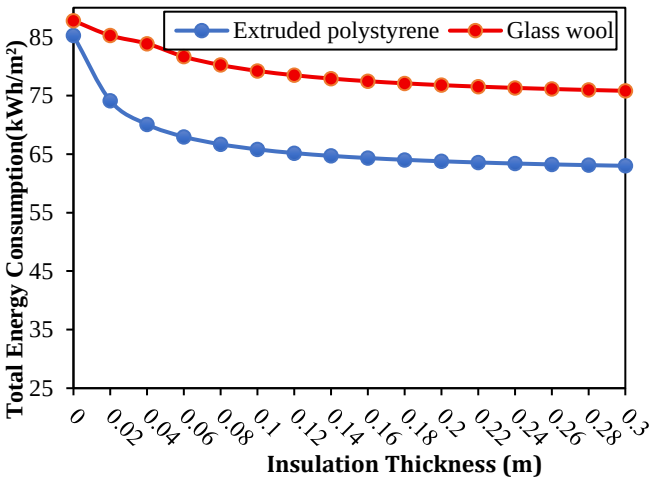
Extruded polystyrene
Glass wool
Total Energy Consumption(kWh/m²)
85
75
65
55
45
35
25
0 0.02 0.04 0.06 0.08 0.1 0.12 0.14 0.16 0.18 0.2 0.22 0.24 0.26 0.28 0.3
Insulation Thickness (m)

(d)

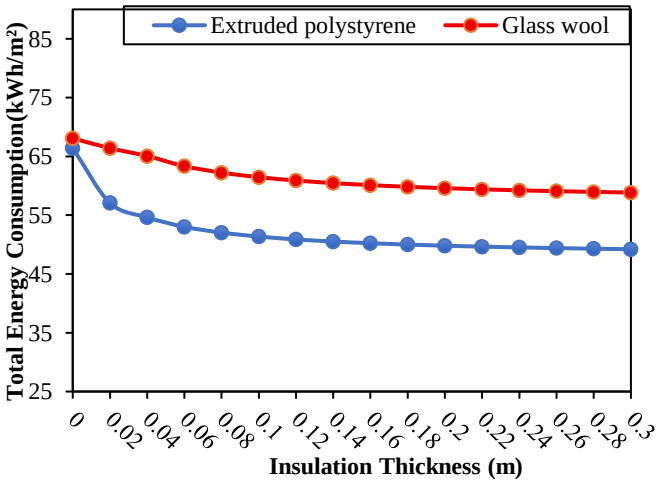
Extruded polystyrene
Glass wool
Total Energy Consumption(kWh/m²)
85
75
65
55
45
35
25
0 0.02 0.04 0.06 0.08 0.1 0.12 0.14 0.16 0.18 0.2 0.22 0.24 0.26 0.28 0.3
Insulation Thickness (m)

(e)

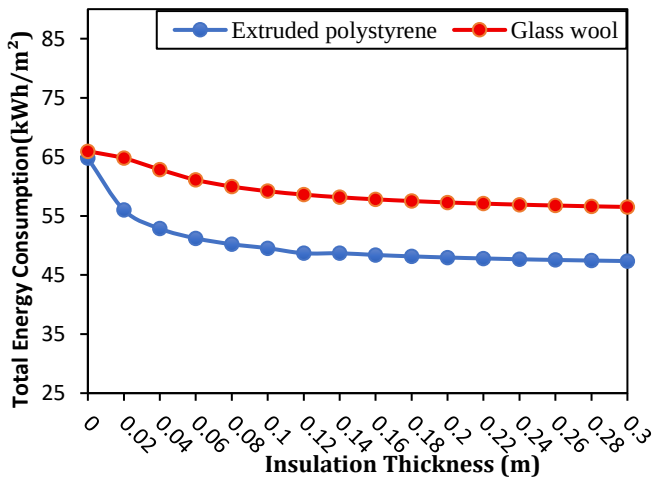
Extruded polystyrene
Glass wool
Total Energy Consumption(kWh/m²)
85
75
65
55
45
35
25
0 0.02 0.04 0.06 0.08 0.1 0.12 0.14 0.16 0.18 0.2 0.22 0.24 0.26 0.28 0.3
Insulation Thickness (m)

(f)

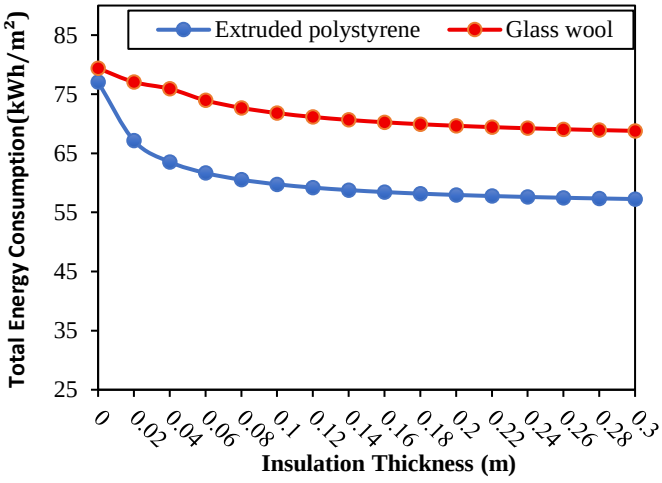

(g)

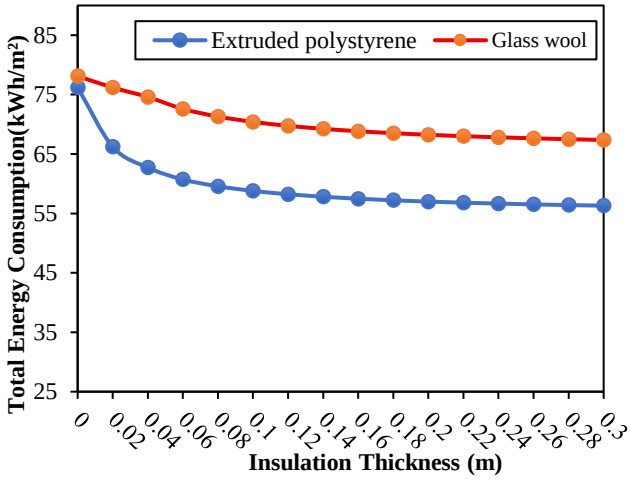

(h)

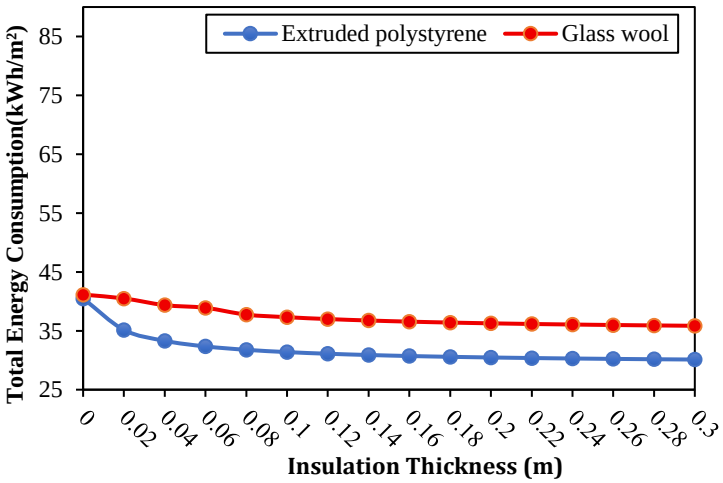

(i)

Figure III.1: Variation of Total Energy Consumption with Insulation Thickness across Different Wilayas. (a) Adrar; (b) Behar; (c) Biskra; (d) Djelfa; (e) Ghardaia; (f) Illizi; (g) Laghouat; (h) Ouargla; (i) Tamanrasset.

The Figure (III.1, a) indicate that as the insulation thickness increases, the annual energy consumption decreases noticeably for both materials. For extruded polystyrene, energy consumption drops from 76.17 kWh/m² without insulation to 55.20 kWh/m² at 0.30 m, while for glass wool, it decreases from 77.22 kWh/m² to 65.52 kWh/m² over the same range. This trend

highlights the clear thermal advantage of extruded polystyrene. The most significant reduction for this material occurs between no insulation and 0.10 m, with values falling from 76.17 to 57.52 kWh/m², suggesting high thermal resistance and insulation performance. In contrast, glass wool's reduction is more gradual over the same interval, moving from 77.22 to 68.84 kWh/m². Beyond 0.18 m, the rate of decrease becomes less pronounced for both materials, indicating that increasing thickness further yields diminishing energy savings. For example, between 0.20 m and 0.30 m, extruded polystyrene drops only from 55.59 to 55.20 kWh/m², while glass wool goes from 66.47 to 65.52 kWh/m². These findings confirm that extruded polystyrene is more efficient than glass wool in reducing energy consumption in the hot and arid climate of Adrar. It achieves greater energy savings even at lower thicknesses, making it a preferable insulation material for such harsh environments.

In Figure (III.1, b) the energy consumption for extruded polystyrene starts at 68.94 kWh/m² at zero thickness and gradually decreases to 50.78 kWh/m² at 0.30 m thickness. In comparison, glass wool consumption decreases from 70.77 to 61.13 kWh/m² over the same thickness range. Extruded polystyrene shows a faster and greater reduction, especially between 0 and 0.10 m, dropping from 68.94 to 53.32 kWh/m², indicating its high thermal insulation efficiency. Glass wool exhibits a more gradual decline during this interval. Beyond 0.18 m thickness, the rate of decrease in energy consumption slows for both materials, suggesting diminishing returns with further thickness increases. Between 0.20 and 0.30 m, polystyrene drops only from 51.69 to 50.78 kWh/m², while glass wool decreases from 61.91 to 61.13 kWh/m². These results confirm that extruded polystyrene is the better choice for improving thermal insulation and reducing energy consumption in the hot and harsh climate of Béchar, achieving significant savings even at lower insulation thicknesses.

Figure (III.1, c) indicates that energy consumption in Biskra for extruded polystyrene starts at 69.18 kWh/m² at 0 thickness and gradually decreases to 51.69 kWh/m² at 0.30 m thickness. For glass wool, consumption begins at 71.18 kWh/m² and reduces to 61.78 kWh/m² over the same thickness range. Extruded polystyrene shows greater effectiveness, with a faster and more significant decrease, especially between 0 and 0.10 m, where consumption drops from 69.18 to 53.88 kWh/m², demonstrating strong thermal insulation capability. In contrast, glass wool exhibits a slower, more gradual decline in energy use during this interval. Beyond 0.18 m thickness, the reduction rate slows for both materials, indicating diminishing returns with further increases in thickness. For example, between 0.20 and 0.30 m, polystyrene consumption decreases slightly

from 52.29 to 51.69 kWh/m², while glass wool decreases from 62.54 to 61.78 kWh/m². These findings confirm that extruded polystyrene offers superior thermal performance and is the better option for enhancing energy efficiency in the warm climate of Biskra.

Figure (III.1, d) illustrates the annual energy consumption in Djelfa using extruded polystyrene and glass wool insulation as thickness increases. For extruded polystyrene, energy consumption starts at 85.25 kWh/m² with no insulation and gradually decreases to 62.99 kWh/m² at 0.30 m thickness. Glass wool begins at 87.78 kWh/m² and reduces to 75.80 kWh/m² over the same thickness range. The results clearly show the superiority of extruded polystyrene in lowering energy consumption compared to glass wool, with a faster and more significant reduction, especially within the first 0.10 m of insulation thickness where consumption drops from 85.25 to 65.80 kWh/m². In contrast, glass wool demonstrates a steadier, more gradual decrease. Beyond 0.18 m thickness, the rate of energy savings slows down for both materials, indicating diminishing returns with further thickness increases. For example, between 0.20 and 0.30 m, polystyrene consumption decreases slightly from 63.77 to 62.99 kWh/m², while glass wool decreases from 76.77 to 75.80 kWh/m². These findings suggest that extruded polystyrene is the better insulation material for improving energy efficiency in Djelfa's climate, offering strong thermal performance and significant energy savings.

Figure (III.1, e) presents the results for the city of Ghardaïa, located in southern Algeria, which experiences a hot and arid desert climate. For extruded polystyrene, the energy consumption begins at 66.40 kWh/m² without insulation and decreases significantly to 49.21 kWh/m² at 0.30 m thickness. In comparison, glass wool starts at 68.08 kWh/m² without insulation and drops to 58.85 kWh/m² over the same range. The results show that extruded polystyrene achieves a faster and greater reduction in energy use, particularly in the early stages. From no insulation to 0.10 m, the consumption falls sharply from 66.40 to 51.36 kWh/m², highlighting its superior thermal performance. On the other hand, glass wool shows a more gradual decline during this interval. After 0.18 m, both materials exhibit slower rates of energy savings, indicating diminishing returns. For instance, between 0.20 m and 0.30 m, extruded polystyrene drops from 49.81 to 49.21 kWh/m², whereas glass wool decreases from 59.59 to 58.85 kWh/m². These results confirm that extruded polystyrene is more effective in reducing energy demand under Ghardaïa's harsh climatic conditions, offering better insulation performance with lower thicknesses.

Figure (III.1, f) presents the results for the city of Illizi, which is characterized by an extremely hot desert climate. The annual energy consumption decreases consistently with the

increase in insulation thickness for both extruded polystyrene and glass wool. For extruded polystyrene, the energy use drops from 64.77 kWh/m² without insulation to 47.36 kWh/m² at 0.30 m. Glass wool follows a similar trend, starting at 65.95 kWh/m² without insulation and decreasing to 56.52 kWh/m². The most significant reductions occur within the first 0.10 m of insulation, particularly for extruded polystyrene, which drops by over 15 kWh/m², indicating high thermal effectiveness at lower thicknesses.

Beyond 0.18 m, both materials exhibit a diminishing rate of energy savings. For example, between 0.20 m and 0.30 m, the reduction for extruded polystyrene is only about 0.60 kWh/m², suggesting that increasing thickness beyond this point yields limited additional benefits. Overall, the results highlight the superior performance of extruded polystyrene, especially in arid climates like Illizi, due to its greater efficiency in reducing energy consumption with thinner layers compared to glass wool.

Figure (III.1, g) presents the results for the city of Laghouat, known for its semi-arid climate with hot summers and cool winters. The analysis shows a clear decrease in annual energy consumption as the insulation thickness increases for both extruded polystyrene and glass wool.

At 0.00 m, energy consumption is 77.05 kWh/m² for extruded polystyrene and 79.39 kWh/m² for glass wool. As the thickness reaches 0.10 m, consumption drops to 59.76 kWh/m² and 71.81 kWh/m², respectively. This indicates that extruded polystyrene reduces energy needs more effectively at lower thicknesses. The decline continues with smaller gains at higher thicknesses. At 0.30 m, consumption reaches 57.27 kWh/m² for extruded polystyrene and 68.80 kWh/m² for glass wool. The difference between the two materials remains significant across all thickness levels. In summary, extruded polystyrene consistently outperforms glass wool in reducing energy consumption in Laghouat's climate, especially in the range of 0.02 m to 0.12 m, making it a more efficient insulation option for buildings in such environments.

Figure (III.1, h) presents the results for the city of Ouargla, illustrating the evolution of annual energy consumption with increasing insulation thickness for extruded polystyrene and glass wool. Without insulation, the energy consumption starts at 76.19 kWh/m² for extruded polystyrene and 78.12 kWh/m² for glass wool. As insulation thickness increases to 0.10 m, consumption decreases significantly to 58.80 kWh/m² and 70.41 kWh/m², respectively. Further increases in thickness to 0.20 m show additional reductions: 56.99 kWh/m² for extruded polystyrene and 68.24 kWh/m² for glass wool. These results confirm the consistent performance advantage of extruded

polystyrene. At the maximum tested thickness of 0.30 m, energy use reaches 56.31 kWh/m² with polystyrene and 67.37 kWh/m² with glass wool. The rate of reduction slows as thickness increases, indicating diminishing returns beyond certain levels. In conclusion, extruded polystyrene outperforms glass wool at all thicknesses in terms of energy saving, particularly between 0.02 m and 0.14 m, where the most significant reductions occur.

Figure (III.1, i) presents the results for the city of Tamanrasset, illustrating the evolution of annual energy consumption with increasing insulation thickness for extruded polystyrene and glass wool. Without any insulation (0.00 m thickness), the energy consumption is 40.50 kWh/m² for extruded polystyrene and 41.15 kWh/m² for glass wool. Even a small increase in insulation to 0.02 m leads to a noticeable reduction, particularly for polystyrene, lowering energy use to 35.16 kWh/m². As the thickness increases to 0.10 m, consumption continues to decline, reaching 31.38 kWh/m² for polystyrene and 37.32 kWh/m² for glass wool. This downward trend persists with smaller reductions at higher thicknesses. At 0.20 m, energy consumption measures 30.47 kWh/m² for extruded polystyrene and 36.27 kWh/m² for glass wool, reaffirming the superior thermal performance of polystyrene. At the maximum thickness tested, 0.30 m, the lowest values recorded are 30.12 kWh/m² for polystyrene and 35.85 kWh/m² for glass wool. These results demonstrate that extruded polystyrene consistently offers better energy savings than glass wool across all insulation thickness levels in Tamanrasset.

The analysis confirms that extruded polystyrene outperforms glass wool in reducing energy consumption across all studied regions. Its superior thermal insulation efficiency is attributed to lower thermal conductivity, higher density, and better moisture resistance. These physical properties make extruded polystyrene the optimal choice for insulation in hot and arid climates.

Figure III.3 presents the variation in cooling and heating energy consumption as a function of insulation thickness across various Algerian wilayas. This comparative analysis highlights how different climatic conditions influence the effectiveness of thermal insulation in reducing energy demand for both heating and cooling.

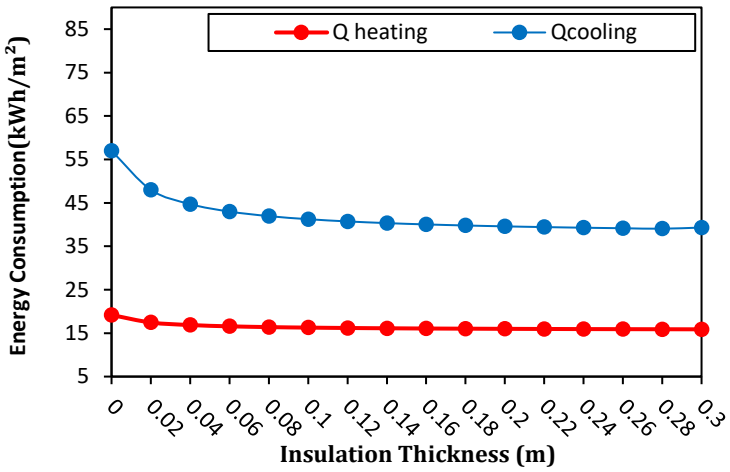
Q heating
Qcooling
Energy Consumption(kWh/m²)
85
75
65
55
45
35
25
15
5
0 0.02 0.04 0.06 0.08 0.1 0.12 0.14 0.16 0.18 0.2 0.22 0.24 0.26 0.28 0.3
Insulation Thickness (m)

(a)

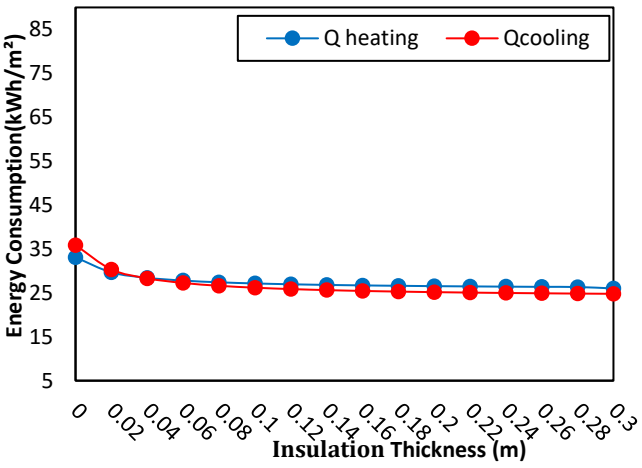
Q heating
Qcooling
Energy Consumption(kWh/m²)
85
75
65
55
45
35
25
15
5
0 0.02 0.04 0.06 0.08 0.1 0.12 0.14 0.16 0.18 0.2 0.22 0.24 0.26 0.28 0.3
Insulation Thickness (m)

(b)

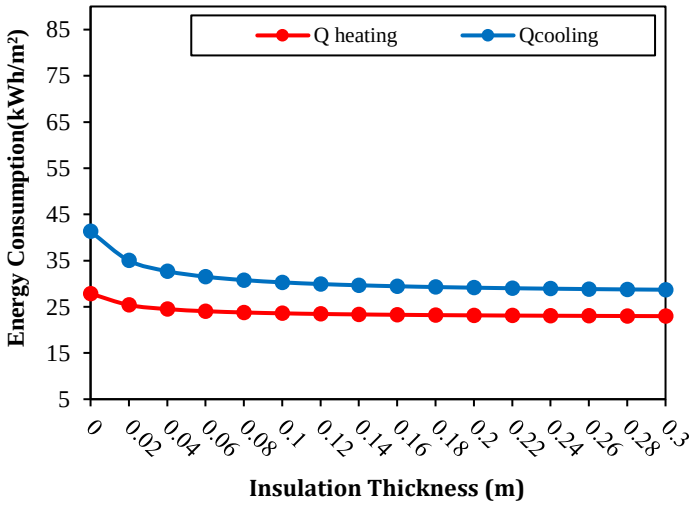
Q heating
Qcooling
Energy Consumption(kWh/m²)
85
75
65
55
45
35
25
15
5
0 0.02 0.04 0.06 0.08 0.1 0.12 0.14 0.16 0.18 0.2 0.22 0.24 0.26 0.28 0.3
Insulation Thickness (m)

(c)

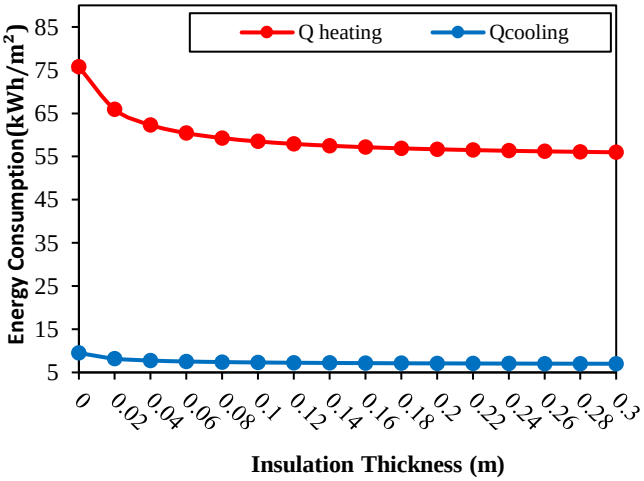
Q heating
Qcooling
Energy Consumption(kWh/m²)
85
75
65
55
45
35
25
15
5
0 0.02 0.04 0.06 0.08 0.1 0.12 0.14 0.16 0.18 0.2 0.22 0.24 0.26 0.28 0.3
Insulation Thickness (m)

(d)

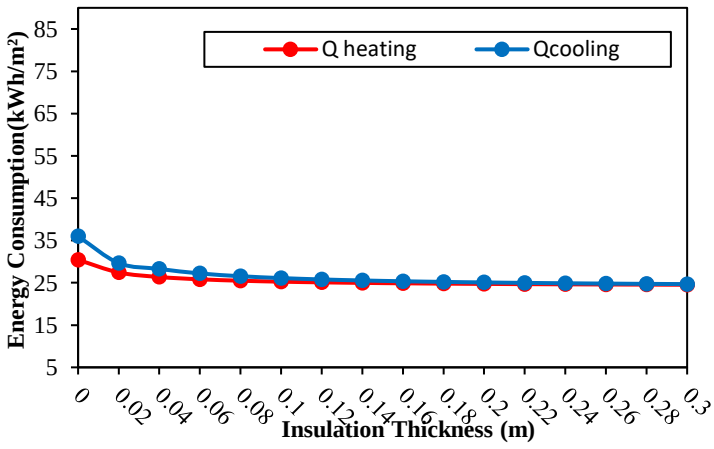
Q heating
Qcooling
Energy Consumption(kWh/m²)
85
75
65
55
45
35
25
15
5
0 0.02 0.04 0.06 0.08 0.1 0.12 0.14 0.16 0.18 0.2 0.22 0.24 0.26 0.28 0.3
Insulation Thickness (m)

(e)

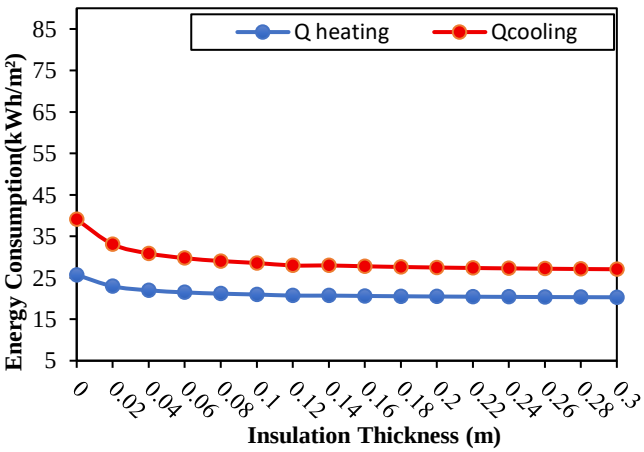
Q heating
Qcooling
Energy Consumption(kWh/m²)
85
75
65
55
45
35
25
15
5
0 0.02 0.04 0.06 0.08 0.1 0.12 0.14 0.16 0.18 0.2 0.22 0.24 0.26 0.28 0.3
Insulation Thickness (m)

(f)

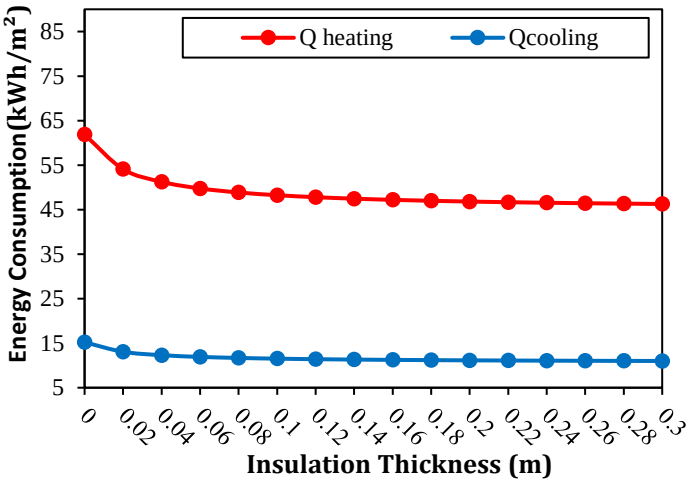

(g)

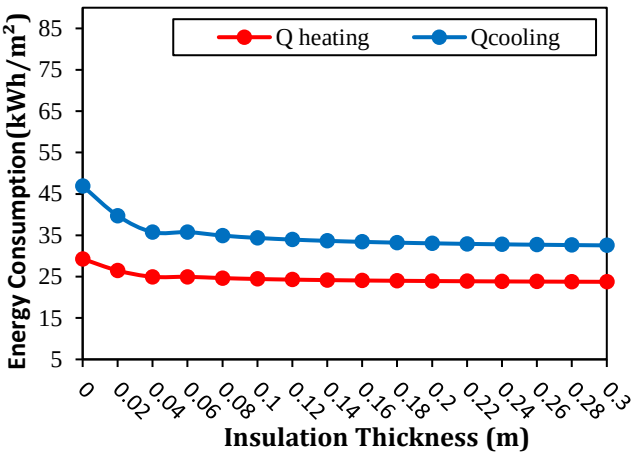

(h)

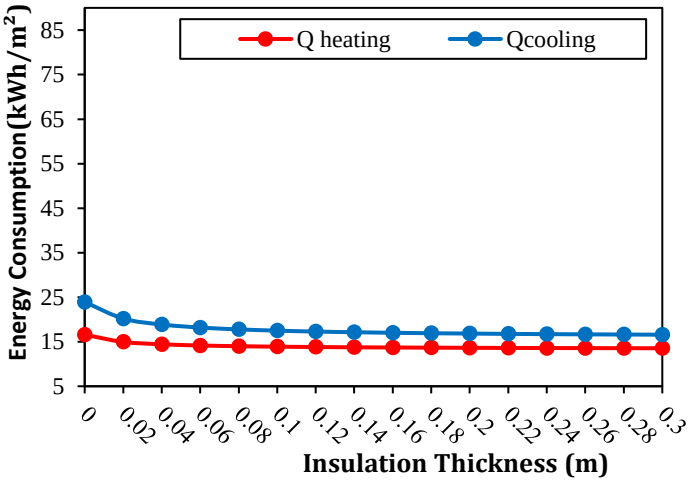

(i)

Figure III.2: Variation of Cooling and Heating Energy Consumption with Insulation Thickness across Different Wilayas. **(a)** Adrar; (b) Behar; (c) Biskra; (d) Djelfa; (e) Ghardaia; (f) Illizi; (g) Laghouat; (h) Ouargla; (i) Tamanrasset.

Figure (III.2, a) illustrates the effect of increasing the thickness of extruded polystyrene insulation on heating and cooling energy consumption in the Wilaya of Adrar. The results show a significant decrease in both heating and cooling demands as the insulation thickness increases from 0 to 30 cm. The reduction is more pronounced at lower thicknesses (from 0 to 6 cm) and gradually

slows down as thickness increases further. Heating energy consumption decreases from approximately 19.18 kWh/m² to about 15.88 kWh/m² at 30 cm thickness, while cooling energy consumption reduces from 56.99 kWh/m² to 39.32 kWh/m². These findings confirm the effectiveness of extruded polystyrene insulation in lowering thermal loads, particularly in the hot climate conditions of Adrar, thereby contributing to improved energy efficiency in residential buildings throughout the year.

Figure (III.2, b) shows the effect of increasing insulation thickness on heating and cooling energy demands in the Wilaya of Béchar. Heating consumption decreases from about 33.08 kWh/m² without insulation to 26.00 kWh/m² at the maximum thickness studied. Cooling demand also reduces from 35.86 kWh/m² to 24.78 kWh/m². The largest reductions occur with the initial increases in insulation thickness, while further increases result in smaller incremental savings. This confirms that thermal insulation significantly lowers energy needs for both heating and cooling. These improvements are particularly relevant for Béchar's climate, which has hot summers and cool winters. Overall, adding insulation is an effective strategy to enhance energy efficiency and reduce energy costs in buildings in this region.

The figure (III.2, c) illustrates the effect of increasing thermal insulation thickness on the energy demand for heating and cooling in the Wilaya of Béchar. The data show that heating energy consumption decreases from approximately 27.86 kWh/m² without insulation to about 22.98 kWh/m² with the greatest insulation thickness. Similarly, cooling consumption drops from 41.32 kWh/m² to around 28.70 kWh/m². The results indicate that improvements in energy efficiency are most pronounced with the initial increases in insulation thickness, where thermal loads significantly decrease, followed by a slowdown in the rate of reduction as thickness continues to increase.

Figure (III.2, d) illustrates the effect of increasing thermal insulation thickness on the energy consumption for heating and cooling in the Wilaya of Djelfa. Heating energy consumption decreases from 75.75 kWh/m² without insulation to approximately 55.98 kWh/m² at an insulation thickness of 30 cm. Meanwhile, cooling consumption drops from 9.50 kWh/m² to around 7.01 kWh/m² with the increase in insulation thickness. The results indicate that the greatest energy savings occur during the initial increments of insulation thickness, where there is a significant reduction in thermal loads, followed by a gradual slowdown in the rate of decrease as insulation thickness increases further. This behavior highlights the importance of thermal insulation in

reducing energy consumption, especially in the Djelfa climate characterized by cold winters and mild summers.

Figure (III.2, e) illustrates the impact of increasing thermal insulation thickness on heating and cooling energy consumption in the Wilaya of Ghardaia. Heating demand decreases significantly from 30.42 kWh/m² without insulation to approximately 24.53 kWh/m² at an insulation thickness of 30 cm. Similarly, cooling consumption reduces from about 35.98 kWh/m² to 24.68 kWh/m² over the same insulation range. The data show a marked reduction in both heating and cooling loads during the initial increases in insulation thickness, with the rate of decrease becoming more gradual as the insulation thickness grows.

The figure (III.2, f) illustrates the effect of increasing thermal insulation thickness on heating and cooling energy consumption in Illizi, Algeria. Heating demand decreases from approximately 25.70 kWh/m² without insulation to about 20.30 kWh/m² at 30 cm insulation thickness. Similarly, cooling consumption reduces from 39.07 kWh/m² to nearly 27.06 kWh/m² over the same range. The results indicate a marked reduction in energy loads during the initial increases in insulation thickness, followed by a gradual slowdown in the rate of decrease as the insulation becomes thicker.

Figure (III.2, g) illustrates how increasing the thermal insulation thickness in Laghouat affects the reduction of energy consumption for both heating and cooling. Heating energy consumption significantly decreases from about 61.85 kWh/m² without insulation to 46.27 kWh/m² at 30 cm thickness, with a noticeable slowdown in the rate of decrease after 20 cm. Cooling energy consumption in Laghouat gradually declines from 15.21 to 11.00 kWh/m², with the curve tending to stabilize at higher insulation thicknesses. This behavior indicates that small to medium insulation thicknesses provide substantial energy savings, making them an optimal choice for insulation design in Laghouat's climate.

In Ouargla, Figure (III.2, h) shows a sharp decline in heating energy consumption from 29.29 to 23.75 kWh/m² as insulation thickness increases. The heating consumption curve decreases rapidly at first, then the rate of decrease slows down after 10 cm, resulting in a flatter curve at greater thicknesses. Cooling energy consumption also exhibits a significant drop from 46.90 to 32.56 kWh/m², with a trend toward stabilization beyond 20 cm thickness. This reflects that insulation in Ouargla achieves the greatest impact in reducing thermal loads during the initial increases in thickness, with diminishing returns as thickness grows.

In Tamanrasset, Figure (III.2, i) shows a distinct variation in the shape of the energy consumption curves. Heating consumption decreases from 16.58 to 13.54 kWh/m², while cooling consumption declines more gradually from 23.92 to 16.58 kWh/m². The curves in Tamanrasset exhibit a slower change after 15 cm thickness, indicating that further increases provide smaller benefits. This pattern reflects the hot desert climate of Tamanrasset, where insulation has a more pronounced effect on cooling loads, making insulation highly effective at small to medium thicknesses, while thicker insulation requires economic consideration.

The results from Figure III.3 clearly demonstrate that increasing the thermal insulation thickness significantly reduces heating and cooling energy consumption across all studied wilayas, with the most substantial savings occurring at small to moderate thicknesses, followed by a gradual slowdown in energy reduction as thickness increases further. Based on these findings, it is essential to determine the optimal insulation thickness that balances maximum energy savings with the associated economic and technical considerations.

2.2.Economic analysis

Figure III.3 illustrates the variation of installation cost relative to insulation thickness across different wilayas. This comparison provides insight into the economic implications of increasing insulation thickness in diverse climatic regions of Algeria.

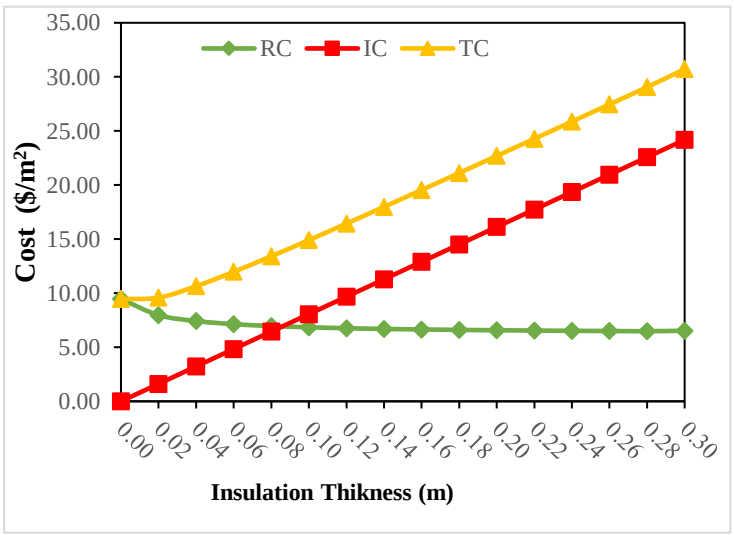

(a)

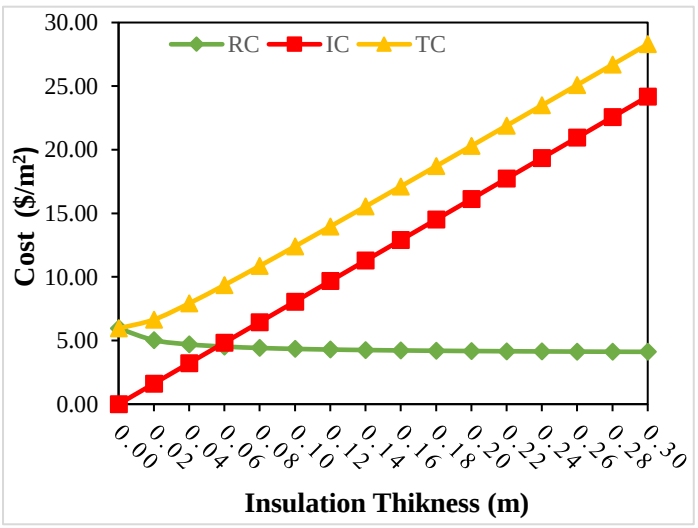

(b)

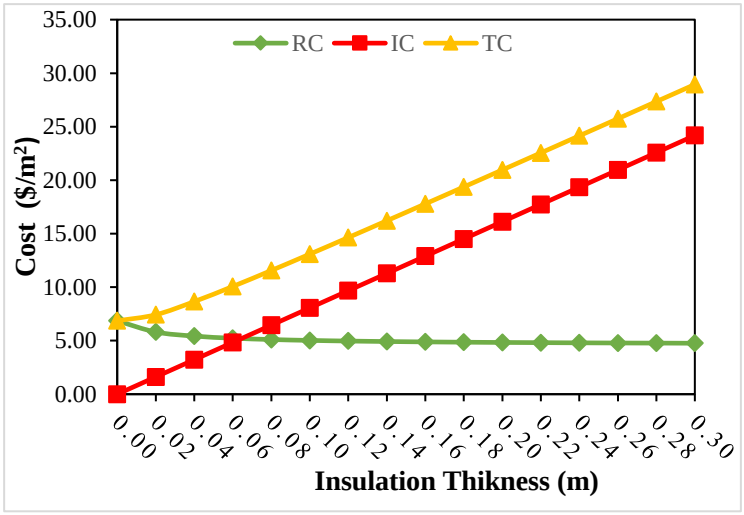
RC
IC
TC
Cost ($/m²)
Insulation Thikness (m)

(c)

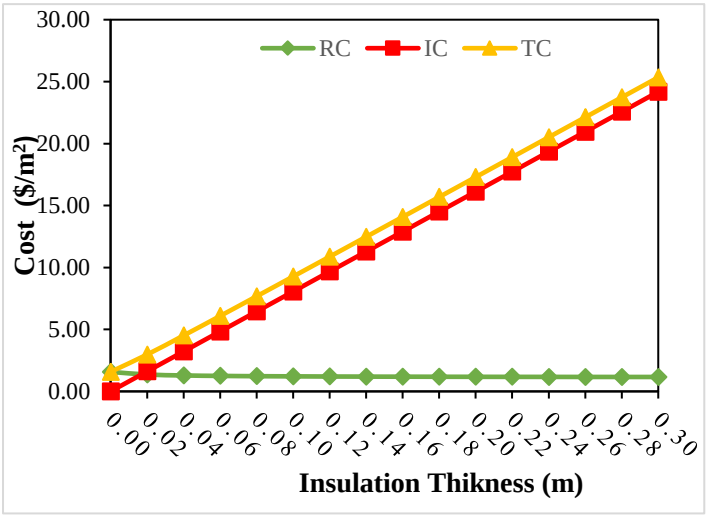
RC
IC
TC
Cost ($/m²)
Insulation Thikness (m)

(d)

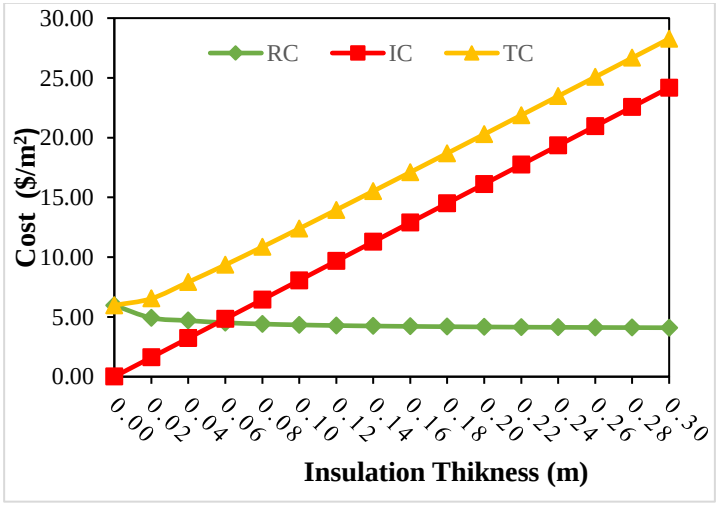
RC
IC
TC
Cost ($/m²)
Insulation Thikness (m)

(e)

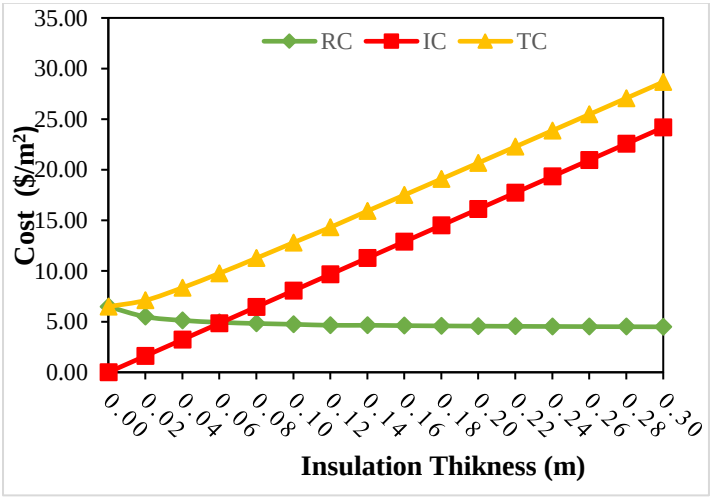
RC
IC
TC
Cost ($/m²)
Insulation Thikness (m)

(f)

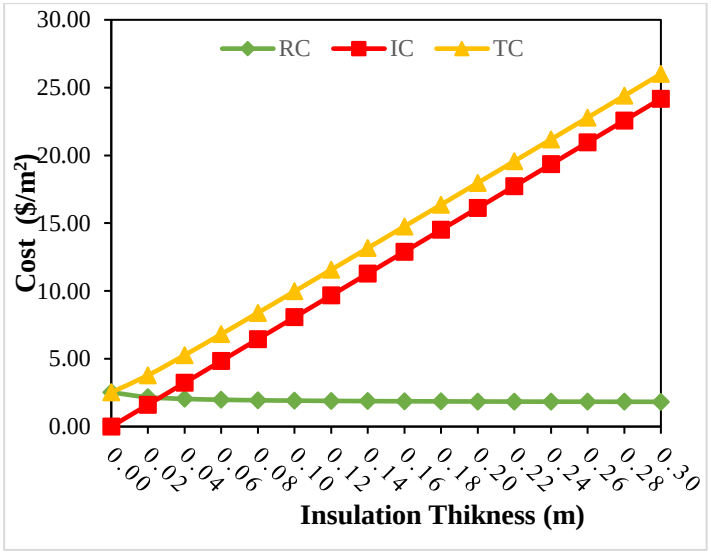

(g)

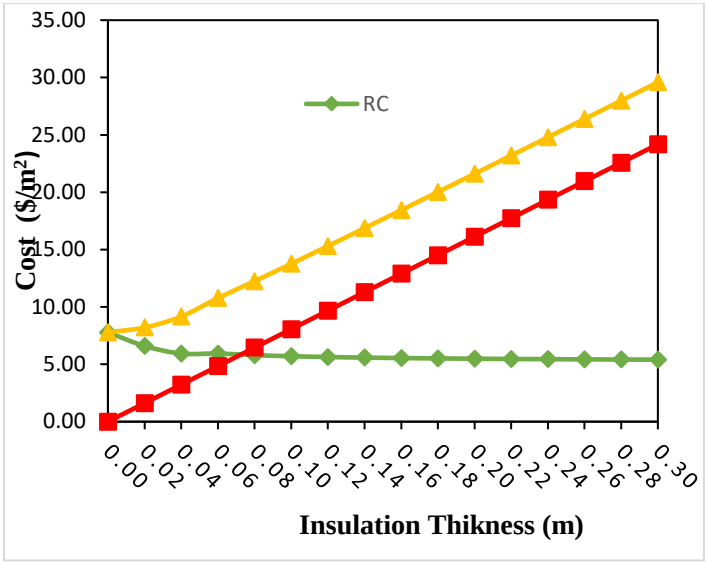

(h)

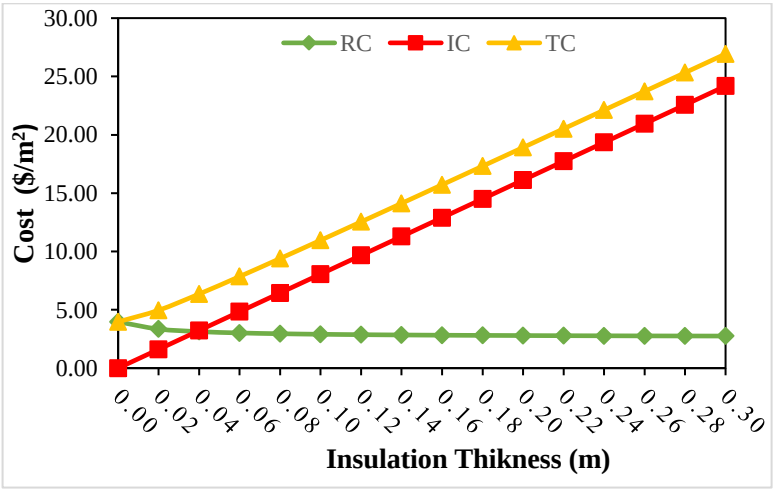

(i)

Figure III.3: Variation of cost with insulation thickness across Different Wilayas. **(a)** Adrar; (b) Behar; (c) Biskra; (d) Djelfa; (e) Ghardaia; (f) Illizi; (g) Laghouat; (h) Ouargla; (i) Tamanrasset.

Figure (III.3, a), which corresponds to the Adrar region, shows that the running cost (RC) decreases significantly with the increase in insulation thickness, dropping from 9.46 $/m² without insulation to approximately 6.90 $/m² at a thickness of 0.09 m—a reduction of about 27%. In contrast, the initial cost (IC) increases gradually from 0 $/m² to around 7.25 $/m² for the same thickness. The total cost (TC), representing the sum of RC and IC, reaches its minimum value of 14.15 $/m² at the insulation thickness of 0.09 m. The results also show that the intersection point

between the RC and IC curves occurs at 0.09 m, indicating an ideal balance between operating and investment costs. It is concluded from this that 0.09 m represents the optimal insulation thickness for the climate of Adrar, as it achieves the lowest possible total cost. Beyond this point, the return on additional insulation becomes economically inefficient due to the linear increase in IC and the slower reduction in RC.

In Figure (III.3, b), which presents the results for the Béchar region, it is observed that the running cost (RC) decreases noticeably with increasing insulation thickness. It drops from \$5.95/m² without insulation to 4.52\$/m² at a thickness of 0.06 m, representing a reduction of approximately 24%. In contrast, the initial cost (IC) rises progressively from \$0/m² to 4.84 \$/m² for the same thickness. The total cost (TC), defined as the sum of RC and IC, reaches its minimum value of 9.36 \$/m² at an insulation thickness of 0.06 m, highlighting this point as the most cost-effective solution. This conclusion is further supported by the fact that the intersection point between the RC and IC curves also occurs at this thickness, indicating an optimal balance between operational and investment costs. Beyond 0.06 m, the reduction in RC becomes marginal, while IC continues to increase almost linearly. This leads to a steady rise in the total cost, making additional insulation economically unjustifiable. Therefore, 0.06 m is identified as the optimal insulation thickness for the climatic conditions of Béchar, as it minimizes the total cost without incurring unnecessary investment.

In Figure (III.3, c), which illustrates the data for the Biskra region, the running cost (RC) shows a significant decrease as the insulation thickness increases. Specifically, RC drops from 6.86 \$/m² without insulation to 5.23 \$/m² at a thickness of 0.06 m, reflecting a reduction of approximately 24%. Meanwhile, the initial cost (IC) increases steadily from 0 \$/m² to 4.84 \$/m² at the same thickness. The total cost (TC), calculated as the sum of RC and IC, reaches its lowest value of 10.07 \$/m² at the insulation thickness of 0.06 m, which also corresponds to the intersection point between the RC and IC curves. This intersection indicates the most balanced and economically optimal point, where the investment in insulation is justified by the resulting savings in running costs. Beyond the 0.06 m thickness, any additional insulation results in minimal reductions in RC, while IC continues to rise substantially. As a result, the total cost begins to increase, making further investment less cost-effective. Therefore, an insulation thickness of 0.06 m is identified as the optimal choice for the climatic conditions of Biskra, offering the best compromise between energy savings and initial investment.

In Figure (III.3, d) for the Djelfa region, the running cost (RC) drops from 1.58 $/m² (at 0.00 m) to 1.36 $/m² at 0.02 m, while the initial cost (IC) rises from 0 to 1.61 /m². The total cost (TC) reaches its minimum value of 2.97 $/m² at this thickness, marking the intersection point between RC and IC. Beyond 0.02 m, RC decreases only slightly (to 1.16 $/m² at 0.30 m), while IC continues increasing significantly, reaching 24.18 /m². This leads to a steady rise in TC, up to 25.34 /m². Hence, 0.02 m is the optimal insulation thickness for Djelfa, balancing cost and performance.

In Figure (III.3, e) corresponding to the Ghardaïa region, the running cost (RC) decreases from 5.97 $/m² at zero insulation thickness to 4.52 $/m² at 0.06 m, whereas the initial cost (IC) rises from 0 to 4.84 $/m² over the same range. The total cost (TC) attains its lowest point of 9.35 $/m² at 0.06 m, marking the intersection of the RC and IC curves. Beyond this thickness, the RC shows a gradual decline, reaching 4.10 $/m² at 0.30 m, while the IC steadily climbs to 24.18/m², resulting in a continual increase in TC up to 28.28/m². Consequently, the optimal insulation thickness for Ghardaïa is identified as 0.06 m, delivering the most economical balance between costs.

For the Illizi region, illustrated in Figure (III.3, f), the RC drops from 6.49 $/m² with no insulation to 4.94 $/m² at 0.06 m, while the IC rises from zero to 4.84 $/m² within this thickness. The TC reaches a minimum value of 9.77 $/m² at 0.06 m, which is also the point where RC and IC curves intersect. After this point, the RC declines slightly to 4.49 $/m² at 0.30 m, but the IC increases steadily to 24.18/m², pushing the TC upwards to 28.67/m². Thus, 0.06 m is the recommended insulation thickness for Illizi to minimize total expenditure.

In Figure (III.3, g) representing Laghouat, the RC decreases from 2.52 $/m² at zero thickness to 2.17 $/m² at 0.02 m, and further down to 1.98 $/m² at 0.06 m. Simultaneously, the IC rises from 0 to 1.61 $/m² at 0.02 m, reaching 4.84 $/m² at 0.06 m. The total cost (TC) attains its minimum of 3.78 $/m² around 0.03 m thickness, coinciding with the intersection of the RC and IC curves. Beyond this thickness, although the RC decreases marginally, the IC grows significantly, causing TC to rise steadily, reaching 26.01 $/m² at 0.30 m. Therefore, the optimal insulation thickness for Laghouat is estimated at 0.03 m, striking a cost-effective balance between initial and running costs.

Figure (III.3, h) details the Ouargla region, where the RC declines from 7.78 $/m² at zero insulation to 5.93 $/m² at 0.06 m, while the IC increases from 0 to 4.84 $/m² at the same thickness.

The TC reaches its lowest value of 10.77 $/m² near 0.07 m, which is also the point where RC and IC meet. Beyond 0.07 m, RC falls slowly to 5.40 $/m² at 0.30 m, while IC rises considerably to 24.18/m², resulting in a steady rise in TC up to 29.58/m². Hence, an insulation thickness of approximately 0.07 m is optimal for Ouargla to balance upfront and operational expenses effectively.

Finally, in Figure (III.3, i) illustrating the Tamanrasset region, the RC decreases from 3.97 $/m² without insulation to 3.02 $/m² at 0.06 m, while the IC grows from zero to 4.84 $/m² within this thickness range. The TC achieves its minimum value of 7.86 $/m² at 0.04 m, which corresponds to the intersection point of RC and IC. Beyond this, the RC shows a slight decrease, but the IC continues rising, pushing the total cost to 26.93 $/m² at 0.30 m. Accordingly, the best insulation thickness for Tamanrasset is 0.04 m, optimizing the trade-off between initial investment and running cost.

The optimal insulation thickness varies between regions due to differences in climatic conditions, ranging from 0.02 m in Djelfa to 0.09 m in Adrar. For example, 0.09 m is the most suitable thickness for Adrar, while 0.06 m is optimal for Béchar, Biskra, Ghardaïa, and Illizi. In Laghouat, the optimal thickness is 0.03 m, in Ouargla 0.07 m, and in Tamanrasset 0.04 m. This variation is attributed to differences in temperature and humidity, which affect the balance between initial insulation costs and long-term energy savings.

Figure (III.4) shows the impact of extruded polystyrene insulation, applied at the optimal thickness for each region, on reducing annual electricity consumption. The results highlight the percentage decrease in energy use achieved within one year, reflecting the balance between insulation investment and operational savings tailored to each local climate.

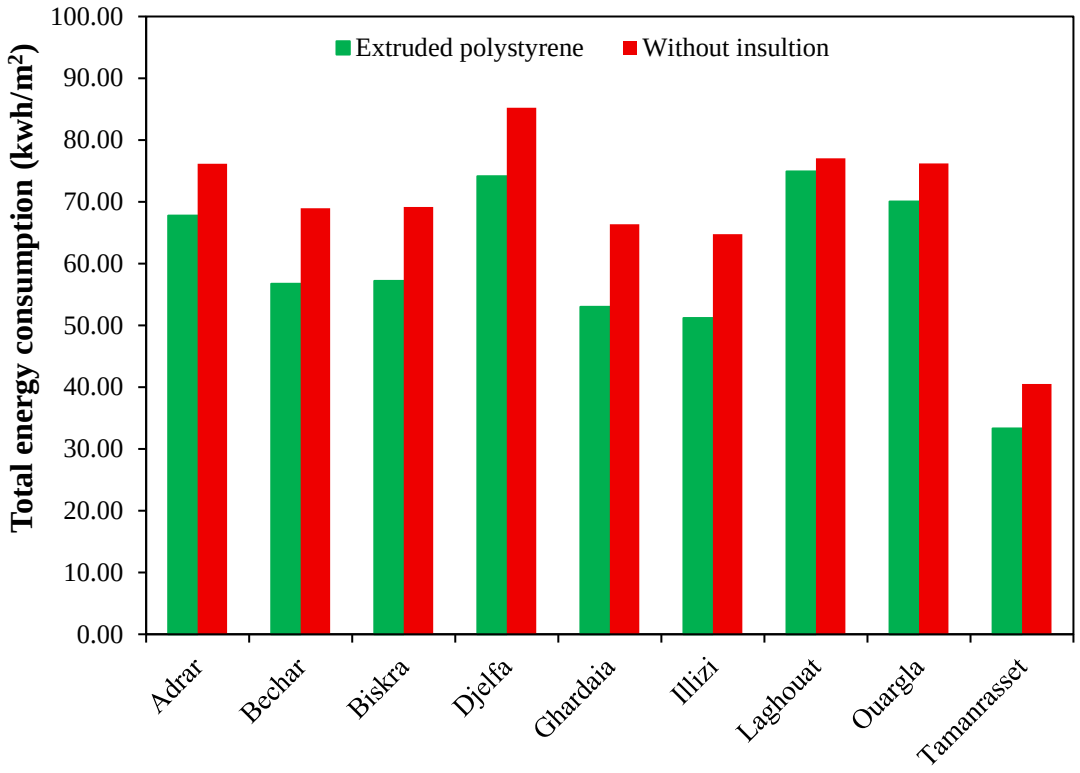

Figure III.4: Effect of extruded polystyrene insulation on energy consumption in various regions.

The optimal insulation thickness varies across regions due to differing climatic conditions, impacting electricity consumption reduction over the course of one year. In Adrar, with an insulation thickness of 0.09 m, electricity consumption decreases by 11.00% annually, reflecting significant energy savings in this hot, arid climate. Bechar, Biskra, Ghardaia, and Illizi all share an optimal thickness of 0.06 m, where annual consumption reductions range between approximately 17% and 21%, demonstrating substantial efficiency gains. Djelfa shows a smaller annual consumption decrease of 13.06% with a minimal insulation thickness of 0.02 m, likely due to its milder climate conditions. Laghouat's optimal thickness is 0.03 m, resulting in a modest 2.76% reduction over the year, indicating limited benefits from insulation in this area. Ouargla, with an optimal 0.07 m thickness, achieves an 8.05% reduction annually, balancing upfront investment and operational savings. Finally, Tamanrasset, at 0.04 m thickness, experiences a 17.78% decrease in yearly electricity consumption, reflecting effective insulation performance for its desert environment. These variations highlight the crucial role of local climate in determining the most cost-effective insulation thickness, optimizing energy efficiency while minimizing costs throughout the year.

2.3.Environmental Impact: CO_2 Emissions Assessment Before and After Insulation

The results shown in Figure (III.5) illustrate the impact of thermal insulation on reducing carbon dioxide (CO2) emissions measured in kg/m² per year across several provinces.

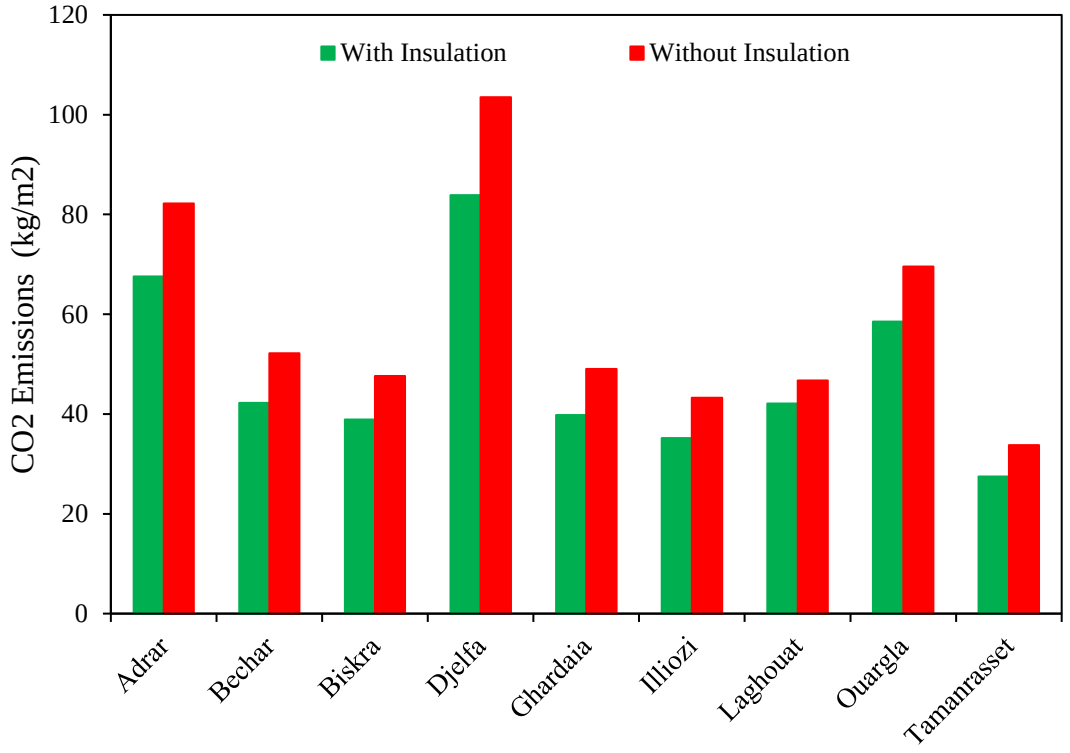

Figure III.5: Impact of extruded polystyrene insulation on annual CO_2 emissions (kg/m²) in residential buildings across different provinces.

The figure clearly demonstrates a significant decrease in CO_2 emissions when insulation is applied compared to cases without insulation. For instance, in Adrar, emissions drop from 82.21 kg/m²/year without insulation to 67.57 kg/m²/year with insulation, representing a reduction of approximately 17.8%. Similar trends are observed in Bechar and Biskra, where emissions decrease by roughly 18.9% and 18.4%, respectively.

The data also reveal that Djelfa, which shows the highest emission rates, experiences a notable improvement, with a 19% reduction following insulation highlighting the effectiveness of insulation particularly in high-emission areas. Other provinces such as Ghardaia, Illizi, and Laghouat exhibit reductions ranging between 9.9% and 18.1%, reinforcing the role of insulation in minimizing heat loss and lowering energy demand.

In Ouargla and Tamanrasset, despite their relatively lower emissions, the figure still shows a considerable decline of 15.8% and 18.6%, respectively. The consistent reduction across all provinces confirms that thermal insulation is an effective and widespread strategy to reduce carbon footprints and improve energy efficiency in residential buildings.

These findings align with existing literature, which emphasizes that thermal insulation reduces heat losses through building envelopes, thereby decreasing the energy required for heating and cooling. Consequently, this leads to a substantial reduction in CO_2 emissions, supporting sustainable development goals.

3. Heat pump

In order to assess the performance of different thermal regulation strategies in Algeria's desert regions, four scenarios were applied across nine provinces with hot arid climates. These scenarios include: (1) Heat Pump combined with Insulation, representing both active and passive thermal control; (2) Heat Pump only, relying solely on active systems; (3) Insulation only, reflecting passive control without mechanical aid; and (4) a baseline scenario with no Heat Pump and no Insulation, illustrating natural indoor temperature response to external climate conditions.

3.1.Adrar

Figure III.6 illustrates the indoor temperature variation throughout the year in the region of Adrar under four different thermal control scenarios: Heat Pump combined with Insulation, Heat Pump only, Insulation only, and a reference case with neither Heat Pump nor Insulation. This figure highlights the impact of each scenario on maintaining thermal comfort under the extreme desert climate of Adrar.

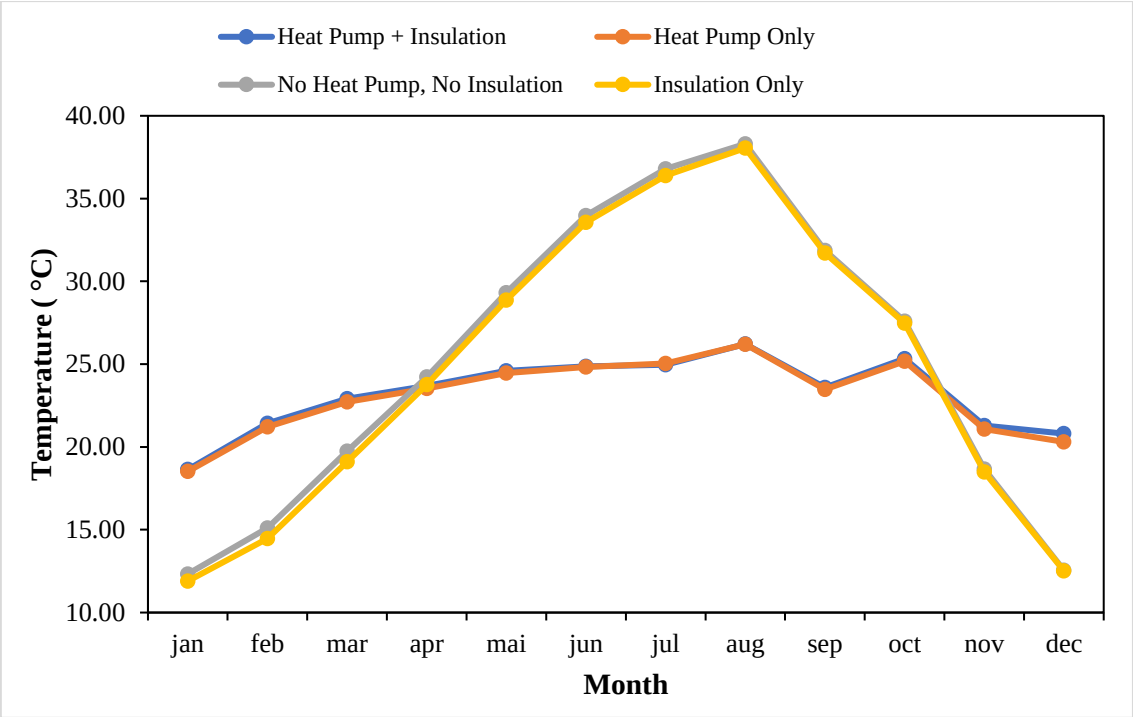

Figure III.6: Indoor temperature profiles throughout the year for different thermal control scenarios in Adrar.

In the heat pump combined with insulation scenario, indoor temperatures remained relatively stable, ranging from 18.64°C in January to 26.21°C in August, with a modest annual variation of 7.57°C. This demonstrates excellent thermal regulation and reduced heat exchange with the exterior environment. Notably, the summer peak of 26.21°C falls within the acceptable range for thermal comfort, making this solution the most effective and energy-efficient option among the four. The integration of both passive and active systems ensures consistent comfort throughout the year with minimal energy consumption.

In the heat pump only scenario (without insulation), the indoor temperature profile was similar, ranging from 18.52°C in January to 26.21°C in August, with a slightly higher annual variation of 7.69°C. While this scenario also maintains indoor temperatures within the comfort range, the absence of insulation results in higher energy demand as the heat pump compensates for thermal losses. Thus, although comfort is achieved, the system is less energy-efficient than the combined solution.

In the insulation only scenario, temperatures varied significantly from 11.90°C in January to 38.05°C in August, leading to an annual range of 26.15°C. While insulation helps reduce heat loss, it does not actively control the indoor temperature. As a result, indoor conditions become

uncomfortable during both winter and summer extremes, exceeding the recommended thermal comfort limits and demonstrating insufficient climate control.

Finally, in the no heat pump and no insulation scenario, indoor temperatures closely mirrored outdoor fluctuations, ranging from 12.33°C in winter to 38.31°C in summer, with a broad annual variation of nearly 26°C. This scenario offers the least thermal comfort and lacks any meaningful thermal control, resulting in severe discomfort for occupants and high potential energy usage if manual heating or cooling is later introduced.

This analysis clearly demonstrates that the combined heat pump and insulation scenario is the most effective in maintaining thermal comfort and reducing energy needs in Adrar's desert climate. The heat pump alone can maintain comfort but requires higher energy input. In contrast, insulation alone or lack of any system results in unacceptable indoor environments due to large temperature swings.

3.2. Béchar

Figure III.7 illustrates the indoor temperature variations over the course of a year in Béchar, comparing the performance of different thermal control strategies.

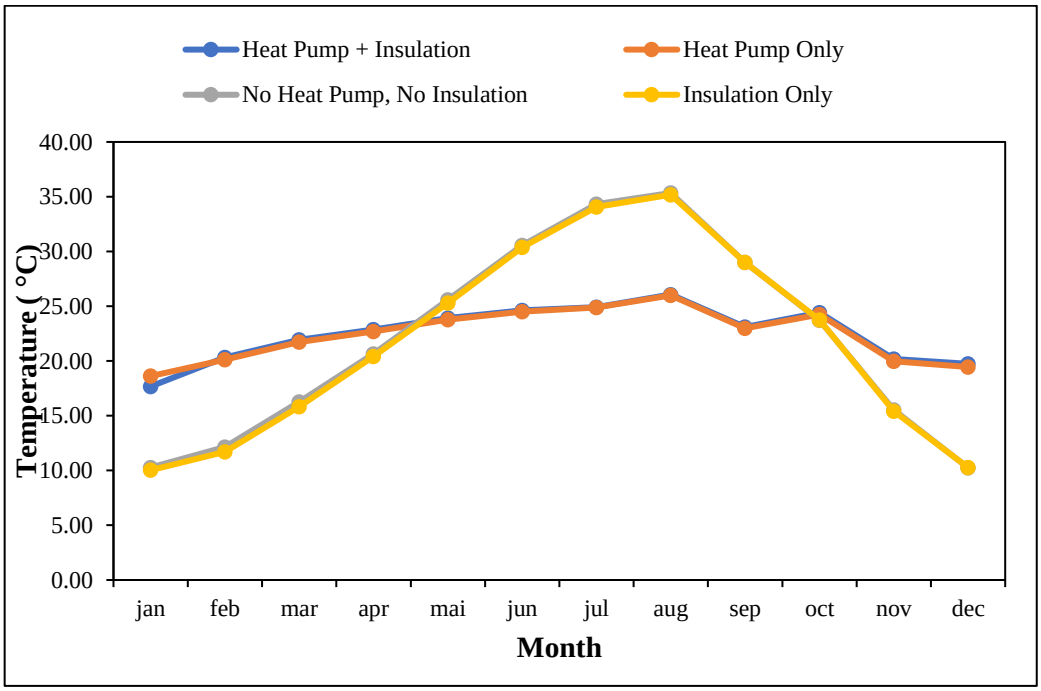

Figure III.7: Indoor temperature profiles throughout the year for different thermal control scenarios in Béchar.

In Béchar, the analysis of indoor temperature profiles under four different thermal control scenarios reveals notable variations in performance and comfort levels.

In the first scenario, which combines a heat pump with insulation, indoor temperatures range from 17.67°C in January to 26.06°C in August, resulting in an annual variation of 8.39°C. This limited fluctuation demonstrates a strong capacity for maintaining thermal stability, as insulation reduces heat transfer while the heat pump actively regulates indoor temperature. The system keeps indoor conditions close to the thermal comfort threshold of 26°C during summer, making it particularly effective in managing the region's hot and dry climate.

The second scenario involves using the heat pump alone, without insulation. Here, temperatures range from 18.62°C in January to 25.99°C in August, with the smallest annual variation of 7.37°C among all configurations. This indicates good thermal control, but the absence of insulation means that more energy is required to maintain comfort, reducing system efficiency. Heat losses are higher, forcing the heat pump to work harder, which may increase energy consumption over time.

In contrast, the third scenario, which features no heat pump and no insulation, exhibits extreme temperature fluctuations. Indoor temperatures span from 10.26°C in January to 35.34°C in August, a wide annual range of 25.07°C. This scenario closely mirrors the outdoor climate, resulting in very uncomfortable conditions inside the building, especially during winter nights and summer afternoons. The lack of any thermal control measures leads to the poorest indoor thermal comfort.

The fourth scenario uses insulation only, without a heat pump. Indoor temperatures vary between 10.02°C in January and 35.18°C in August, with an annual range of 25.16°C. Although insulation helps reduce heat exchange, the absence of active heating or cooling mechanisms results in poor thermal comfort. The building remains cold in winter and hot in summer, highlighting the need for supplementary systems to maintain comfort.

3.3. Biskra

Figure III.8 presents the year-round indoor temperature profiles in Biskra under various thermal control scenarios, highlighting their impact on maintaining thermal comfort.

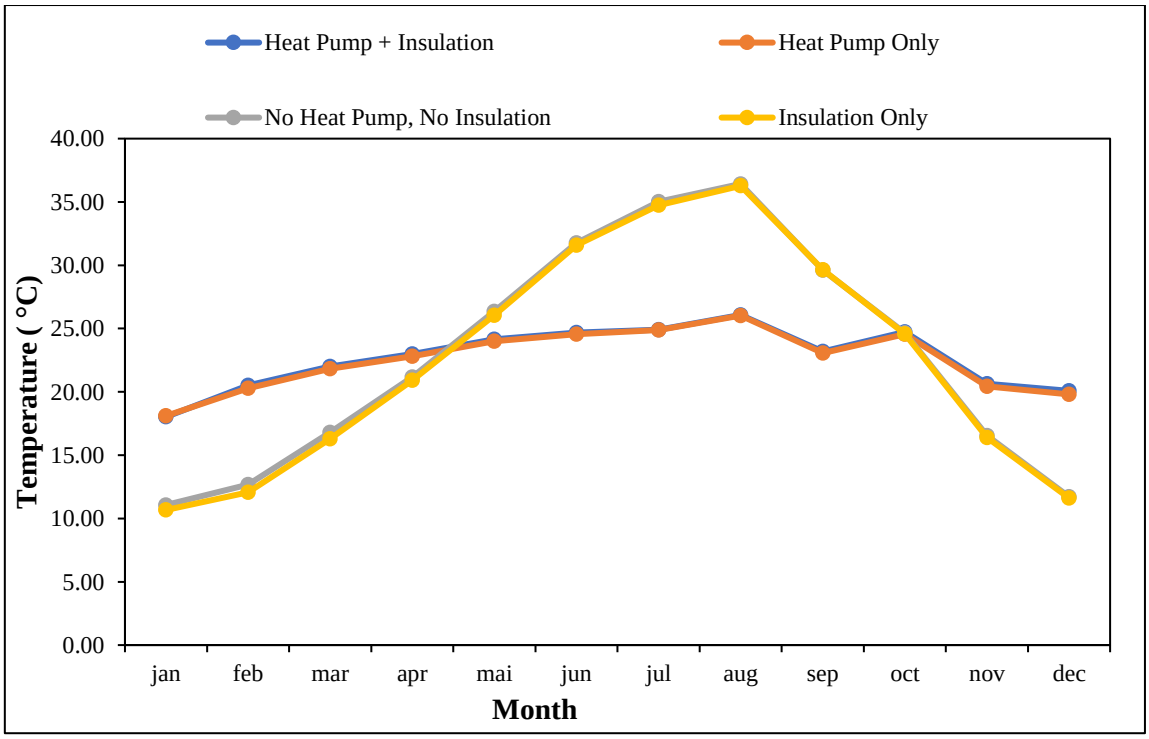

Figure III.8: Indoor temperature profiles throughout the year for different thermal control scenarios in Biskra

In Biskra, the analysis of indoor temperature variations under four different thermal control scenarios provides a comprehensive view of their effectiveness in ensuring thermal comfort, especially given the region's hot climate.

In the scenario combining a heat pump with insulation, indoor temperatures range from 18.02°C in January to 26.07°C in August, resulting in a modest annual temperature fluctuation of 8.05°C. This configuration maintains relatively stable and comfortable temperatures throughout the year. During summer months, temperatures hover close to the upper thermal comfort threshold (26°C), while winter months remain well above the minimum comfort level, indicating a balanced and efficient thermal environment.

In the second configuration using the heat pump only, temperatures span from 18.10°C in January to 26.02°C in August, with a slightly narrower fluctuation of 7.92°C. This setup also provides stable indoor conditions but at the expense of higher energy consumption due to the absence of insulation. The heat pump compensates for heat loss or gains more frequently, especially in extreme weather periods, which may reduce long-term energy efficiency.

In the case of no heat pump and no insulation, temperature values vary significantly from 11.07°C in January to 36.42°C in August, a large annual variation of 25.35°C. These figures reflect near-outdoor thermal behavior, with insufficient mitigation of external climatic extremes. As a result, occupants would experience uncomfortable cold conditions in winter and extreme overheating in summer, making this the least effective scenario.

The scenario using insulation only, without a heat pump, results in indoor temperatures between 10.67°C in January and 36.27°C in August, indicating an annual variation of 25.60°C. Despite the presence of insulation, which slightly reduces the temperature amplitude, the absence of active thermal control leads to severe discomfort during both hot and cold seasons.

3.4.Djelfa

Figure III.9 shows the indoor temperature trends throughout the year in Djelfa, comparing the effects of different thermal control methods on indoor climate stability.

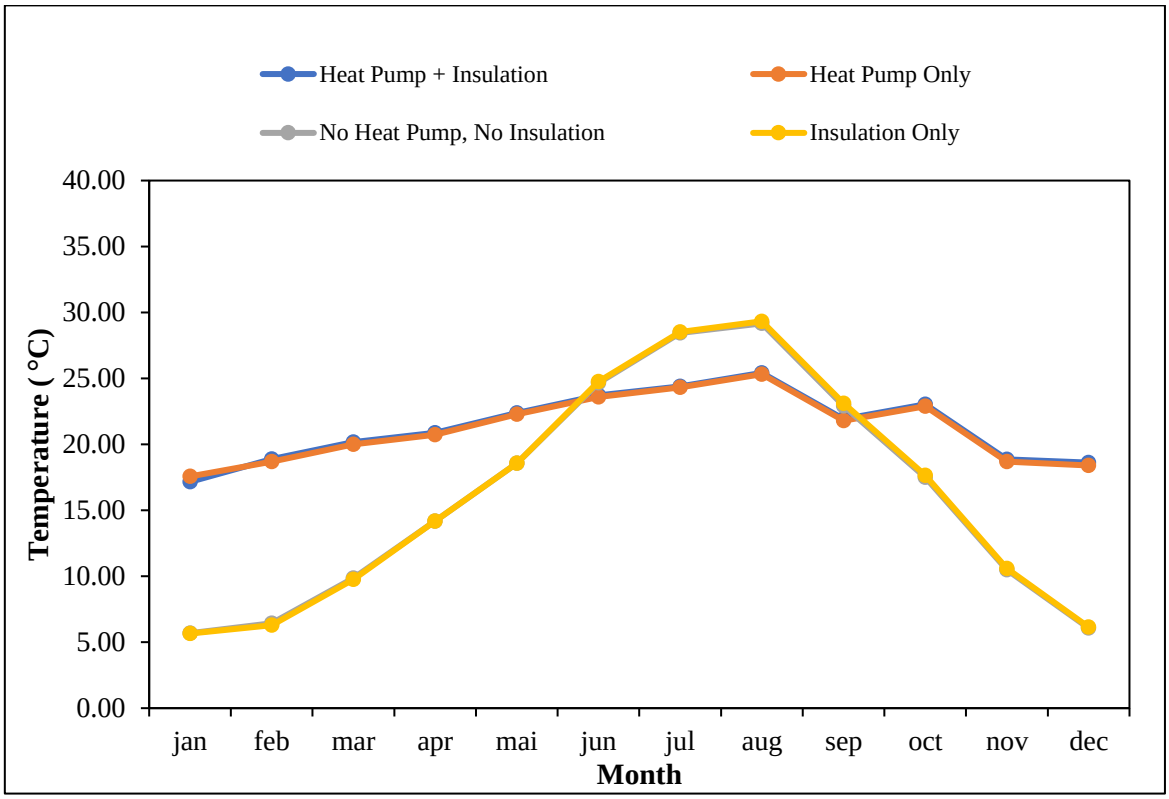

Figure III.9: Indoor temperature profiles throughout the year for different thermal control scenarios in Djelfa.

The analysis of indoor temperature variations in Djelfa reveals the performance of four different thermal control scenarios, highlighting their effectiveness in providing a comfortable indoor environment throughout the year under a dry and moderately cold to warm climate. In the scenario combining a heat pump with insulation, indoor temperatures range from 17.16°C in January to 25.42°C in August, with an annual fluctuation of about 8.26°C. This scenario demonstrates good stability in indoor temperatures year-round, with mild winter temperatures meeting comfort requirements and relatively moderate summer temperatures without extreme overheating, indicating the effectiveness of combining insulation with a heat pump to maintain comfort and reduce temperature fluctuations.

In the case of using the heat pump only, temperatures vary between 17.57°C in January and 25.32°C in August, with a slightly smaller annual fluctuation of 7.75°C. This setup provides stable and acceptable indoor temperatures but lacks insulation, which could reduce heat loss or gain, potentially resulting in higher energy consumption due to more frequent operation of the heat pump to compensate for external temperature changes.

On the other hand, when both the heat pump and insulation are absent, indoor temperatures show significant variations between 5.68°C in January and 29.17°C in August, resulting in a large annual fluctuation of 23.49°C. This scenario clearly reflects outdoor climate influence, with very cold winter temperatures and extreme summer heat creating an uncomfortable indoor environment lacking effective thermal control. In the scenario with insulation only and no heat pump, temperatures range from 5.66°C in January to 29.33°C in August, with an annual fluctuation of 23.67°C, similar to the previous case.

Despite the presence of insulation, the absence of an active heat control system means indoor temperatures are still subject to large uncomfortable fluctuations, especially during cold winters and hot summers, highlighting the necessity of an active thermal control system to ensure occupant comfort. Based on these results, it is clear that the combination of a heat pump with insulation offers the best stable and comfortable indoor environment while enhancing energy efficiency, whereas the lack of an active thermal control system leads to significant temperature variations detrimental to indoor comfort.

3.5. Ghardaia

Figure III.10 illustrates the annual indoor temperature variations in Ghardaia, highlighting the influence of various thermal control scenarios on indoor comfort.

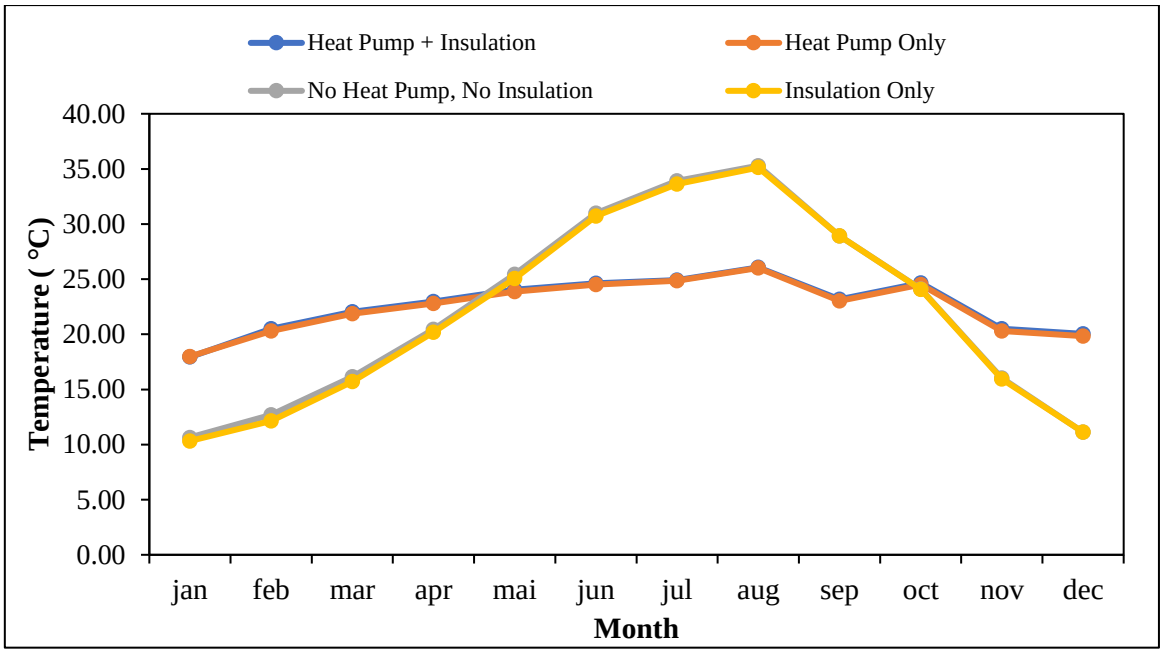

Figure III.10: Indoor temperature profiles throughout the year for different thermal control scenarios in Ghardaia.

The results of the indoor temperature analysis for Ghardaïa under four different thermal control scenarios highlight the impact of each strategy on maintaining comfortable indoor conditions in a hot desert climate. When combining a heat pump with insulation, indoor temperatures range from 17.93°C in January to 26.07°C in August, with an annual fluctuation of about 8.13°C. This scenario ensures good temperature stability throughout the year, providing mild and comfortable winter temperatures and summer conditions that remain close to the upper comfort limit, demonstrating the efficiency of pairing insulation with active thermal control.

In the case of using only the heat pump, indoor temperatures vary between 17.99°C in January and 26.01°C in August, with a similar annual fluctuation of around 8.02°C. Although this scenario maintains stable indoor temperatures, the absence of insulation leads to higher heat losses and gains, causing the heat pump to operate more frequently and potentially increasing energy consumption.

On the other hand, when both the heat pump and insulation are absent, indoor temperatures show a wide range from 10.65°C in January to 35.29°C in August, resulting in a significant annual variation of approximately 24.64°C. This large fluctuation reflects strong influence from the outdoor climate, with very cold winters and extremely hot summers, creating uncomfortable indoor conditions.

Similarly, the scenario with insulation only, without a heat pump, experiences temperatures from 10.32°C in January to 35.12°C in August, with an annual fluctuation close to 24.80°C. Although insulation reduces temperature extremes slightly, the lack of active thermal control results in large and uncomfortable indoor temperature variations during both winter and summer.

3.6. Illizi

Figure III.11 depicts the indoor temperature fluctuations over the year in Illizi, comparing the effectiveness of different thermal control strategies in maintaining comfort.

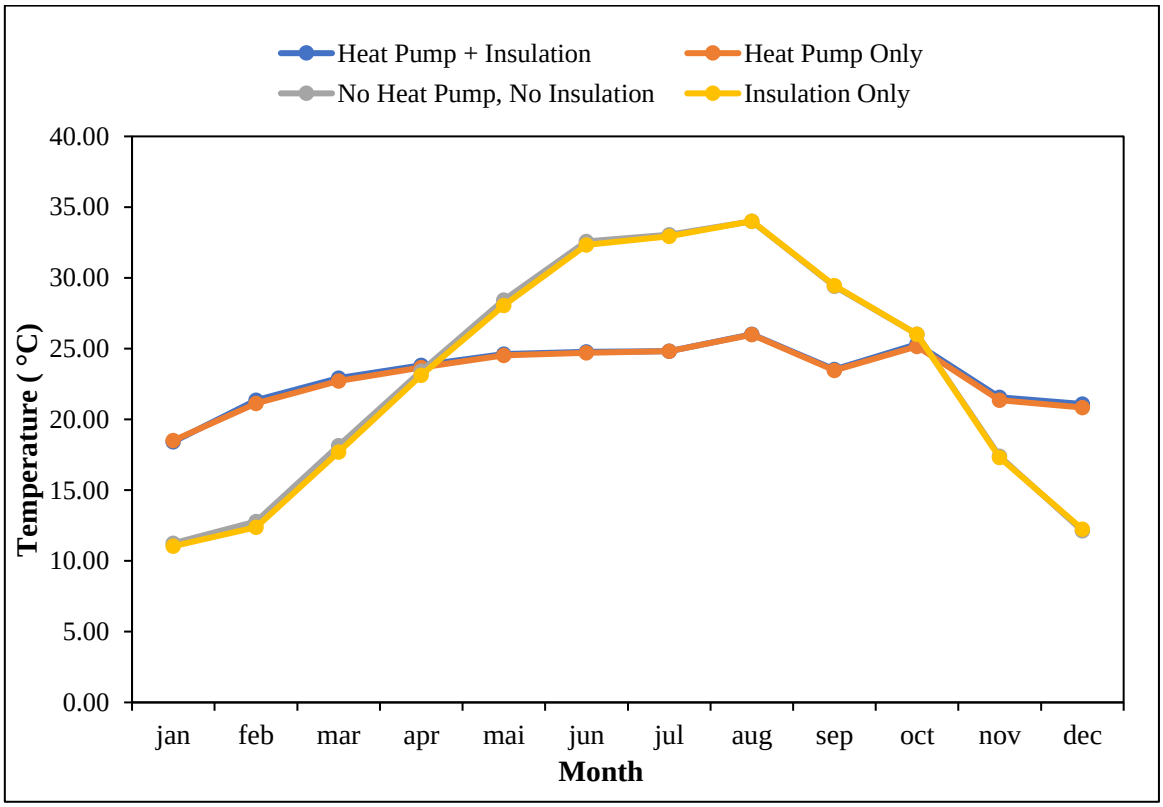

Figure III.11: Indoor temperature profiles throughout the year for different thermal control scenarios in Illizi.

The analysis of indoor temperature variations in Illizi under four different thermal control scenarios highlights the effectiveness of each strategy in ensuring thermal comfort in this region's hot climate. When combining a heat pump with insulation, indoor temperatures range from 18.42°C in January to 26.01°C in August, with an annual variation of approximately 7.59°C. This setup maintains stable and comfortable indoor conditions throughout the year, with mild winters and summer temperatures near the upper comfort threshold, demonstrating the benefits of combining insulation with active thermal regulation.

Using the heat pump only, temperatures vary slightly from 18.51°C in January to 25.99°C in August, with an annual fluctuation close to 7.48°C. While this scenario offers relatively stable temperatures, the absence of insulation causes higher heat losses and gains, leading to more frequent operation of the heat pump and potentially greater energy consumption.

In the case of no heat pump and no insulation, indoor temperatures fluctuate widely between 11.25°C in January and 34.00°C in August, resulting in a large annual variation of roughly 22.75°C. This reflects strong influence from outdoor extremes, causing uncomfortable cold winters and excessively hot summers.

Similarly, with insulation only and no heat pump, indoor temperatures range from 11.04°C in January to 34.01°C in August, with an annual variation near 22.97°C. Although insulation reduces temperature swings somewhat, the lack of active thermal control results in significant discomfort during both cold and hot seasons.

3.7. Laghouat

Figure III.12 displays the yearly indoor temperature variations in Laghouat, illustrating the impact of various thermal control scenarios on indoor thermal comfort.

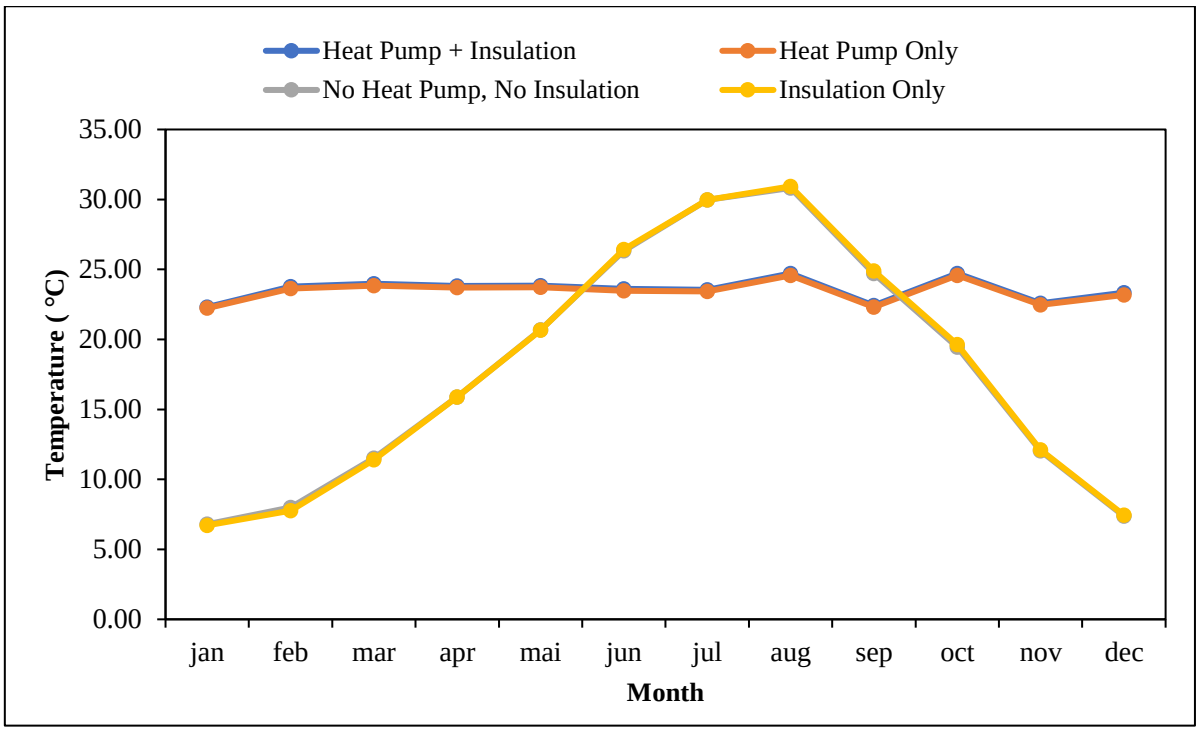

Figure III.12: Indoor temperature profiles throughout the year for different thermal control scenarios in Laghouat.

The evaluation of indoor temperature variations in Laghouat under four different thermal control scenarios reveals significant differences in thermal comfort outcomes. When combining a heat pump with insulation, indoor temperatures remain quite stable, ranging from 22.31°C in January to 24.71°C in October, with relatively small annual fluctuations. This scenario ensures a comfortable indoor environment year-round, with temperatures staying well within typical thermal comfort limits, highlighting the synergy of active heating/cooling with insulation.

Using the heat pump only, temperatures show a similar trend, fluctuating between 22.23°C in January and 24.58°C in October. While this setup also maintains stable indoor conditions, the lack of insulation likely leads to higher energy consumption due to increased heat transfer through the building envelope.

In the absence of both heat pump and insulation, indoor temperatures vary widely, ranging from a low of 6.79°C in January to a high of 30.82°C in August, showing a large annual variation of nearly 24°C. This wide fluctuation reflects significant influence from external weather extremes, resulting in cold indoor conditions in winter and excessive heat in summer, which is far from ideal for occupant comfort.

Similarly, when only insulation is used without a heat pump, indoor temperatures range from 6.72°C in January to 30.93°C in August, with temperature swings nearly as large as the no-control scenario. Although insulation slightly reduces thermal variation, the lack of active heating or cooling means indoor comfort is still compromised during extreme weather periods.

3.8. Ouargla

Figure III.13 presents the indoor temperature variations over the year in Ouargla, highlighting the effects of different thermal control scenarios on maintaining indoor comfort.

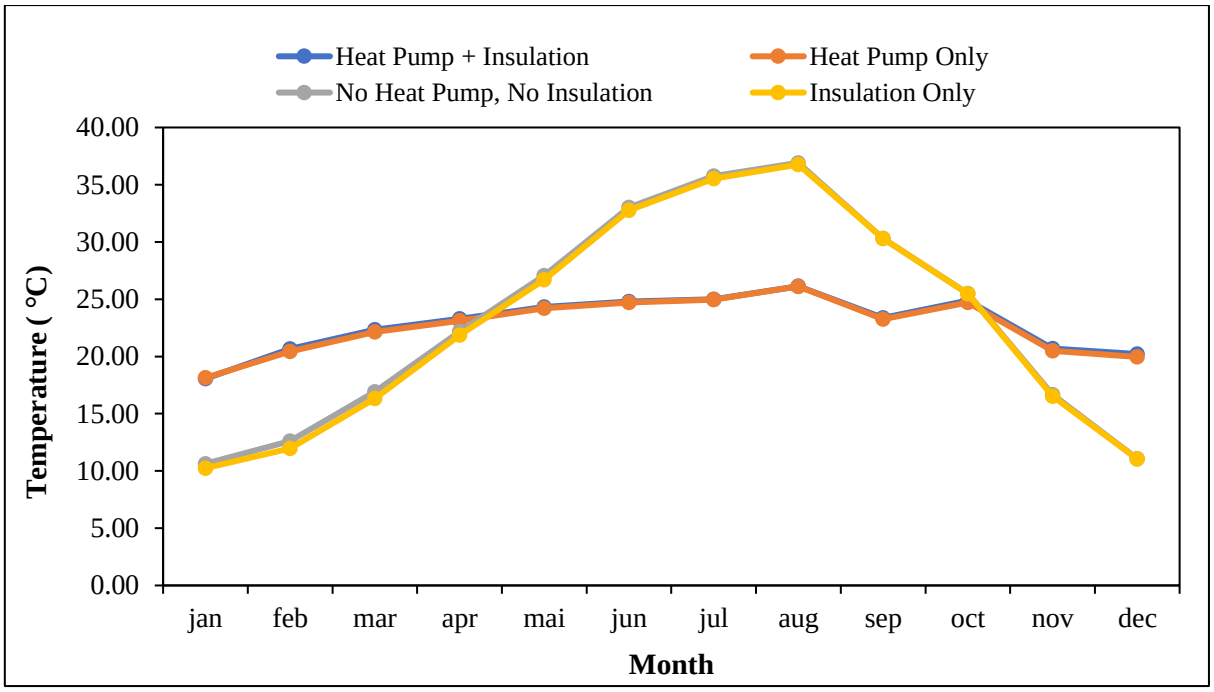

Figure III.13: Indoor temperature profiles throughout the year for different thermal control scenarios in Ouargla.

The evaluation of indoor temperature fluctuations in Ouargla under four different thermal management approaches reveals clear contrasts in their capacity to sustain thermal comfort. When both a heat pump and insulation are used, indoor temperatures remain fairly steady, ranging from 18.06°C in January up to 26.13°C in August. This setup effectively moderates indoor climate, ensuring comfort throughout the year by minimizing the impact of outdoor temperature extremes.

In the heat pump only scenario, indoor temperatures show a similar pattern, varying between 18.13°C in January and 26.12°C in August. However, the lack of insulation means more heat is lost or gained through the building envelope, likely resulting in increased energy consumption to maintain these conditions.

Without either a heat pump or insulation, indoor temperatures experience significant swings, dropping to 10.63°C in January and rising to 36.91°C in August. These wide variations mirror outdoor conditions closely, causing cold interiors in winter and excessive heat in summer, thus compromising occupant comfort.

With insulation alone, but no heat pump, temperatures fluctuate from 10.24°C in January to 36.76°C in August, showing only slight improvement compared to having no controls. While

insulation helps to somewhat buffer temperature changes, the absence of active heating or cooling leaves occupants vulnerable to discomfort during seasonal extremes.

3.9. Tamanrasset

Figure III.14 illustrates the annual indoor temperature patterns in Tamanrasset, comparing the performance of various thermal control strategies in ensuring indoor comfort.

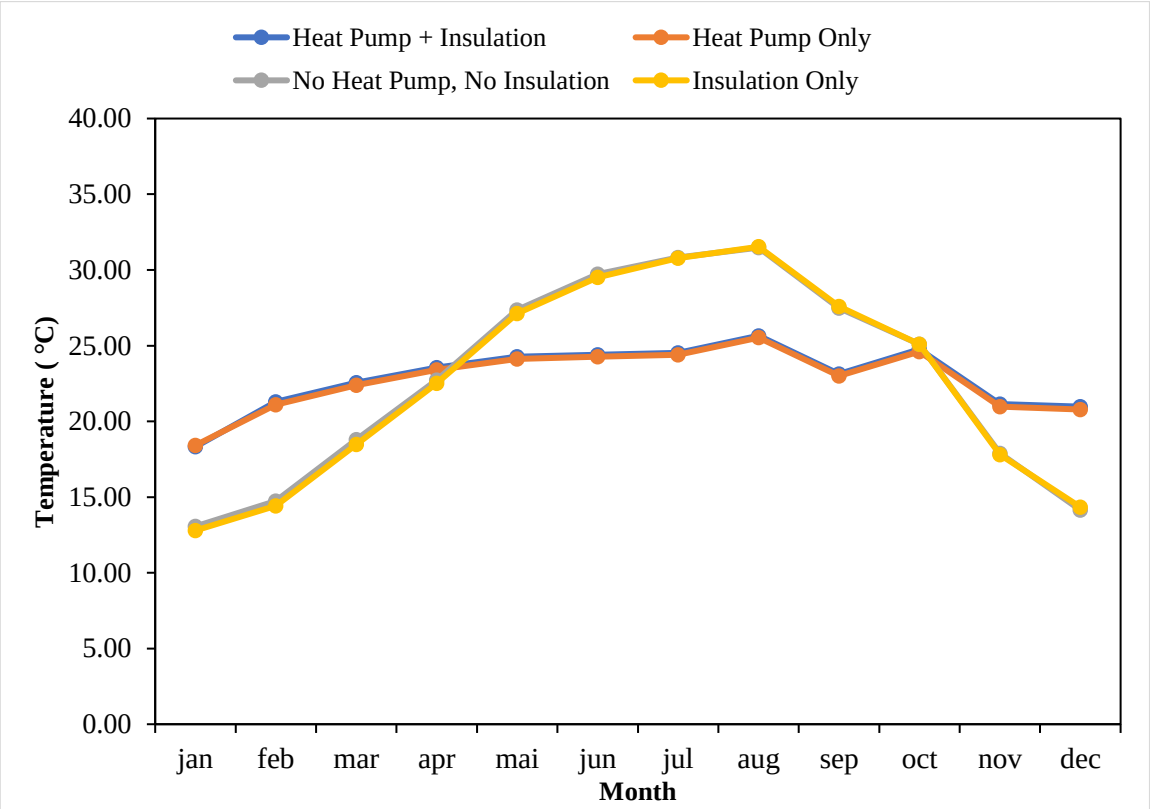

Figure III.14: Indoor temperature profiles throughout the year for different thermal control scenarios in Tamanrasset.

The evaluation of indoor temperature patterns in Tamanrasset under four distinct thermal control scenarios reveals notable differences in maintaining a comfortable indoor climate. The scenario combining both a heat pump and insulation results in the most consistent indoor temperatures, ranging from 18.32°C in January to 25.66°C in August. This setup effectively minimizes the impact of external weather extremes, providing a steady and pleasant indoor environment year-round.

When relying solely on the heat pump without insulation, temperatures fluctuate slightly between 18.42°C in January and 25.53°C in August. While this approach can maintain comfort,

the lack of insulation means the building loses or gains heat more rapidly, which likely leads to increased energy consumption.

In the absence of both heat pump and insulation, indoor temperatures vary dramatically, with lows around 13.06°C in January and highs reaching 31.48°C in August. This wide variation mirrors outdoor conditions closely, exposing occupants to cold winters and excessively hot summers, which significantly compromises comfort.

Using insulation alone, without a heat pump, results in indoor temperatures from 12.79°C in January up to 31.53°C in August. Although insulation helps to some extent by reducing temperature swings, the lack of active heating or cooling means that the indoor environment still faces uncomfortable extremes during the year.

4. Conclusion

The detailed analyses concluded that thermal insulation using expanded polystyrene provides superior thermal performance compared to fiberglass, especially in hot regions. It was also found that combining insulation with a heat pump offers the best thermal comfort conditions inside the building with minimal energy consumption, while using either system alone remains less efficient. From an economic perspective, the optimal insulation thickness was identified based on the intersection of initial cost and operational cost curves, which varies from one region to another depending on the climate. Additionally, insulation contributed to a significant reduction in carbon emissions across all studied areas. These results reflect the great potential of applying climate-adapted design solutions to enhance the sustainability of buildings in desert environments.

General Conclusion

General Conclusion

In conclusion, this study highlights the effectiveness of integrating thermal insulation with an air-to-air heat pump system as a strategic solution for enhancing energy efficiency and indoor thermal comfort in hot and semi-arid regions of Algeria. Through detailed numerical simulations across nine provinces, it was demonstrated that the combination of passive and active systems yields the most significant improvements in energy performance, economic feasibility, and environmental impact.

The addition of thermal insulation alone led to substantial reductions in energy consumption, with heating loads decreasing by up to 60% and cooling loads by approximately 40% in some regions such as Adrar and Biskra. In Laghouat, for instance, heating demand was reduced from 61.85 kWh/m² to 46.27 kWh/m² and cooling demand from 15.21 to 11.00 kWh/m² by applying insulation up to 30 cm thick

Furthermore, insulation thicknesses as low as 6 cm in Biskra and Béchar resulted in annual electricity savings ranging between 17% and 21%

From an environmental perspective, insulation significantly lowered CO_2 emissions. In Adrar, emissions decreased from 82.21 to 67.57 kg/m²/year—representing a reduction of 17.8%. Similar trends were observed in Béchar (−18.9%) and Biskra (−18.4%). Even in provinces with initially lower emission levels, such as Ouargla and Tamanrasset, reductions of 15.8% and 18.6%, respectively, were achieved.

Regarding thermal comfort, the scenario combining insulation with a heat pump consistently delivered indoor temperatures within the optimal comfort range. In Adrar, indoor temperatures ranged from 18.64°C in January to 26.21°C in August, maintaining a limited annual variation of only 7.57°C. In contrast, the reference case without any thermal control exhibited extreme indoor temperatures from 12.33°C to 38.31°C, leading to a 26°C fluctuation and severe discomfort

Similar performance was confirmed in Tamanrasset, where the combined system maintained indoor temperatures between 18.32°C and 25.66°C year-round

Altogether, the study validates that neither insulation nor heat pumps alone are sufficient to achieve ideal performance in harsh climates. Only their synergy provides stable thermal conditions, lowers operational costs, and significantly reduces environmental impact. These findings support a strong case for promoting combined passive and active energy strategies in national policies for sustainable building development, especially in Algeria's desert and semi-desert regions.

References

References

1. ADEME. (2023). L'efficacité énergétique dans le secteur résidentiel : Défis et opportunités. Hors collection. https://librairie.ademe.fr [Consulté le 18 avril 2025]
2. **Alger Froid.** (2023). *Laine de verre 1.20cm/40cm*. Alger Froid. Retrieved [15/05/2025], from: https://alger-froid.com/index.php/produit/laine-de-verre-1-20cm-40cm/
3. Assly. (2025). *Plaque polystyrène D25 0.5 cm d'épais feuille de 02 m².* Retrieved June 10, 2025, from https://www.assly.dz/product/plaque-polystyrene-d25-05-cm-d-epais-feuille-de-02-m/
4. Awan, U. K. (2012). Experimental analysis of variable capacity heat pump system equipped with vapour injection and permanent magnet motor (Master's thesis). Royal Institute of Technology, Stockholm, Sweden.
5. Barbouchi, S. (2007). Pompe à chaleur air/eau haute température pour la réhabilitation du chauffage dans l'habitat existant (Doctoral dissertation). École des Mines de Paris.
6. Bechahe, K. (2021). *Situation de l'élevage camelin laitier dans la zone péri-urbaine de la région de Ouargla : contraintes et perspectives* [Master's thesis, Université Kasdi Merbah Ouargla].
7. Benamrane, N., Boukdir, A., & Bounoua, L. (2018). Urban microclimate and energy demand in coastal cities: The case of Algiers. Energy and Buildings, 173, 135–146.
8. Benouar, D., & Messaoud, M. (2019). Towards energy efficiency in Algerian buildings: Challenges and opportunities. Journal of Sustainable Architecture and Civil Engineering, 25(2), 45–55.
9. Benouaz, T., & Belhamel, M. (2002). Passive cooling and energy conservation in buildings in hot and dry climates. *Renewable Energy*, *27*(3), 339–347. https://doi.org/10.1016/S0960-1481(01)00191-0
10. Bensaid, A., Boukhatem, M. N., & Touil, D. (2021). Assessment of energy consumption in Algerian residential buildings: A review. Renewable and Sustainable Energy Reviews, 145, 111058.
11. Bhatia, A. (2024.). Heat Pumps for Heating and Cooling Cours. CED Engineering. Retrieved, [03/04/2025], from https://www.cedengineering.com/userfiles/M06-047%20-%20Heat%20Pumps%20for%20Heating%20and%20Cooling%20-%20US.pdf

12. Bhatia, S. C. (2014). Solar thermal energy. In *Advanced Renewable Energy Systems* (pp. 94–143). Elsevier. https://doi.org/10.1016/B978-1-78242-269-3.50004-8
13. Bouabdallah, S., Amara, M., & Belarbi, R. (2020). Climate change and energy demand in Algeria: An overview. International Journal of Environmental Science and Technology, 17(3), 1439–1450.
14. Chamoun, M. (2012). Modélisation, conception et étude expérimentale d'une pompe à chaleur industrielle à eau à haute température (Doctoral dissertation). Institut National des Sciences Appliquées de Lyon.
15. Chel, A., Messaoudi, L., & Gharbi, L. (2019). Energy performance analysis using dynamic simulation tools: Case of TRNSYS and EnergyPlus. Energy Reports, 5, 1275–1283.
16. Cherif, H., Khettab, N., & Chikhi, A. (2017). Passive design strategies for mountainous regions in Algeria. Building Simulation, 10(6), 877–889.
17. CNES. (2021). Évaluation des zones sahariennes pour les applications solaires. Centre National d'Études Spatiales d'Algérie.
18. CSTB. (2022). Heat pumps in building regulations: RE2020. Centre Scientifique et Technique du Bâtiment.
19. Daouas, N. (2011). A study on optimum insulation thickness in walls and energy savings in Tunisian buildings based on analytical calculation of cooling and heating transmission loads. *Applied Energy, 88*(1), 156–164. https://doi.org/10.1016/j.apenergy.2010.07.030
20. Derradji, L., Bounoua, M., & Haddadi, M. (2017). Impact of expanded polystyrene insulation thickness on thermal performance of prototype buildings in Algeria. Energy and Buildings, 140, 270–281.
21. Dobayci, S. (2007). Energy efficiency improvement of a thermal power plant. *Energy Conversion and Management, 48*(7), 2147–2153. https://doi.org/10.1016/j.enconman.2007.01.013
22. Ecodom. (2013). La qualité thermique des bâtiments dans les DOM: Guide technique.
23. Elsayed, M. F., Malkawi, A. M., & Abed, S. (2019). Life cycle cost analysis for optimum insulation thickness of building walls in Palestine. Energy Reports, 5, 1124–1134.
24. Eurostat. (2024). *Electricity price statistics*. European Commission. Retrieved [17/04/2025], from https://ec.europa.eu/eurostat/statistics-explained/index.php?title=Electricity_price_statistics
25. Gaussen, H. (1957). *Zones climatiques du globe terrestre*. Toulouse: Centre National de la Recherche Scientifique (CNRS).

26. Ghedamsi, R., Settou, N., Gouareh, A., & Khamouli, A. (2016). A bottom-up approach for forecasting residential energy demand in Algeria. Energy Policy, 92, 93–105.

27. Ghedamsi, R., Settou, N., Gouareh, A., Khamouli, A., Saifi, N., Recioui, B., & Dokkar, B. (2016). Modeling and forecasting energy consumption for residential buildings in Algeria using bottom-up approach. *Energy and Buildings, 121*, 309–317. https://doi.org/10.1016/j.enbuild.2015.12.030

28. Ghrib, T., Labed, A., & Abene, A. (2018). Climate variability and its impact on building energy needs in Algeria. Energy Procedia, 153, 130–135.

29. Hamdi, K. (2016). *Étude thermique d'une maison traditionnelle de la ville de Tamanrasset* [Master's thesis, Université Saâd Dahlab Blida].

30. International Energy Agency (IEA). (2021). Heat pumps..]. Retrieved [21/02/2025], from https://www.iea.org/search/charts?q=Heat%20Pumps&page=1

31. IRENA. (2020). Renewable energy integration with heat pumps. International Renewable Energy Agency.

32. Itho Daalderop. (2024). Une pompe à chaleur convient-elle à votre maison ? [Brochure PDF]. Retrieved [21/02/2025], from:www.ithodaalderop.be

33. Jason Brown Plumbing & Gas. (2005). Energy efficient hot water heat pump systems. Retrieved [15/02/2025], from:https://www.jasonbrownplumbing.com.au/hot-water-heat-pumps.

34. Kadraoui, H., Bekkouche, S. M. E. A., & Chikhaoui, A. (2019). Analysis of energy consumption for Algerian buildings in extreme North-African climates. *International Journal of Sustainable Energy Planning and Management, 19*, 45–58. https://doi.org/10.5278/IJSEPM.2019.19.5

35. Kaushik, A. K., Arif, M., Syal, M. M. G., Rana, M. Q., Oladinrin, O. T., Sharif, A. A., & Alshdiefat, A. S. (2022). Effect of indoor environment on occupant air comfort and productivity in office buildings: A response surface analysis approach. *Sustainability*, *14*(23), 15719. https://doi.org/10.3390/su142315719

36. Khenfer, A., Chacha, A. (2018). Modélisation des consommations d'énergie du secteur résidentiel en Algérie à long terme. Mémoire Master. Université Kasdi Merbah Ouargla.

37. Khoukhi, M. (2018). Effects of heat and humidity on thermal conductivity of polystyrene insulation in building applications. Building and Environment, 136, 182–190.

38. Kimco Insulation. (2024). Glass wool insulation blanket specification. Retrieved [10/04/2025], from: https://pdt.static.globalsources.com/IMAGES/PDT/SPEC/269/K1215809269.pdf.
39. Kinab, E. (2009). Optimisation des performances non nominales des pompes à chaleur réversibles pour le secteur tertiaire (Doctoral dissertation). École Nationale Supérieure des Mines de Paris. https://pastel.archives-ouvertes.fr/pastel-00566590
40. Mebarki, A., Amirat, M., & Hamidat, A. (2020). Modeling uncertainty in energy consumption predictions for residential buildings. Energy and Buildings, 223, 110062.
41. Medjelekh, A. (2006). Classification climatique de l'Algérie. Office National de la Météorologie. These magister en genie climatique , Université Frère Mentouri - Constantine 1
42. Messaoudi, L., Chel, A., & Touati, F. (2021). Evaluation of energy-saving strategies in Algerian buildings. Energy Efficiency, 14(2), 25–37.
43. Messaoudi, L., Settou, B., Belkheir, A., & Gouareh, A. (2024). Climate-based bottom-up modeling of residential energy demand in Algeria. Journal of Building Performance, 15(1), 45–63.
44. Ministère de l'Habitat et de l'Urbanisme. (MHU) (2010). *Document de Réglementation Thermique dans les Bâtiments (DTR C3.5)*. Centre National d'Études et de Recherches Intégrées du Bâtiment (CNERIB), Algeria.
45. Mokhtara, C., Negrou, B., Bouferrouk, A., Yao, Y., Settou, N., & Ramadan, M. (2020). Integrated supply–demand energy management for optimal design of off-grid hybrid renewable energy systems for residential electrification in arid climates. *Energy Conversion and Management, 221*, 113192. https://doi.org/10.1016/j.enconman.2020.113192
46. Mokhtara, C., Negrou, B., Settou, N., Gouareh, A., & Settou, B. (2019a). Pathways to plus-energy buildings in Algeria: Design optimization method based on GIS and multi-criteria decision-making. *Energy Procedia, 162*, 171–180. https://doi.org/10.1016/j.egypro.2019.04.019
47. Mourshed, M. (2012). Relationship between annual mean temperature and degree-days. *Energy and Buildings, 54*, 418–425. https://doi.org/10.1016/j.enbuild.2012.07.024
48. Neya, I., Chikhi, A., & Mebarki, A. (2021). Thermal performance evaluation of compressed stabilized earth blocks with different insulation materials in hot dry climates. Sustainable Cities and Society, 72, 103057.

49. Office National de la Météorologie (ONM). (2018). *Données climatiques de la station de Laghouat (2008–2017)* [Climatic data set]. Algeria: ONM.
50. Office National de la Météorologie. (ONM). (2021). Régionalisation des normales annuelles des températures en Algérie par la méthode K-means. Retrieved [07/05/2025], from: https://onm-blog.meteo.dz/wp-content/uploads/2024/08/Article_Bousri.pdf
51. Omer, A. M. (2012). *Performance analysis of ground source heat pumps for building applications* [PhD thesis, University of Nottingham]. https://doi.org/10.17863/CAM.13766
52. Özel, M. (2011). Thermal performance and optimum insulation thickness of building walls with different structure materials. *Applied Thermal Engineering, 31*(17), 3854–3863. https://doi.org/10.1016/j.applthermaleng.2011.07.033
53. Ozel, M. (2019). Influence of glazing area on optimum thickness of insulation for different wall orientations. *Applied Thermal Engineering, 147*, 770–780. https://doi.org/10.1016/j.applthermaleng.2018.10.104
54. Ozel, M. (2019). Numerical investigation of glazing area and wall orientation effects on optimum insulation thickness: Case study Elazığ, Turkey. Energy and Buildings, 199, 120–132.
55. Rahhal, C. (2006). Conception d'une pompe à chaleur air/eau à haute efficacité énergétique pour la réhabilitation d'installations de chauffage existantes (Doctoral dissertation). École des Mines de Paris.
56. Rosti, M., Aghamolaei, R., & Tahsildoost, M. (2020). Optimal insulation thickness in buildings for different climate zones of Iran. Journal of Building Engineering, 32, Article 101790. https://doi.org/10.1016/j.jobe.2020.101790
57. Saheb, Y., Chikhi, A., & Mebarki, A. (2019). Solar potential and energy performance in desert regions of Algeria. Renewable Energy, 132, 1088–1097.
58. Saif, N., Belatrache, D., Ghedamsi, R., Messaoudi, D., Dokkar, B., Rahmouni, S., & Settou, N. (2024). Modeling energy consumption of the residential sector in Algeria in the long term. *Euro-Mediterranean Journal for Environmental Integration*.
59. Sârbu, I., & Sebarchievici, C. (2010). Heat pumps – Efficient heating and cooling solution for buildings. Buletinul Institutului Politehnic din Iași. Secția Construcții și Arhitectură, 56(2), 45–56.

60. Self, S. J., Reddy, B. V., & Rosen, M. A. (2013). Ground source heat pumps for heating: Parametric energy analysis of a vapor compression cycle utilizing an economizer arrangement. Applied Thermal Engineering, 52(2), 245–254.

61. Semahi, S., Benbouras, M. A., Mahar, W. A., Zemmouri, N., & Attia, S. (2020). Development of spatial distribution maps for energy demand and thermal comfort estimation in Algeria. *Sustainability, 12*(15), 6066. https://doi.org/10.3390/su12156066

62. Shuyang, Z., Lun, Z., & Xiaosong, Z. (2017). Performance evaluation of existing ground source heat pump systems in buildings using auxiliary energy efficiency index: Case study in Jiangsu, China. Energy and Buildings, 147, 90–100.

63. Staffell, I., Scamman, D., Velazquez Abad, A., Balcombe, P., Dodds, P. E., Ekins, P., Shah, N., & Ward, K. R. (2019). The role of hydrogen and fuel cells in the global energy system. *Energy & Environmental Science, 12*(2), 463–491. https://doi.org/10.1039/C8EE01157E

64. The Weather Channel. (n.d.). *10-Day Weather Forecast for Illizi, Algeria* [Website]. Retrieved from https://weather.com/ar-SY/weather/tenday/l/Illizi%2BIllizi%2BAlgeria

65. TRNSYS 18. (2015). *A TRaNsient SYstem Simulation program: Volume 4 – Mathematical Reference*. Solar Energy Laboratory, University of Wisconsin-Madison. Retrieved from http://sel.me.wisc.edu/trnsys

66. United Nations Development Programme (UNDP). (2022). Climate resilience and energy policy in arid regions: Algeria report. Retrieved [03/02/2025], from: https://www.undp.org/sites/g/files/zskgke326/files/2023-04/Annual-Report-2022.pdf

67. Weather and Climate. (n.d.). *Average monthly Rainfall, Sunshine, Temperatures in Illizi, Algeria* [Website]. Retrieved from https://weather-and-climate.com/average-monthly-Rainfall-Temperature-Sunshine%2CIllizi%2CAlgeria

68. Xiao, B., He, L., Zhang, S., Kong, T., Hu, B., & Wang, R. Z. (2020). Comparison and analysis on air-to-air and air-to-water heat pump heating systems. Renewable Energy, 146, 1888–1896.

69. Yuan, Z., Wu, H., & Luo, X. (2017). An efficient algorithm for multi-objective optimization of building energy consumption and indoor environment. *Energy and Buildings, 140*, 356–367. https://doi.org/10.1016/j.enbuild.2017.01.057

70. Zhang, Q., Wang, Z., Yang, C., Niu, Q., & Jia, L. (2017). Field test analysis of an urban sewage source heat pump system performance. Energy Procedia, 143, 131–136. https://doi.org/10.1016/j.egypro.2017.12.062ز

71. Zhuang, Z., Zhao, J., Mi, F., Zhang, T., Hao, Y., & Li, S. (2023). Application and analysis of a heat pump system for building heating and cooling using extracting heat energy from untreated sewage. Department of Thermal Energy Engineering, Shandong Jianzhu University, China.
72. Alyami, M. M. (2022). An approach to enhancing energy performance in residential buildings in hot climate regions (The case of Saudi Arabia) Doctoral dissertation, University of Nottingham.
73. Meftah, N., & Mahri, Z. L. (2022). Analysis of Algerian energy efficiency measures in buildings for achieving sustainable development goals. Journal of Renewable Energy and Environment, 1(1). https://doi.org/10.54966/jreen.v1i1.1030

Annex A

Overview of TRNSYS 18:

TRNSYS is a transient systems simulation program with a modular structure. It recognizes a system description language in which the user specifies the components that constitute the system and the manner in which they are connected. The TRNSYS library includes many of the components commonly found in thermal and electrical energy systems, as well as component routines to handle input of weather data or other time dependent forcing functions and output of simulation results. The modular nature of TRNSYS gives the program tremendous flexibility, and facilitates the addition to the program of mathematical models not included in the standard TRNSYS library. TRNSYS is well suited to detailed analyses of any system whose behaviour is dependent on the passage of time. TRNSYS has become reference software for researchers and engineers around the world. Main applications include: solar systems (solar thermal and photovoltaic systems), low energy buildings and HVAC systems, renewable energy systems, cogeneration, fuel cells (TRNSYS 18., 2015).

Table 1: Description of components and capabilities in thermal simulation

Type	Component name	Logo	Description
56	Multi-Zone Building	 Building	This component models the thermal behavior of multi-zone buildings using a building description file generated by TRNBuild.
15	Weather Data Processor	 Weather	This component reads and interpolates weather data, providing it to TRNSYS and calculating key temperatures and seasonal factors.
77	Soil Temperature Profile	 Type77	models ground temperature profiles using annual surface temperature data and soil properties. Detailed info is in the referenced document
65	Online graphical plotter	 Q_heat_cool_Plotter	The Online Graphics component displays selected system variables in real-time during simulation. It helps users quickly identify performance issues but does not generate an output data file.
25	Printer	 Type25b	The Printer outputs system variables at set time intervals, using either relative or absolute time. It includes unit labels, can add a header, and either appends or overwrites the output file.

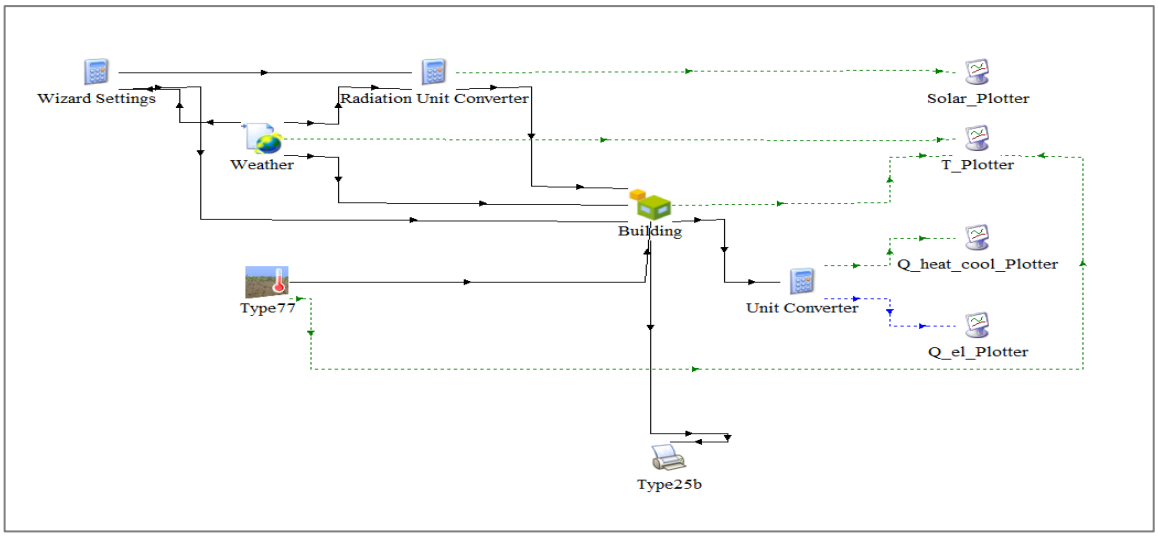

Figure 1: TRNSYS 18 interface and Type56 configuration

Abstract

In hot and semi-arid regions like southern Algeria, achieving thermal comfort while reducing energy consumption is a major challenge due to significant temperature fluctuations. This study focuses on combining thermal insulation and heat pump systems as a joint strategy to enhance energy performance and reduce environmental impact. The TRNSYS software was used to simulate a typical residential building across nine southern provinces such as Adrar, Biskra, and Laghouat, evaluating different insulation materials like glass wool and polystyrene.

Results showed that insulation reduced heating needs by up to 60% and cooling demands by around 40%. In Laghouat, heating consumption dropped from 61.85 to 46.27 kWh/m², while CO_2 emissions decreased by 17.8% in Adrar and 18.9% in Béchar. Indoor temperature fluctuations were also significantly minimized. The study confirms that combining insulation with a heat pump is more effective than using either alone and recommends applying this integrated strategy in building policies for Algeria's arid regions.

ملخص

في المناطق الحارة وشبه الجافة مثل جنوب الجزائر، يشكل تحقيق الراحة الحرارية مع تقليل استهلاك الطاقة تحديًا كبيرًا بسبب التفاوت الكبير في درجات الحرارة. تركز هذه الدراسة على دمج العزل الحراري ومضخات الحرارة كاستراتيجية لمحاكاة مبنى سكني نموذجي في تسع TRNSYS مشتركة لتحسين الأداء الطاقوي وتقليل الأثر البيئي. تم استخدام برنامج ولايات جنوبية مثل أدرار وبسكرة والأغواط، مع دراسة مواد عزل مختلفة كالصوف الزجاجي والبوليسترين.

أظهرت النتائج أن العزل يقلل من احتياجات التدفئة بنسبة تصل إلى 60% والتبريد بحوالي 40%. في الأغواط، بنسبة 17.8% في أدرار و18.9% CO_2 انخفض استهلاك التدفئة من 61.85 إلى 46.27 ك.و.س/م²، وانخفضت انبعاثات في بشار. كما قلّت تقلبات درجات الحرارة داخل المبنى بشكل ملحوظ. تؤكد الدراسة أن الجمع بين العزل ومضخة الحرارة أكثر فعالية من استخدام كل منهما على حدة، وتوصي بتطبيق هذه الاستراتيجية في سياسات البناء في المناطق الجافة بالجزائر.